Production and Properties of Photoactive Collagen-Based Wet Spun Fibres

Jessica Margaret Rickman

Submitted in accordance with the requirements for the degree of PhD

The University of Leeds
School of Design and School of Dentistry

2020

The candidate confirms that the work submitted is her own, except where work which has formed part of jointly-authored publications has been included. The contribution of the candidate and the other authors to this work has been explicitly indicated below. The candidate confirms that appropriate credit has been given within the thesis where reference has been made to the work of others.

Rotation-assisted wet-spinning of UV-cured gelatin fibres and nonwovens.

Rickman, J., Tronci, G., Liang, H. and Russell, S.J. 2019.
Journal of Materials Science. 54(14), pp.10529-10547.

Acknowledgements

I am grateful to my supervisors Professor Stephen Russell and Dr. Giuseppe Tronci, and for the support of Dr He Liang. Thank you to Professor Parikshit Goswami, and Dr Subhadeep Paul of Huddersfield University for assistance with tensile testing during Covid-19 lockdown measures. I thank wider members of the group, Sarah Myers, Jackie Hudson, and Matthew Percival from the School of Dentistry, and Jianguo Qu and Tim Smith from the School of Design. I would also like to thank family and friends who have supported me both during my research.

Abstract

The excellent biocompatibility of collagen-based biomaterials make them highly relevant in the field of medical textiles. The manufacture of continuous filaments and staple fibres permits their incorporation into textiles with more easily controllable properties than other material structures such as sponges, electrospun meshes, and hydrogels. However collagen-based biomaterial spinning has thus far presented a challenge with issues such as wet instability, triple helix denaturation, rapid *in vivo* biodegradation and poor mechanical properties, particularly for gelatin fibres.

Herein, to address these challenges alternative crosslinking strategies have been developed to stabilise the protein structure, without the need for chemical treatments post-spinning that carry the risk of residual cytotoxic effects. To provide a novel approach, selected photo-active crosslinking moieties are grafted onto the collagen-based material before spinning and then crosslinked in the presence of a light source and a specific water-soluble photoinitiator. The vinybenzylation approach enables unreacted reagents to be washed away in the precipitation stage following functionalisation of the collagen-based material minimising potential for adverse reactions when the material is *in vivo*.

Preparation of gelatin-4 vinyl benzyl chloride (Gel-4VBC) materials was studied, including the feasibility of spinning, effects of varying wet-spinning coagulants, and comparisons between the spinning of gelatin-4VBC and methacrylated gelatin, another photoactive material widely used in the biomaterials industry. Results showed the vinylbenzylated material had a better combination of mechanical (UTS= 74 ± 3 MPa) and swelling index (SI= 260 ± 24 a%), was more readily wet spun into room temperature, using aqueous coagulants, and was significantly more biocompatible than gelatin-methacrylate (Gel-MA) after 7 days of incubation.

Collagen-4VBC staple fibres were also prepared and wet spun and characterised with factors such as coagulant type, extrusion and collection rate, and spinneret dimensions' influence upon collagen triple helix denaturation, swelling, and enzymatic, tensile, and thermal resistance observed. A triple helix retention of 82% was measured using circular dichroism, indicating low levels of denaturation during the functionalisation and spinning processes. Increased stretching of the fibre during spinning was shown to increase fibre strength as compared to increasing shear stress induced by higher extrusion rates. Reducing the needle aperture was shown to increase fibre tensile strength and modulus by a factor of 2.3 and 2.9 respectively. The staple fibres had high ultimate tensile strength (UTS) and modulus, comparable to native collagen reported in the literature with a UTS of 286 ± 38 MPa and modulus of 4 ± 0.5 GPa recorded.

The feasibility of converting the staple fibres into nonwoven and braided textile structures was then confirmed. The prototypes were tested with respect to morphological, swelling, collagenase degradation and cell tolerance characteristics showing suitable properties for use in medical devices. Overall this work demonstrates that 4VBC functionalisation of collagen-based materials followed by UV-crosslinking is a promising route for manufacture of biocompatible wet spun staple fibres relevant to applications in healthcare.

List of Abbreviations

4VBC- 4-vinylbenzyl chloride

ARDS- Automated Rotational Deposition System

ATR-FTIR- attentuated total resistance Fourier-transform infrared

CD- circular dichroism

Coll-4VBC- Collagen-4VBC

DMEM- Dulbecco's modified eagles solution

DMSO- dimethyl sulfoxide

DR- draw ratio

DSC- differential scanning calorimetry

ECM- extracellular matrix

EDC- 1-ethyl-3-(3-dimethylaminopropyl) carbodiimide

ER- endoplasmic reticulum

EtOH- ethanol

F- functionalisation %

GMA- glycidyl methacrylate

GTA- glutaraldehyde

Gel-4VBC- gelatin-4VBC

Gel-MA- Gelatin-methacrylate

HFC- hydrolysed fish collagen

HFP- 1,1,1,3,3,3- heaxafluoro-2-propanol

I2925- Irgacure 2959

LOX- lysyl oxidase

MA- methacrylic acid

MMPs- matrix metalloproteases

Mw- molecular weight

NHS- N-hydroxysuccinimide

NW- nonwoven

PCL- polycaprolactone

PEG- polyethylene glycol

Ph- phenylenediaceticacid

PI- photoinitiator

RER- rough endoplasmic reticulum

RF- riboflavin

RTC-rat tail collagen

SEM- scanning electron microscopy

SI- swelling index

TE- tissue engineering

TEA- triethylamine

TFE- 2,2,2, trifluoroethanol

Tm- melting temperature

TNBS- 2,4,6-Trinitrobenzenesulfonic acid

TR- tissue regeneration

UTS- ultimate tensile strength

WU- water uptake

YM- Young’s modulus

Table of Contents

List of Tables

List of Figures

List of Equations

Chapter 1

Introduction

1.1 Collagen-Based Materials

Collagen-based materials have long been incorporated into medical devices used for healthcare due to their excellent biocompatibility and mechanical properties. The native protein consists of three polyproline II-type (PPII) helices predominantly composed of proline, hydroxyproline and glycine arranged in a triple helix predominantly stabilised with hydrogen bonds. These helices are covalently crosslinked together and aligned in a staggered formation endowing the material with high strength. Motifs within the protein encourage cellular recruitment and attachment and allow for the material to be degraded and reabsorbed. These characteristics make the material suitable for implantation.

Whilst decellularised collagen in its native structure may be used directly for the manufacture of medical devices, synthetic processing of the material is often necessary to allow it to be delivered in formats not available in nature, but useful for the clinic. Such formats include membranes, hydrogels, textile staple fibres, yarns and fabrics, of various dimensions with physical characteristics meeting the requirements of devices such as regenerative scaffolds and wound dressings.

Spinning collagen feedstocks into fibres also facilitates biomimicking of the native cellular environment in terms of fibre dimensions and geometric structure, whilst enabling textile materials to be produced with the high surface area and porosity required for cellular support and nutrient exchange. In recent years, specifically in relation to applications in healthcare, intensive research has been conducted on the manufacture of collagen submicron fibres by electrospinning, with the intention to minimic the diameter of native collagen fibrils found in vivo. However, the volatile polar solvents needed for process disrupt hydrogen bonding in the collagen

helices resulting in denaturation, and the formation of gelatin fibres with relatively poor mechanical properties and wet-stability. Furthermore electrospinning only produces thin, membrane-like fabrics with small pore sizes that can inhibit cellular infiltration and nutrient exchange.

This has renewed interest in more conventional methods of fibre manufacture such as wet or solution spinning, where voltage-free production of collagen fibres is possible, in conditions that can be controlled, to produce fibres of uniform dimensions. Conversion into a range of textile formats is then possible from fibres, continuous filaments, fabrics and braids, for example.

Wet-spinning, involves extrusion of a spinning dope into a non-solvent causing coagulation and solidification by diffusional exchange. Once spun collagen fibres are crosslinked to increase mechanical strength, reduce collagenase bio-susceptibility and improve thermal and wet stability. Common modes of crosslinking have been shown to have significant limitations such as limited mechanical strength and cytotoxicity.

Recent developments in this field have seen the synthesis of functionalised collagen materials being developed, directed mainly at the manufacture of high strength hydrogels. One recently introduced variant of functionalised collagen involves the grafting of photo-active moieties onto the collagen backbone. Ultra-violet (UV) light irradiation of the resulting photosensitive material is then used to initiate the synthesis of a covalently crosslinked network, therefore yielding a mechanically competent hydrogel.

This UV-irradiation approach is attractive because unlike the use of liquid crosslinking reagents, it ensures that any cytotoxic material is removed from the collagen material in the precipitation stages prior to spinning and has the potential to produce excellent mechanical properties and biocompatibility in collagen hydrogels. The compatibility of this approach with the manufacture of collagen-based materials using wet spinning is therefore of significant interest.

1.2 Aims and Objectives

Until now, very few previous studies of wet spinning of functionalised collagen materials have been reported. This research aims to address this knowledge gap by developing a functionalised collagen fibre manufacturing platform based on a wet spinning route for producing photoactive, crosslinked fibres, using methods previously developed for the manufacture of collagen hydrogels. The specific objectives are:

1. To critically review the production of collagen-based materials by wet spinning and related manufacturing methodologies.
2. To investigate the feasibility and methods for wet spinning of UV-photoactive functionalised gelatin (f-gelatin) and collagen (f-collagen) fibres.
3. To study the effects of process parameters with respect to resulting fibre morphology and physical properties.
4. To determine the feasibility of converting functionalised, photoactive collagen-based fibres in to nonwovens and braids.

Chapter 2

Literature review

2.1 Introduction

Collagen is the most abundant protein found within living systems. There are multiple types of collagen all of which differ slightly in primary amino acid sequence. This primary structure endows the molecule with a distinct triple helical structure which forms a fibrillary macromolecule complete with binding sites and regions which interact with cells and other extracellular matrix components. This gives the material and its derivatives, notably gelatin, unique properties as a building block for incorporation into textile materials intended for medical devices. This Chapter reviews essential aspects of collagen-based materials, relating to structure and properties, applications in medical devices, their value as biomaterials and the potential modes of processing collagen into fibres and textile assemblies.

2.2 Collagen and gelatin materials

2.2.1 Structure and properties

The proteinaceous structure of collagen can be conveniently described by considering its hierarchical features. Starting from the smallest units, the primary amino acid structure of collagen endows the protein with high tensile strength and stability. The three most common amino acids within collagen are glycine, proline, and hydroxyproline, the structures of which are shown

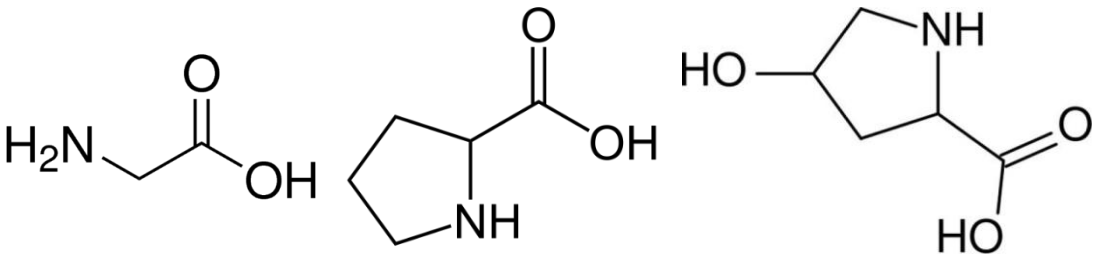

Figure 2.1: From left to right: glycine, proline, and hydroxyproline - the three main amino acids in collagen

in Figure 2.1 (Shoulders and Raines, 2009; Balasubramanian et al., 2013; Engel and Bachinger, 2005).

The small, simple structure of glycine, found at every third site along the chain (X-Y-Gly), allows the collagen fibrils to align closely together, facilitating the formation of many stabilising hydrogen bonds. Within the collagen alpha helices, the glycine residues are positioned pointing inwards. This is due to the limited space that is available within the helix, allowing only glycine's small hydrogen R-group to be accommodated. By contrast, the proline and hydroxyproline components, point outwards with their cyclic side chains giving the structure conformational rigidity, with hydroxyproline's hydroxyl group supporting the sharp twists of the helix (Shoulders and Raines, 2009).

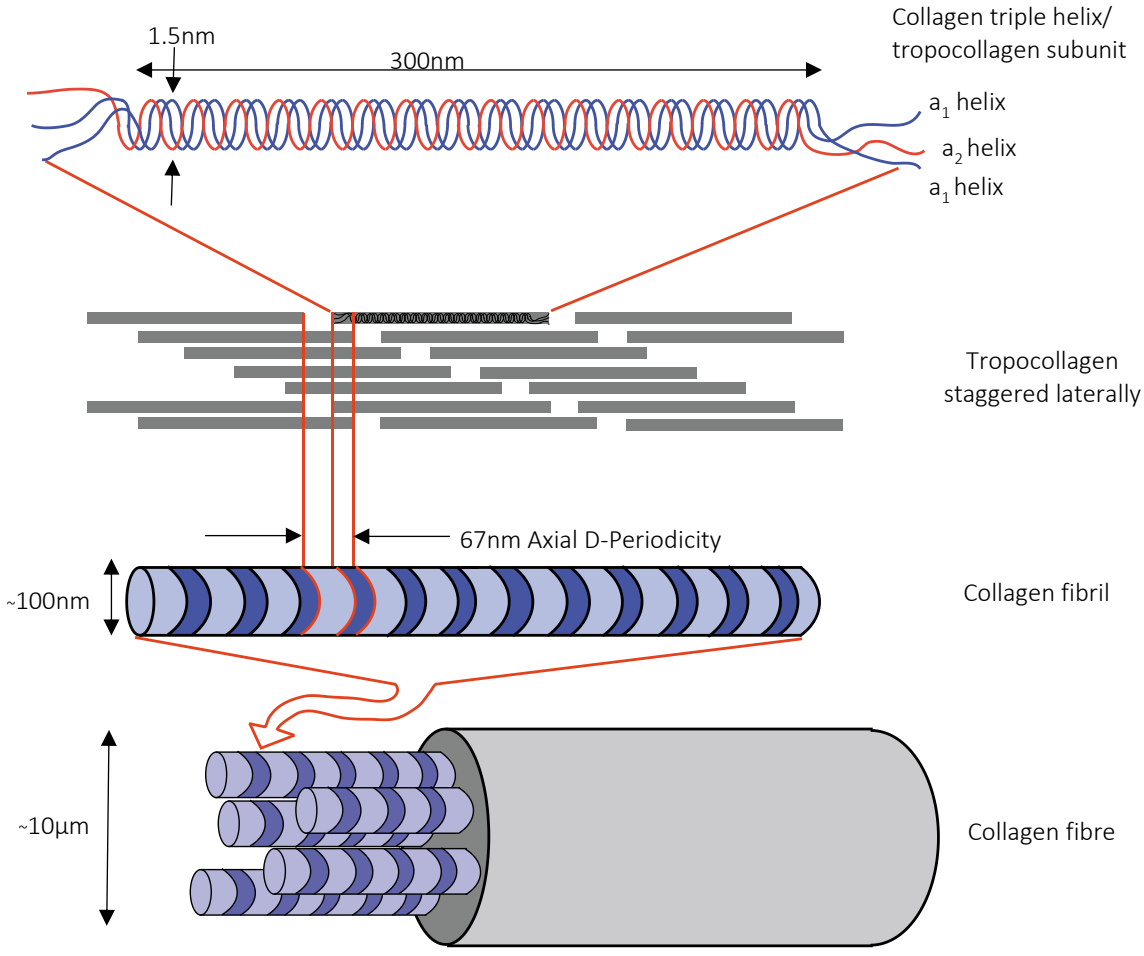

Figure 2.2: The hierarchical structure and organisation of collagen fibres

The collagen protein consists of three amino acid left handed alpha helices, (two α1 and one α2), wound into a triple helix, which measures 300nm along the length with a width of 1.5 nm. This monomer is also known as a tropocollagen subunit (Hulmes et al., 1973).

The subunits are staggered forming sections of overlap held together by covalent bonds, as shown in Figure 2.2. This is called D-periodicity and forms characteristic striations in the collagen at a distance of 67 nm. This alignment is thought to involve charge-charge and hydrophobic interactions, and is likely to contribute towards the protein's mechanical strength, and proteolytic resistance. Indeed, it has been reported that the triple helical structure is a prerequisite for fibril self-assembly and that it blocks antigenic and proteolytic cleavage sites (Caves et al., 2010; Lynn et al., 2004; Shepherd, D.V. et al., 2015).

Gelatin is the result of chemical, thermal or electrical disruption to the H-bonds that stabilise the collagen triple helix, causing denaturation. This process leads to irreversible triple helix disentanglement into separate randomly organised polypeptide chains due to hydrogen bond disruption (Figure 2.3). Gelatin does retain the ability to form triple helices at low temperature, however when exposed to physiological conditions, i.e. aqueous environments at 37ºC, the disruption of the hydrogen bonding lead to the material reverting back to randomly oriented polypeptide chains (Mukherjee and Rosolen, 2013). This leads to a reduction in the mechanical and thermal stability normally associated with collagen and its highly ordered lateral formation, leading to gelatin dissolution under physiological conditions.

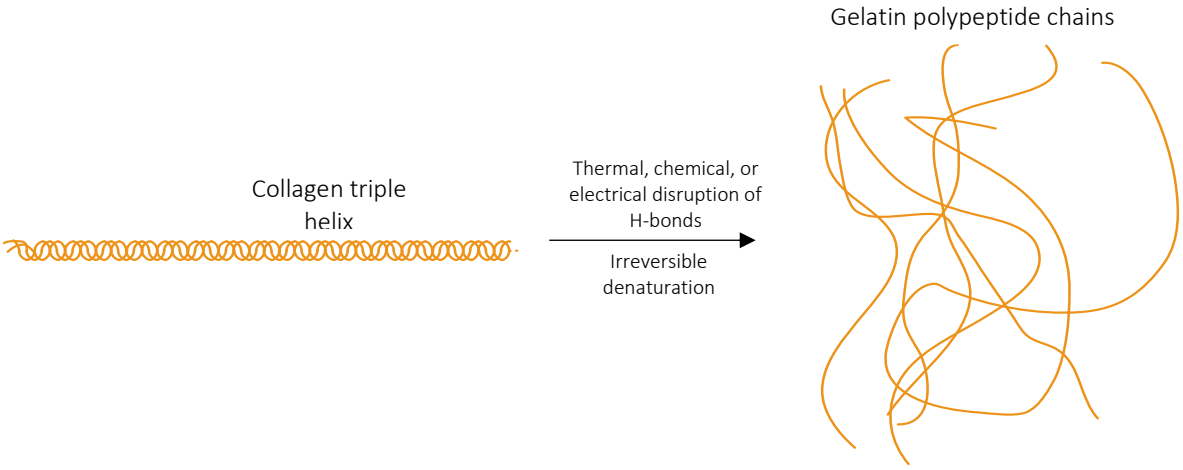

Figure 2.3: Gelatin formation by collagen denaturation

Although denaturation does lead to adverse effects in terms of material properties, these can be combatted to some extent by crosslinking which stabilises the chain structure at higher temperatures in a polypeptide hydrogel network, preventing dissolution. It has also been reported to induce a lower level of immune reaction when implanted, due to (a) the absence of telopeptides from the terminal ends of the polypeptide chain and, (b) from the increased levels of processing during gelatin production, which is hypothesised to improve sterilisation and removal of antigens (Gorgieva, 2011). Owing to lower levels of sensitivity and ease of processing, gelatin is also considerably cheaper, as well as having the same primary amino acid structure as collagen. This means it is also biodegradable and compatible with the physiological environment due to its collagenase target sequences (Vandooren et al., 2013; Liu, Y.X. and Chan-Park, 2010).

2.2.2 Synthesis *in vivo*

Consideration of collagen synthesis *in vivo* is useful to gain understanding of the cellular complexity required to form fibres within the body, and the different orders of the molecular structure. The process takes place initially in the rough endoplasmic reticulum (RER) of the cell where the alpha chains are synthesised at the ribosomes embedded in the organelle's walls. These chains are called preprocollagen. They have registration peptides and a signal peptide at the end of each chain. Released into the lumen of the RER the chains have their signal peptides cleaved and selected lysine and proline

amino acids hydroxylated. Hydroxylysine residues are then further glycosylated to form procollagen (Kadler et al., 2008; Shoulders and Raines, 2009).

The triple helical structure of procollagen is formed in the endoplasmic reticulum (ER) and transported to the Golgi apparatus. Here it is packaged and exocytosis occurs. Outside of the cell, the registration peptides are cleaved enzymatically by procollagen peptidase. This decreases the solubility of the procollagen and triggers the self-assembly of collagen triple helices. These are then converted to collagen fibrils. This is overseen by the enzyme lysyl oxidase (LOX) which catalyses aldol condensation reactions between the hydroxylysine and lysine residues on the triple helices resulting in covalent bonds between the tropocollagen molecules. Multiple collagen fibrils are grouped together to form a collagen fibre.

2.2.3 The Extracellular Matrix (ECM)

As shown in Figure 2.4, the ECM is the non-cellular region between cells within all tissue (Frantz et al., 2010). It works to provide physical support by acting as a cell scaffold, as well as overseeing biochemical and biomechanical cues which initiate differentiation and homeostasis. Each tissue type has varying functional requirements from an ECM, and therefore it is structurally tailored according to tissue type.

This specific organisation of ECM decides the mechanical properties of the tissue, such as elasticity, compressive or tensile strength. For example bone ECM must have a high compressive strength to support impact (Jones et al., 2009). Nerve axons by contrast must be softer and more flexible (Siriwardane et al., 2014). The binding of growth factors to the ECM determines this organisation.

The ECM is made up of two components; the proteoglycans, and the fibrous proteins. These fibrous proteins are collagens, elastins, fibronectins, and laminins. Collagen is the most abundant of these proteins and regulates tensile strength, cell adhesion, chemotaxis and the development of tissues (Rozario and DeSimone, 2010). Collagen protein is secreted by fibroblasts which align the collagen fibres by exerting tension upon the extracellular

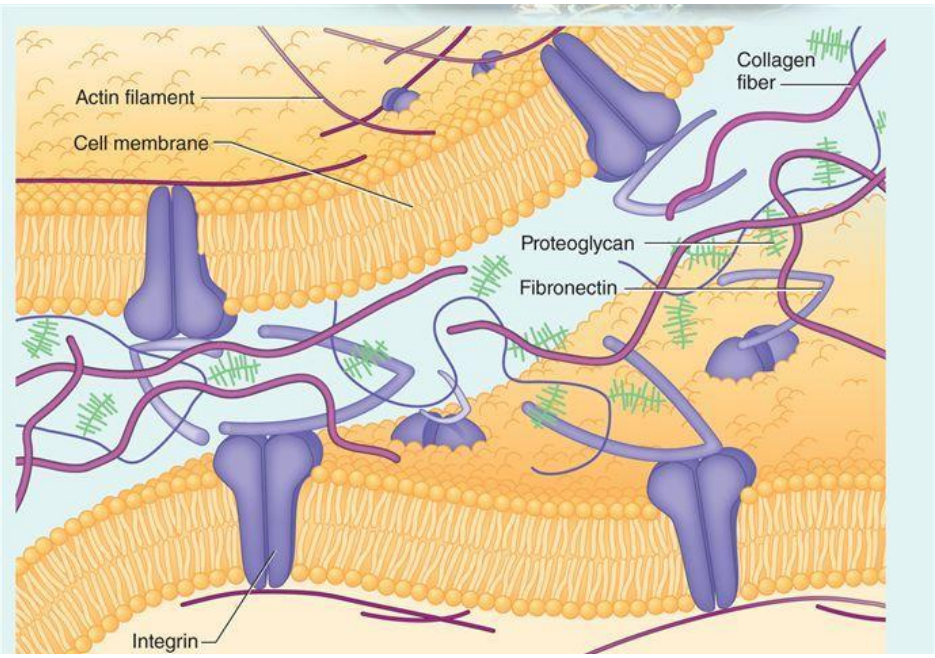

Figure 2.4: The extracellular matrix (ECM) between cells in tissue. It acts as a medium for cell anchoring, signalling, and support. A large majority of the ECM is made up from collagen. (StudyBlue, 2016)

matrix, thereby defining the tensile properties of the fibre (Tracy et al., 2016). This mechanism is conceptually similar to that used in synthetic fibre drawing, where fibres undergo uniaxial tension, to align them relative to each, making the structure more oriented, and increasing the uniaxial strength.

2.3 Spinning Techniques for Collagen-Based Materials

Amongst the various approaches that have been developed for the production of collagen-based medical devices, textile processes are attractive because of the ability to manufacture a wide variety of different

formats. This includes, fibres (including micro and nanofibres), woven and knitted fabrics, braids and nonwovens. Methods capable of producing continuous collagen fibres are particularly attractive because of the potential to convert resulting yarns in to woven, knitted, braided or other textile structures, in addition to nonwovens. This section considers the two most reported techniques compatible with collagen fibre spinning (electrospinning and wet spinning), and the key parameters controlling fibre morphology, dimensions and physical properties. The implications for retention of native protein structure are also considered, since this can affect both mechanical and biological properties. A critical summary of each spinning technique in relation to collagen fibre production is given in Table 2.1**: Comparison of spinning techniques for collagen-based materials**.

2.3.1 Electrospinning

Electrospinning is the process by which fibres are spun by extruding an electrically charged polymeric spinning dope, which due to electrostatic repulsion, counteracting the liquid surface tension, results in the stretching of a liquid stream. The resulting instabilities and whipping of the polymer stream in air, leads to progressive attenuation, which following evaporation of the solvent in the polymer dope, leads to the formation of solid fibres. (Reneker and Yarin, 2008). The basic elements of a simple electrospinning process are shown in Figure 2.5. Fibre dimensions, morphology and physical properties can be adjusted by varying parameters such as dope flow rate, viscosity, concentration, and molecular weight, spinning orifice size, spinning distance, and ambient conditions, notably humidity and temperature (Liu, H. et al., 2013; Haghi, 2012; Teule, 2008).

Depending on spinning dope viscosity and process conditions, the resulting fibres are of small fibre diameter ranging from <100 nm to <10 microns, which depending on polymer composition, allows for biomimicking of the ECM, where fibrillar collagen structures are found from 20nm and up to 40µm (Silver et al., 2003; Jarvinen et al., 2004; Huang, Y.F. et al., 2001). Electrospinning has therefore been reported in multiple studies aimed at the

production of collagen based textile materials (Hlavata et al., 2017; Kovalenko et al., 2017; Delyth et al., 2009; Farzamfar et al., 2018; Cumming et al., 2018; Alexander

Table 2.1: Comparison of spinning techniques for collagen-based materials

Spinning method	Wet-spinning	Electrospinning
Technique summary	Polypeptide dope/ suspension is extruded into a non-solvent causing a phase transition from liquid dope to solid fibre by diffusional exchange	Charged dope extruded onto oppositely charged collection plate. Volatile dope solvent rapidly evaporates from fibre causing solidification
Parameters to control	Dope concentration, molecular weight and viscosity Coagulation polarity Coagulation bath concentration Post drawing conditions Temperature and humidity Needle/ spinneret size and shape	Dope concentration, molecular weight and viscosity Dope conductivity Solvent evaporation rate Dope flow rate Applied voltage Tip to collector distance Temperature and humidity
Fibre/textile properties	Diams: 10µm-2000µm (Kew et al., 2011) Single continuous filaments	Diams: 100nm-1µm (Haghi, 2012) Thin meshes <1mm wide
Advantages for collagen spinning	Diams: 10µm-2000µm (Kew et al., 2011) Single continuous filaments Voltage free and no heat input, low levels of denaturation Diameter and fibre alignment highly controllable Fibres continuous, therefore able to form nonwovens with controlled morphologies Higher levels of cell infiltration	Low fibre diameters mimic native collagen fibres
Disadvantages for collagen spinning	Blockages and breakages common	Voltage input and volatile denaturing chemicals cause collagen triple helix disruption Difficult to control fibre and nonwoven morphology

et al., 2019; Turker et al., 2019; Kim, J.Y. et al., 2019). Although electrospinning is normally associated with the production of nonwoven webs, methods of forming multifilament yarns by electrospinning is also possible by convergence of the as-spun electrospun fibres (Badrossamay et al., 2014).

There are several significant drawbacks to collagen electrospinning. The spinning itself is difficult to control leading to unpredictable fibre morphologies and large diameter distributions (Kew et al., 2012). It is also difficult to process the fibres once spun due to their sensitivity to moisture and low tensile strength. Electrospinning also results in a thin, membrane-like structure, which may not be suitable for many practical applications, and key dimensional properties such as porosity are difficult to control (Stepanyan et al., 2014; Khorshidi et al., 2016). In the context of medical devices, wet-spun fibres allow for greater liquid or exudate absorbency, cell infiltration and shape forming, supporting cell survival as compared to electrospun fibres assembled into nonwovens (Kalaithong et al., 2017).

Preparation of the dope followed by electrospinning of collagen are also believed to result in denaturation of the polymer. As a protein, the structure of collagen is stabilised by hydrogen bonds, which are especially sensitive to heat, voltage and volatile or highly polar chemicals. Exposure to these conditions causes the collagen triple helices to denature due to the disruption of hydrogen bonding, and take up a randomly organised, semi-crystalline, polypeptide chain configuration, commonly known as gelatin. As discussed in Section 1.1 this can lead to a reduction in tensile strength as well as thermal and wet stability, which undermines the utility of the material in physiological conditions. In addition to the collagen dope being electrically charged during electrospinning, highly volatile solvents are used to form the spinning dope. Most commonly used are the fluoroalcohols 1,1,1,3,3,3-hexafluoro-2-propanol (HFP) and 2,2,2, trifluoroethanol (TFE) (Zeugolis, Dimitrios I. et al., 2008)

Zeugolis *et al.* confirmed that electrospinning of collagen dissolved in HFP or TFE, effectively resulted in the production of gelatin fibres, due to denaturation (Zeugolis, Dimitrios I. et al., 2008). They compared fibres spun by electrospinning using TFE and HFP, self-assembled collagen fibres dissolved in TFE and HFP, self-assembled collagen fibres not exposed to these solvents, and native rat-tail tendon. They observed that the electrospun collagen fibres did not exhibit triple helical structure and were not crystalline. There was no internal structure, D-spacing, or staggering of the fibrils. This lack of characteristic structure resulted in the denaturation temperatures of the collagen electrospun fibres being significantly lower than native collagen: 29 ºC ±3 vs 58 ºC ±1, and lower, even, than the gelatin electrospun fibres at 30 ºC ±2. The electrospun fibres were also found to be pepsin susceptible, which is also indicative of collagen denaturation.

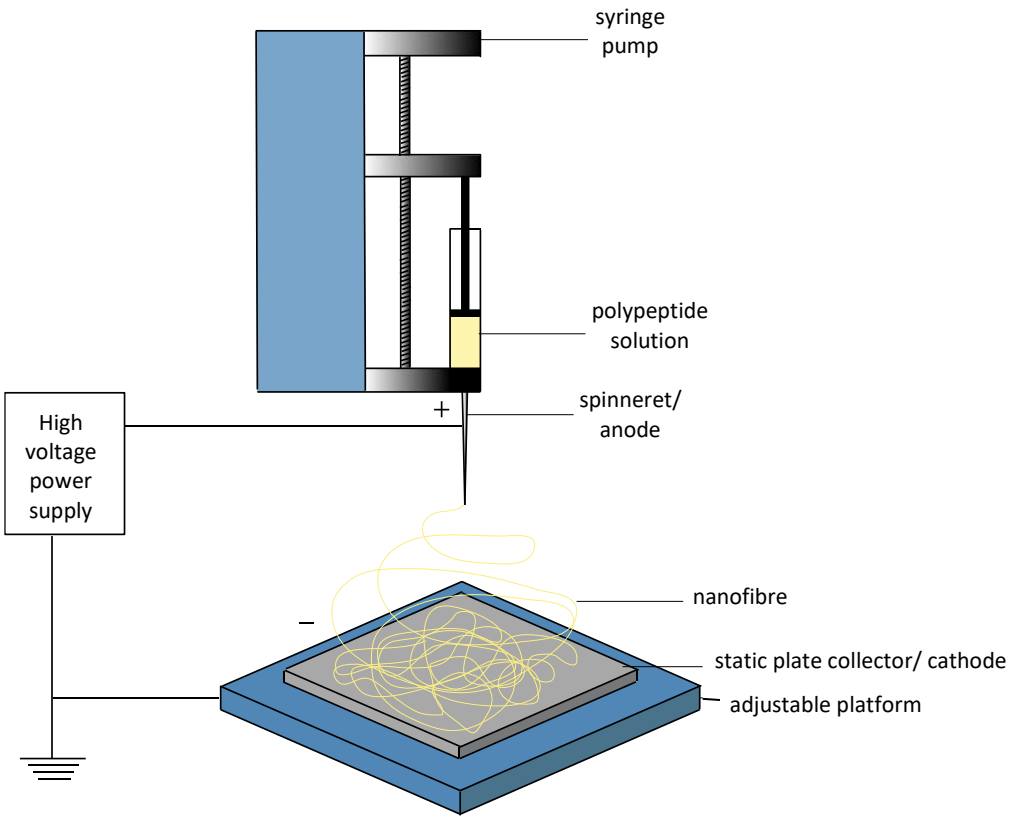

Figure 2.5: Elements of a Simple Electrospinning Rig

Some success has recently been achieved in retaining the triple helix structure of collagen during electrospinning (Wakuda et al., 2018). Collagen was electrospun in a core-shell (sheath) configuration, with a PVP protective shell, which was subsequently washed away to produce collagen nanofibers. The fibres had an average diameter of 461nm with similar triple helix retention to native collagen, as determined by circular dichroism (CD). Although this approach is promising in terms of preserving collagen structure during electrospinning, the process is far from straightforward because of the need for a sacrificial polymer, and the issues around controlling the dimensional properties of the resulting fibres still remain since they are inherent to the electrospinning process. It is therefore important to consider alternative approaches to collagen and gelatin fibre formation, which are voltage-free and potentially circumvent the basic limitations of electrospinning.

2.3.2 Alternative spinning techniques

Other work in collagen based fibres spinning has looked at methods from outside the dominant spinning techniques used in literature. Due to the solubility and sensitivity of collagen in most cases these works use gelatin to produce their fibres.

Centrifugal spinning

Centrifugal spinning is performed by placing a dope into a rotating head with a nozzle. Upon the head rotating at a critical speed the centrifugal force upon the dope overcomes it’s surface tension, this causes the solution to be ejected in a liquid jet from the tip of the nozzle. The liquid jet is then stretched and dried in the air and a solid web of fibres is deposited on a 2D collector surface, similar to electro-spinning. Although there is limited literature on centrifugal spinning of collagen based fibres Freudenberg have patented a process for spinning gelatin for use as a haemostat (Vogt, 2015).

Although centrifugal spinning is a rapid and cheap means of spinning fibres, it does have drawbacks when regarding its suitability towards collagen

spinning. As with electrospinning, only 2D meshes with small pore sizes are able to be produced. In addition the high viscosity of collagen solutions would inhibit spinning due to the high centrifugal forces required to overcome the dope's surface tension.

Dry-spinning and gel-spinning

The techniques of dry spinning and gel-spinning are very similar. Dry spinning is the process by which a dope is forced through a spinneret forming a continuous stream of liquid dope which then forms a solid fibre as the solvent evaporates in the air. Gel spinning involves the same process with a secondary step of phase separation within a coagulation bath. Both techniques have been seen for the formation of gelatin fibres, again, this process is unsuited to collagen spinning due to its dope viscosity (Fukae et al., 2005; Fukae and Midorikawa, 2008; Midorikawa et al., 2012, Chaochai et al., 2016).

Chaochai *et al* investigated using dry spinning for the preparation of gelatin fibres. Gelatin dissolved in water, held at 50 ºC was extruded through a nozzle, dried off with high speed stretching in the air and crosslinked. Resulting fibres were 50-60 µm and showed good water resistance after crosslinking. Drawbacks to the material were its porous internal architecture, indicating that the drying process was not well controlled (Chaochai et al., 2016).

Gel-spinning has so far mostly been performed in search of a substitute for wool in the garment industry (Fukae et al., 2005; Fukae and Midorikawa, 2008; Midorikawa et al., 2012). Resultingly the toxic chemicals used, such as DMSO, methanol, and ethylene glycol would likely cause toxicity to cells if residue remained post-spinning. Fukae *et al* used a process by which gelatin dissolved at 15 wt % into DMSO was extruded into a -20 ºC bath post air exposure (Fukae et al. 2008). The resulting fibres showed a tensile strength of 146 MPa when drawn to a ratio of 1:16. In addition to the toxic chemicals used in this study, the use of a -20 ºC bath would be impractical and costly when utilized for large scale production. As such wet-spinning is

proposed as a more practical, biocompatible options for the formation of gelati and collagen fibres.

2.3.3 Wet-spinning

An alternative mode of collagen-based fibre spinning is wet-spinning where a polypeptide dope, is extruded through spinneret into a non-solvent bath to coagulate the polymer stream that is formed (Figure 2.6**Error! Reference source not found.**) (Aishanjiang et al., 2016; Teule, 2008; Tronci et al., 2015b; Arafat et al., 2015; Enea et al., 2013; Enea et al., 2011; Meyer et al., 2010; Kew et al., 2011; Shepherd, D.V. et al., 2015; Zeugolis et al., 2009b; Zeugolis, D. I. et al., 2008c; Zeugolis et al., 2010; Yaari et al., 2016; Haynl et al., 2016; Fukae et al., 2005; Fukae and Midorikawa, 2008; Midorikawa et al., 2012; Caves et al., 2010; Wang, Y. et al., 2019; Tonndorf et al., 2020).

Wet spinning is one of the most established methods of spinning naturally occurring polymers, from animal or plant sources. Historically, although production was discontinued in 1959, commercial manufacture of wet spun collagen-based fibre has been pursued by Carl Freudenberg, who produced a product under the tradename ‘Marena’ made from split hides for use in brushes (Cook, 2001). Kaneka in Japan also produce a highly crosslinked collagen fibre under the tradename ‘Kanecaron Collagen Fiber’, which finds applications as synthetic hair (Kaneka-Corporation, 2013). More recently ‘Umorfil’ fibre has been launched, which incorporates collagen-based material extracted from fish scales in Japan combined with regenerated cellulose, and the product is directed at fashion applications (Camangi-Corp, 2020). These previously developed collagen-based materials involve significant modification of the native collagen material through either combination with other polymers or chemical cross-linking such that they are not intended for use in invasive medical devices.

The wet spinning process relies on diffusional exchange to induce a phase separation, by which the solvent diffuses out of the polymer dope to be replaced with the non-solvent causing solidification and the formation of a fibre. The rate of diffusional exchange can greatly influence the internal and

external fibre morphology. Following coagulation, attenuation of the fibre via drawing and other treatments can be implemented to influence fibre properties.

Fibres produced by wet-spinning can have a mean fibre diameter ranging from 10-2000μm, depending on process conditions, controlled by spinneret orifice size, coagulation and drawing arrangements. Wet-spinning produces continuous filaments that can be wound on to packages ready for conversion in to fabrics using a variety of textile and nonwoven processes. It is also this versatility that is attractive from a manufacturing perspective, since there is the possibility to make a range of reproducible textile architectures that is somewhat more difficult to achieve using electrospinning as an additional level of control is introduced by separating the fibre spinning and textile manufacture stages.

As summarised in Table 2.2, in relation to the wet spinning of polypeptides such as collagen and gelatin, there are several parameters that influence the fibre spinning process, which will now be considered in greater depth.

2.3.4 Variables influencing wet-spun fibre properties

The key variables affecting wet spun fibre properties can be conveniently divided into three sub-groups. The first is the liquid stage, wherein key factors are the dope viscosity and the solvent used for dissolution. The second is the solidification stage, which is largely controlled by the selection of the coagulant, the concentration, polarity, and viscosity. The third relates to the post-spinning treatment stage, which includes drawing, and potential crosslinking steps.

Of major significance in wet spinning are the variables adjuvant to the basic phase transition, which include the rate of extrusion, draw ratio, spinneret aperture shape and size, and post-treatment crosslinking of the fibre (Lu et al., 2020).

Table 2.2: Polarity and viscosity of FFBs used by Tronci *et al* (2015b) Solvent polarity parameter ($E_T(30)$/kcal mol^{-1}) and the viscosity values (μ/Pa s (×10−3)) of DMSO, TFE, acetone, and ethanol (Paul, 1968)

Solvent	DMSO	TFE	Acetone	Ethanol
$E_T(30)$/kcal mol^{-1}	45.1	59.8	42.2	51.9
μ/Pa s (×10^{-3})	1.99	1.75	0.31	1.07

The first two factors (the liquid and solidification stages) influence the nature of the phase transition, by affecting the rate of diffusional exchange. The faster the diffusional exchange, the less homogenous the fibre will be as rapid exchange will cause the outer surface of the fibre to quickly solidify, forming a barrier against diffusion from the fibre core. A consequence of this can be a fibre morphology in which there is a porous core, and a dense outer sheath. This lack of homogeneity in the structure can negatively affect the mechanical properties of the fibre, as the internal discontinuities within the fibre lead to disproportionate load bearing by the outer fibre surfaces. A very slow diffusional exchange can by contrast lead to difficulties in forming a coherent fibre (Tronci et al., 2015b; Adanur, 1995).

2.3.5 Liquid stage: wet-spinning dope

The viscosity of dope is important to consider with respect to the basic wet-spinning process. The dope must be viscous enough to produce a coherent liquid stream without the need for excessive back pressure at the spinneret, or orifice blockage. Within these limits, dope viscosity can be tuned within to produce fibres with the required attributes. Viscosity refers to *"the tendency of a liquid or gas to resist by internal friction the relative motion of its molecules and hence any change of shape; the magnitude of this, as measured by the force per unit area resisting a flow." (OED, 2018)*

In terms of diffusional exchange the more viscous the dope the slower the diffusional exchange will be. This is due to reduced mobility within the

polypeptide chains in solution, caused by increased internal friction, reducing the rate of outward diffusion of the solvent from the forming fibre (Tronci et al., 2015b).

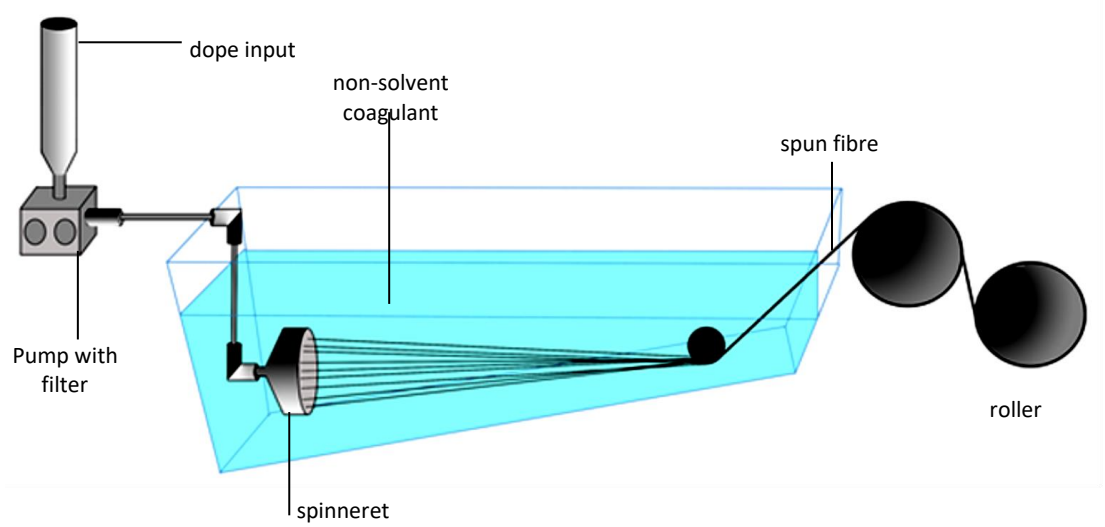

Figure 2.6: Components of a simple wet-spinning process. Dope is pumped through and filter and tubing leading up to a spinneret with multiple holes. The dope exits the spinneret into the coagulant where it solidifies and forms fibres. Spun fibres are then collected on rollers for drawing and further downstream processing

Viscosity also influences the crystallinity of the resulting fibre because of the effect of molecular alignment, and the internal friction created by axial stretching in the direction of the polypeptide chains (Arafat et al., 2015). An increase in crystallinity has been shown to increase the fibre's resistance to temperature, mechanical forces, and enzymatic breakdown (Pins et al., 1997b; Pins et al., 1997a). Multiple factors influence dope viscosity including, molecular weight, concentration, temperature, and solvent selection. These parameters are now discussed in further detail because of their relevance to the present research.

2.3.4.1 Dope concentration

Increasing polypeptide dope concentration in wet spinning usually leads to an increase in viscosity due to the dope becoming denser and the effect on molecular chain mobility. Arafat *et al* dissolved rat tail collagen at

concentrations of 1.2, 1.4, and 1.6 wt. % and an inverse relationship was found between dope concentration and fibre diameter, ultimate tensile strength (UTS) and modulus. The tensile strength and modulus of fibres spun using 1.2 wt.% being 2200 MPa and 71.76 MPa respectively (Arafat et al., 2015).

Other experimental work, involving spinning of different collagen concentrations dissolved into 0.01M of ethanoic acid, also exhibited this trend, with a mean dry fibre diameter of 77±10 μm and a UTS of 237±104 MPa being recorded for fibres spun from 3 mg/ml dopes, compared to 161±19 μm and 130±31 MPa for fibres spun at 7mg/ml (Zeugolis et al., 2009b).

2.2.4.2 Polypeptide molecular weight

Increasing the molecular weight normally increases viscosity because of increased polypeptide chain entanglement and reduced chain mobility. Changes in mechanical and enzymatic response can also be linked to an increase in chain length (Neffe et al., 2010; Tronci et al., 2015b). Practically, this has been illustrated by comparing the properties of fibres made from collagen-based materials having different molecular weights. Wet spun gelatin produced fibres with tensile strength in the range 25-250kPa whereas hydrolysed fish collagen (HFC) produced fibres with values between 10-20 kPa, following crosslinking. In this particular study, it was observed that the longest chain gelatin material produced fibres with the highest uniformity and tensile strength (Tronci et al., 2015b).

2.2.4.3 Dope temperature

An increase in temperature leads to an increase in the thermal kinetic energy within the polypeptide spinning dope, enhancing chain mobility and decreasing the viscosity (Khan et al., 2009; Al-Shammari et al., 2011; Briefer and Cohen, 1927). However due to the tendency of collagen to denature at

temperatures above 37ºC, modulating the temperature is not a suitable strategy for controlling viscosity during collagen fibre spinning.

2.2.4.4 Dope solvent

The choice of solvent is a potential means to tune overall dope viscosity depending upon the solubility of the polypeptide in the specific solvent system.

It is also important to reflect upon solvent type within the context of protein denaturation as this can easily occur when working with collagen particularly with regard to electrospinning. This leads to reduced wet stability and tensile strength, even after cross-linking. Care must therefore be taken in the dissolution of collagen to consider the polarity of the solvent, as highly polar solvents risk denaturation.

Another consideration when assessing risk of denaturation is the presence of bulky molecules which may disrupt the organisation of collagen triple helices. Lu *et al* discovered that mixing PEG

The use of low concentration acetic acid as a solvent is convenient and has been shown to enable up to 94% preservation of triple helixes (Arafat et al., 2015). Use of weak ethanoic and hydrochloric acid has also been shown to preserve triple helix structure (Zeugolis, Dimitrios I. et al., 2008; Zeugolis, D. I. et al., 2008b; Caves et al., 2010).

2.3.6 Solidification stage: the coagulant

The relative polarity and viscosity of the coagulation medium plays a large part in the diffusional exchange process. The coagulant is normally a non-solvent with a similar polarity to that of the dope solvent, and has a relatively high viscosity or concentration, resulting in a gradual downwards diffusion gradient. It must also be of a low enough polarity to be able to preserve the

hydrogen bonding within the collagen triple helices. Various coagulation solutions have been experimented with in relation to wet spinning of collagen-based materials, notably polyethylene glycol (PEG), NaCl, and ethanol (Zeugolis, D. I. et al., 2008b; Zeugolis et al., 2009a; Zeugolis et al., 2009b; Arafat et al., 2015).

Zeugolis *et al* experimented with various concentrations of NaCl in a 118mM PBS coagulation bath (Zeugolis et al., 2009b). Salt concentrations of 5%, 20%, and 40% wt were used. It was found that 20% NaCl was the optimal concentration producing fibres with the smallest dry diameter, highest stress and strain at break, and the highest modulus. They hypothesised that the reason for this was due to the ionic interactions with the NaCl electrolytes. Up to 20% wt salting-in occurs, wherein the increase in the ionic strength of the coagulant increased the solubility of the protein, allowing for the collagen to configure itself into a more structurally stable conformation. Salting out occurred at higher concentrations, as observed with the 40% concentration. Here the electrolytes caused a decrease in protein solubility preventing the stable arrangement of protein subunits from occurring (Luescher et al., 1974).

A similar experiment was performed using the polyethylene glycol (Mw 8000). Again, it was discovered that of 5%, 20%, and 40% wt PEG, in a PBS coagulation bath, the 20% PEG bath was the optimal condition for fibre formation, producing the smallest diameter and most thermally stable fibres. This again was thought to be due to the salting-in effect (Zeugolis et al., 2009a).

A smaller difference in polarity is also likely to decrease the rate of diffusion. Previously, wet-spun gelatin fibres have been produced using either dimethylsulfoxide (DMSO) or 2,2,2 trifluoroethanol as a dope solvent and ethanol or acetone as the coagulating non-solvent (Table 2.1) (Paul, 1968).

Gelatin fibres produced with DMSO (solvent polarity parameter, $E_T(30)$ =45.1 kcal mol^{-1}) as the solvent produced a less homogeneous fibre in terms of internal structure, with dissimilar outer sheath and inner core morphologies. This was thought to be due both to the low concentration of the gelatin/DMSO solutions, and also to relatively similar polarities between DMSO and acetone (polarity= 42.2 kcal mol^{-1}), where the most heterogenous fibres were observed. This allowed for instantaneous diffusional exchange to occur on the outer surface of the fibre (Tronci et al., 2015b).

There is evidence that manipulation of pH during coagulation can stimulate fibrillogenesis and self-assembly, a characteristic of triple helix markers seen in native collagen fibres (Zeugolis, Dimitrios I. et al., 2008; Zeugolis, D. I. et al., 2008b; Caves et al., 2010). Caves et al used an offline PBS incubation step in conjunction with fibre drawing to create fibres which exhibited D-periodicity (discussed in Section 2.1.1) during Second Harmonic Generation (SHG) Microscopy and Transmission Electron Microscopy. An initial acidic dope of 2, 5, or 7.5mg/ml dissolved in HCl was coextruded from a dual syringe pump with a PEG/PBS buffer of pH 8 into a rinsing bath of 70% vol ethanol. Fibres were collected automatically and dried, then incubated in PBS pH 7.4 at 37ºC for 48 hr before subsequent drying and GTA crosslinking. This stage allowed the collagen chains to self-assemble into the D-periodic assembly (Caves et al., 2010).

Post spinning treatments such as this are used extensively throughout collagen spinning to impact tensile strength, stability, and fibre organisation.

2.3.7 Post spinning treatment

2.3.7.1 Drawing

A common method of modifying the mechanical properties of fibres, particularly tensile strength, is by drawing the as-spun fibre. This involves progressive tensioning to encourage axial molecular alignment, and can also lead to increased crystallinity. The draw ratio (DR) quantifies the degree of drawing and thereby attenuation of the fibre, and is governed by the input and output velocities of the fibre within the spinning system. For example, if the dope is extruded at a rate of 0.1m/s and taken up at a rate of 0.2m/s, the associated DR would be 0.1:0.2 or 1:2.

Yaari *et al* (2016) incorporated a drawing step into their spinning process for human recombinant collagen. High concentration collagen dopes were extruded into a bath of PBS and salt and drawn within the bath (Yaari et al., 2016). The fibres were spun and characterised with reference to the draw ratio. Seeding and alignment of rat tenocytes *in vitro* along the fibres was observed. A glutaraldehyde crosslinker was used to enhance tensile strength and for the purposes of producing a biocompatible fibre for the cell seeding, experiments based on EDC/NHS crosslinking were also conducted.

It was found that up to a draw ratio of 1:8.1, the fibre tensile strength increased as the draw ratio increased. Drawing lead to elimination of the core/sheath morphology previously observed in wet spun collagen-based fibres, and enabled production of small mean fibre diameters. Beyond a threshold draw ratio of 1:8.1, microscopic imperfections and fractures began to form, weakening the fibre and reducing its UTS and Young’s modulus. Notably, relatively high tensile strength was obtained (150 MPa) following hydration of the fibre, which is important for real world medical device applications. However, this work relied upon glutaraldehyde crosslinking, which produces potentially cytotoxic side chains.

Polarised light microscopy was used to characterise the order and orientation of the collagen fibrils, and at a DR of 1:1, a high level of retardance was observed at the outer surface with low levels within the fibre core. Higher draw ratios produced an almost uniform level or retardance throughout the fibre, indicating that chain alignment was uniform throughout the fibre cross-section.

In an attempt to produce highly aligned biomaterials which could stimulate stem cell elongation Lu *et al* spun acetic acid dissolved collagen and extruded it into a 10% PEG 20k reinforced buffer at 37ºC (Lu et al., 2020). By increasing collection roller speed from 0-120rpm they were able to stimulate collagen fibril alignment and reduce the collagen fibre diameter down to 30µm. This increase in alignment was shown using SEM imaging and Small Angle X-ray Scattering (SAXS). Fibres were carbodiimide crosslinked and a range of characterization performed including collection of wet-strength data. Fibres were equilibrated in PBS and tensile tested.

Increasing the drawing speed produced fibres with a higher tensile modulus and strength. Fibres collected at a rate of 100r gave a mean tensile strength of 3.2 MPa and modulus of 9.32kPa. Those fibres collected at a rate of 60r had a strength of 2.1MPa and modulus of 6.84 kPa (manuscript denoted draw speeds as 60r and 100r, 100r being the faster rotation rate). Carbodiimide crosslinked fibres collected at a rate of 60r gave a significantly higher tensile strength of 25 MPa and modulus of 97 kPa.

Another interesting method of collagen fibre drawing has recently been demonstrated that relies upon microfluidics. Here, streams of coagulant (pH8) and collagen (pH3) were pumped into microchannels at right angles to each other. The movement of the coagulant liquid around the outside of the tube served to draw the collagen fibre whilst preventing it from sticking

to the inside. The rate of coagulant flow was increased from 30µl/hr to 800µl/hr, which increased the draw ratio and produced thinner fibres. Collagen spinning dope flow rate also affected the fibre diameter, with lower flow rates of 50µl/hr creating fibres of just 3-6 µm, the lowest reported diameter for wet-spun collagen fibres, with coagulant flow rates of 300µl/hr (Haynl et al., 2016).

One notable feature of these 3.7µm collagen fibres was the high tensile strength and thermal stability achieved without the use of crosslinking. A modulus of 4138±512 MPa, a tensile strength of 383±85 MPa and a denaturation temperature of 59^{o}C were reported. Whilst an impressive dry tensile strength was reported, there was no report of the wet-strength. The wet strength of collagen-based fibres is a critical indicator of the utility of the material for many medical device applications, because of the presence of body fluids such as whole blood, plasma, exudate or high relative humidity. The absence of crosslinking, and a lack of conformation or triple helix retention is typically associated with poor wet-stability *in vivo*.

2.3.7.2 Crosslinking of Polypeptide Chains

Crosslinking of collagen occurs via lysyl oxidase mediated reaction between hydroxylysine and lysine residues in the production of collagen *in* vivo (Section 2.1.2). This crosslinking serves to stabilise the material, increasing the tensile strength and enzymatic resistance under physiological conditions. For the purpose of implanted medical devices such as regenerative scaffolds or skin substitutes, crosslinking is important for tuning the rate of degradation, ensuring that the biological breakdown of the material is slow enough to fully support the site throughout the healing process. Care must also be taken to prevent encapsulation, which occurs when a foreign material does not break down within the body fast enough to avoid an immune reaction.

The influence of crosslinkers on the properties of collagen based materials depends upon the structure of the crosslink and the nature of the linkages. This section considers common modes of crosslinking in collagen-based materials, including novel methods designed to combat the limitations of traditional methods (Table 2.1).

1-ethyl-3-(3-dimethylaminopropyl) carbodiimide (EDC) is a zero length crosslinker, commonly used in conjunction with N-hydroxysuccinimide (NHS) to increase efficacy (Shepherd, D.V. et al., 2015; Kew et al., 2012). Instead of acting as a physical bridge, it encourages formation of short 1nm crosslinks between Glu/Asp carboxyl groups and the amine groups of Lys and Hyl amino acid residues (Ahn et al., 2013). This is done by acting as an intermediary between the two reactive sites. EDC reacts via an addition reaction to the hydroxyl group of the amino acid facilitated by the breaking of the C=N double bond. This forms the o-acylisourea intermediate. EDC is then substituted by the primary amine group of the second amino acid and is converted to a water soluble isourea byproduct. The byproduct is washed away leaving the crosslinked chains.

EDC is a popular crosslinker as it is a zero length linker, leaving no foreign, potentially cytotoxic residues like many other bridging moieties. However, one drawback is that the short bonds often do no reach between polypeptide chains and helices causing an increase in intramolecular bonding which stabilises locally within the molecule as opposed to the network of covalently bonded polypeptide chains, with longer more flexible bridges allowing for fibre slippage produced by longer crosslinks. (Zeugolis et al., 2009a; Sung et al., 2003).

As a result mechanical properties of the resulting materials are generally quite poor, as has been observed in gelatin fibres with EDC/NHS and 1,3-phenylenediaceticacid (Ph), a dicarboxylic acid, crosslinkers. Activated Ph crosslinked collagen fibres are reported to have superior tensile and swelling

properties when compared to intramolecular EDC crosslinked fibres (Tronci et al., 2013b). This was also confirmed when comparing the hydrated stress at break values for collagen fibres crosslinked with EDC/NHS (3.16±0.63 MPa) compared to those crosslinked with glutaraldehyde (10.85±2.85) and genipin (6.89±2.52) (Zeugolis et al., 2009a).

Bridging monomers

Collagen and collagen-based polypeptide processing has been performed with a host of different crosslinkers such as glutaraldehyde (GTA), 1,3-phenylenediaceticacid (Ph), polyethylene glycol (PEG), genipin (Yaari et al., 2016; Zeugolis et al., 2009a; Tronci et al., 2015b; Arafat et al., 2015; Tronci et al., 2013b; Meyer et al., 2010; Kew et al., 2012; Tonndorf et al., 2020). As an alternative to liquid reagents and chemical crosslinking, recent investigations also include grafting of photoactivated crosslinking molecules onto polypeptides, which following a purification step may activated using blue or UV light. This is a particularly novel approach to collagen-based material crosslinking that leads to good triple helix preservation (Tronci et al., 2013a; Tronci et al., 2015a; Tronci et al., 2016a; Shi et al., 2015).

Each crosslinking strategy aims to provide a physical bridge between residues. Here, the collagen amino acids are functionalised using a synthetic, often bifunctional crosslinking molecule (Zeugolis et al., 2009a). The molecule covalently binds to one strand of the collagen structure at one reactive site and to a different region of the collagen with the other. Zeugolis *et al*. performed a comprehensive review of the many bridging crosslinking materials relevant to collagen fibre formation for regenerative medicine (Zeugolis et al., 2009a). It was concluded that water content significantly affects the strength of the fibre and crosslinking strongly influences this sensitivity. Molecules with higher water affinity, i.e. those with polar water binding sites, naturally lead to an increase in water absorption, eliciting a reduction in strength. It has also been shown that different polarities can affect affinity towards other chemicals, which could aid in drug loading and slow release (Tronci G., 2014)

Table 2.3: Summary of collagen polypeptide crosslinking agents

Crosslinking monomer	Structure	Mode	Advantages	Disadvantages
EDC/NHS	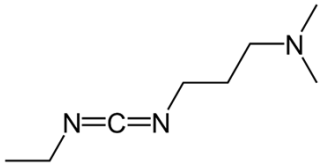	Facilitates formation of 1nm crosslinks	No foreign cytotoxic additives in structure Retains triple helix conformation	Short crosslinks cause low mechanical properties
GTA	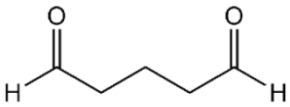	Bridging xl Post-spinning chemical treatment	High mechanical properties Highly efficient reaction Retains triple helix conformation	Cytotoxic residue within material Cytotoxic side chains
GMA	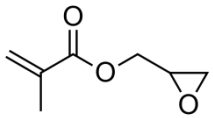	Bridging xl Pre-spinning functionalisation Post spinning UV activation	Long flexible Retains triple helix conformation Purification stage removes excess cytotoxic chemicals Potential for one stage spin and xl Good mechanical and swelling properties	Little literature with collagen polypeptides wet-spinning published
MA	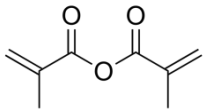	Bridging xl Pre-spinning functionalisation Post spinning UV activation	Retains triple helix conformation Purification stage removes excess cytotoxic chemicals Potential for one stage spin and xl Good mechanical and swelling properties Highly efficient functionalisation	Gel-MA fibres difficult to wet-spin with low controllability and complicated spinning process Low levels of literature with collagen polypeptides and wet-spinning performed
4VBC	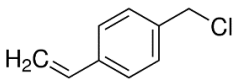	Bridging xl Pre-spinning functionalisation Post spinning UV activation	Retains some triple helix conformation Purification stage removes excess cytotoxic chemicals Potential for one stage spin and xl Good mechanical and swelling properties	Some triple helix formation lost Low levels of literature with collagen polypeptides and wet-spinning performed

Other factors affecting the mechanical behaviour of collagen-based material are the length and flexibility of the molecule. Tronci *et al* compared the properties of swollen collagen hydrogels crosslinked with Ma, GMA and 4VBC in different concentrations (Tronci et al., 2015a). A correlation between the rigidity of the crosslink molecule and the compressive modulus and swelling ratio of the collagen material was observed. The rigid, bulky, aromatic 4VBC crosslinked hydrogels had a higher compressive modulus and swelling ratio than the flexible, aliphatic GMA and short length MA. This was thought to be due to the sharing of the π electrons on the adjacent stacked benzene rings, stabilising the structure further.

This is potentially useful for tuning the properties of collagen materials towards different potential applications. It is understood that in regenerative medicine cells prefer substrates which mimic the mechanical properties of their native environment (O'Brien, 2011). In this instance the flexibility of GMA may suit regenerative scaffolds for neural tissue, which require softer more elastic substrates on which to grow. Conversely, 4VBC would suit bone scaffolds due to its high compressive strength and rigidity.

The level of crosslinking also affect the properties of the resulting collagen-based material. Increased crosslinking usually increases the toughness of a material, requiring more energy to break all of the covalent bonds. Crosslinks also serve to block water binding sites, preventing the material from swelling due to absorption (Tronci et al., 2015a). However, the reduction in water uptake and relative inflexibility caused by high crosslinking density can adversely affect the ability of cells to infiltrate into the material and reduce cell viability.

Interestingly, increasing the functionalisation of collagen with 4VBC has been found to reduce its triple helix organisation (from 79% triple helix

preservation at monomer/lysine molar ratio of 25 vs 98% at a ratio of 10). This is thought

to be due to the bulkiness of the molecule, and the consequent disruption of the internal structure of the collagen, preventing peptide chains from forming hydrogen bonds in close proximity.

Photoactive monomers

The functionalisation of collagen using photoactive monomers represents an interesting new development in the formation of defined collagen systems. Photoactive monomers such as 4-vinylbenzyl chloride (4VBC), and glycidyl methacrylate (GMA), and methacrylic anhydride (MA) contain functional moieties that form crosslinks on exposure to UV light (Tronci et al., 2013b; Tronci et al., 2015a).

In this reaction, light triggers the formation of free radicals from a photoinitiator (PI), at a specified wavelength. These free radicals attack the C=C double bond within the vinyl group causing it to break and reform with adjacent photoactive monomers resulting in a crosslink forming (Figure 2.7).

A large advantage of this family of crosslinkers is that they allow for functionalisation to occur before the spinning of fibres, ensuring the removal or any potentially cytotoxic residues. They also facilitate rapid crosslinking *in*

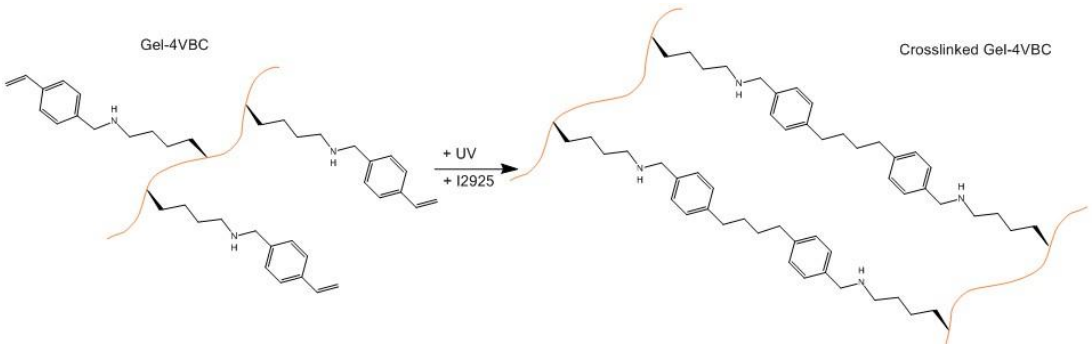

Figure 2.7: UV photoactivation of Gel-4VBC

situ, by exposure to a specific wavelength of light, without the need for immersion in liquid reagents. In traditional crosslinking approaches using liquid reagents such as GTA, a major concern has been cytotoxic residues left within the material, which subsequently leaches out, adversely affecting cell survival (Gorgieva, 2011).

There is a very limited body of published work reporting the processing of photoactive functionalised collagen materials in to wet spun fibres. Photo-crosslinking Gel-MA is frequently researched with respect to biomaterials development, but limited success has been reported in spinning the material into fibres (Lee et al., 2016; Yue et al., 2015; Zhao et al., 2016; Shi et al., 2015). Parameters such as time of UV exposure, stage of processing at which UV exposure occurs, and quantity of crosslinker required in relation to fibre properties are all important areas to investigate with respect to wet spinning production.

2.4 Application of Collagen Nonwovens in Medical Devices

Historically, collagen-based materials have been extensively utilised for the manufacture of a variety of medical devices, including sutures (catgut), wound dressings, dental barrier membranes, replacement heart valves, and meshes for vascular applications for which a high tensile strength, biocompatibility and ability to degrade are required (Zeugolis et al., 2009a; Chaparro et al., 2016; Everaerts et al., 2007). The use of collagen in medical devices is attractive, because of its presence in the tissues of the human body and its biocompatibility (Balasubramanian et al., 2013; DeFrates et al., 2018; Gorgieva, 2011).

In devices such as skin substitutes or guided bone regeneration membranes (GBR), a promising strategy is to introduce tissue-mimicking features at molecular, microscopic or functional level. Collagen is the main protein of the ECM and can communicate with cells via cell-binding peptides present along the protein amino acid sequences (Shoulders and Raines, 2009). Collagen-based medical devices can therefore promote migration, proliferation and differentiation of region-specific cells. Herein, the application and

manufacture of collagen-based textiles used in medical devices are reviewed because they are of primary relevance to the proceeding research.

2.4.1 Wound Healing

Collagen plays a vital role in wound healing and wound dressings are another application where collagen-materials are of clinical value. During wound healing, the protein works to attract fibroblasts and keratinocytes to the wound site, promoting debridement, re-epithelialisation, and angiogenesis (Zaman et al., 2011; Basu et al., 2017). Collagen wound dressings also stimulate the deposition of newly synthesised collagen and wound granulation (Schiefer et al., 2016). For this purpose collagen fibres require the ability to swell, to absorb the high levels of exudate being released by the wound as well as mechanical strength to stay intact once in place at the wound site and fully saturated by liquid (Cutting, 2003; Power et al., 2017).

Collagen is degraded by matrix metalloproteases (MMPs), an enzyme which is in excess at wound sites due to high levels of inflammation (Jabłońska-Trypuć et al., 2016; Kim, S. et al., 2016). MMPs are released by the body during inflammation to help with tissue remodelling. However, in the case of chronic wounds an excess of MMPs can lead to the breakdown of healthy tissue, and stalling of the wound healing process. Provision of an alternative source of collagen by incorporating it into the wound dressing itself, can act as a sacrificial target for the MMPs to work upon (Bohn et al., 2016; Tronci et al., 2016b), accelerating wound healing**.**

Skin substitutes are an intermediate product category between collagen wound dressings and tissue regenarative scaffolds. They are applied to wounds, for example diabetic ulcers or burns, and act as a replacement barrier for the skin. They encourage wound healing, as do collagen wound dressings, and are eventually incorporated into the skin tissue and

remodelled, as with TR scaffolds (Alrubaiy and Al-Rubaiy, 2009; Centanni et al., 2011).

The Integra ™ bilayer wound matrix (BWM) is an excellent example of a commercially available skin substitute (Hodde et al., 2001; Powell, Heather M. and Boyce, 2006).. Made up of a Type I bovine collagen and shark chondroitin 6- sulfate glycosaminoglycan (GAG) matrix reinforced by a silicon membrane, this dressing has been shown to promote healing over a three week period and improve healing outcomes (Papa et al., 2011; Loss et al., 2000; Gottlieb, 2004).

2.4.2 Tissue Engineering and Regenerative Medicine

The disciplines of tissue engineering (TE) and tissue regeneration (TR) frequently use scaffolds and membranes containing collagen-based material. A common function is to provide biomimetic ECM, mechanically supporting the tissue, promoting cell adhesion, tissue growth, leading eventually to remodelling and the breakdown and resorption of the scaffold. The two concepts differ when it comes to the source of progenitor cells which attach to the scaffolds and rebuild the tissue. TE involves seeding the patients stem cells onto the scaffold *in vitro*. Once seeded and after time for the cells to establish themselves the scaffold is implanted into the patient. TR by contrast implants the scaffold directly into the patient and relies upon the recruitment of cells *in vivo.* The scaffold then is eventually remodelled by the body and new native tissue is formed in its place.

The main requirements of a TE or TR scaffold are that it is able to support cell adhesion and viability, allowing the new tissue to grow and survive; it is not cytotoxic; it breaks down at the correct rate, thereby providing adequate mechanical stability throughout the remodelling process; and that it has the required mechanical properties in a wet environment to mimic the target tissue.

The majority of research into tissue engineering and regeneration focusses primarily upon electrospinning of scaffolds (He et al., 2014; Argento et al., 2012; Kalaithong et al., 2017; Enea et al., 2013; Kew et al., 2011; Venugopal et al., 2008; Powell, H. M. and Boyce, 2009; Timnak et al., 2011). As a result other paths of research into collagenous nonwoven techniques have been relatively unexplored. This presents a large opportunity due to the limitations of collagen electrospinning with respect to desired scaffold properties, namely that they are 2D, have a small pore size distribution, obstructing cells from infiltrating into the material, and are often denatured and have low wet strength (Kalaithong et al., 2017; Zeugolis, Dimitrios I. et al., 2008).

In recent years research on needle-punching of collagen fibres has been accumulating focussing on the manufacture of thick 3D nonwovens for the purpose of bone and cartilage regeneration (Sutherland, F.W.H. et al., 2005; Yim et al., 2007; He et al., 2014; Guan et al., 2015). Additional, less conventional techniques have also been developed, such as the reinforcement of crosslinked collagen/ chondroitin sponges using spun collagen fibres (Shepherd, J.H. et al., 2013). Innovation of collagen nonwoven formation presents interesting opportunities to tailor material properties to promote biocompatibility. The feasibility of further unconventional techniques for the formation of collagenous scaffolds will be investigated in Chapter 5. Investigation of textiles techniques outside of the nonwovens field will also be completed in Chapter 5. The background of which also warrants discussion here.

2.4.3 Braided and Knitted textiles

Outside of nonwoven formation other collagenous textiles materials have also been developed, most pronounced of which are knitting and braiding of fibres (Zheng et al., 2017; Tonndorf et al., 2020). These techniques are extremely suited to modulating the macroscopic material mechanical properties, enabling a tighter control on the movement of fibres over one another. In knitting extensibility can be endowed into a material by the intermeshed loop structure. Knitting of collagen fibres has so far yielded some success (Tonndorf et al., 2020), though cytotoxic GTA crosslinking

was required to give the wetspun fibres enough strength to be compatible with knitting machinery.

The braiding and twisting of fibre bundles has also been shown to increase the tensile strength and extension at break of materials, of great use when biomimicking load bearing tissues such as ligaments and tendons (Freeman et al., 2007; Walters et al., 2012). As with knitting, the strength of the fibres must be sufficient to withstand the forces applied during manufacture.

2.5 Summary

Collagen and gelatin are valuable raw materials, but there are challenges in processing them in to formats other than those directly provided by nature for applications in medical devices. The manufacture of high quality collagen-based fibres that are not blended with other polymers or contaminated with toxic residues is a pre-requisite for developing improved devices suitable for wound care and tissue regeneration. Wet spinning is a highly scalable process that is capable of producing high quality collagen-based fibres, but improving the wet stability and wet-mechanical properties of as-spun collagen-based materials without recourse to chemical crosslinking using liquid reagents remains a challenge. Accordingly, the experimental work that follows focuses on developing an alternative route to preparing collagen-based fibre materials, including the feasibility of wet spinning and subsequent UV-crosslinking of photoactive collagen-based fibres, together with an evaluation of the properties of the materials.

Chapter 3

Preparation and Characterisation of Functionalised Gelatin Fibres

This Chapter includes material from the paper: "*Rotation-assisted wet-spinning of UV-cured gelatin fibres and nonwovens*" published in the Journal of Materials Science, July 2019, Volume 54, Issue 14, pp 10529–10547. With co-authors Giuseppe Tronci, He Liang, and Stephen Russell

3.1 Introduction

Given it is derived from the partial denaturation of collagen, gelatin has significant potential as a building block for economic manufacture of medical devices, due to its biocompatibility, wide availability and low cost. As well as regenerative devices, the clinical uses of gelatin encompasses wound dressings, drug delivery, vascular prostheses, orthopaedic membranes and skin substitutes (Ginalska et al., 2005; Choi et al., 1999; Chandra, 2017; Abbasi and Wu, 1996; Tigani et al., 2008; Kiernan et al., 2010; Arellano-Olivares et al., 2016; Huang, Z.L. and Jiang, 2006; Kanokpanont et al., 2012; Farzamfar et al., 2018; Lekakou et al., 2008; Tampieri et al., 2003).

Gelatin is a polypeptide formed by the denaturation of collagen, often thermally or chemically, wherein the hydrogen bonds stabilising the triple helices are disrupted. This process leads to triple helix disentanglement into separate randomly organised polypeptide chains. Gelatin therefore has the same primary amino acidic structure as collagen, which makes gelatin biodegradable and compatible with the physiological environment due to the presence of collagenase-cleavable and cell-binding peptide sequences, respectively (Vandooren et al., 2013; Liu, Y.X. and Chan-Park, 2010).

Spinning of gelatin fibres for use in medical devices has been reported via dry spinning, gel spinning, electrospinning and wet spinning (Fukae and Midorikawa, 2008; Fukae et al., 2005; Delyth et al., 2009; Stoessel et al.,

2015b; Shi et al., 2015; Tronci et al., 2015b; Yang et al., 2009; Farzamfar et al., 2018), yielding varied fibre properties. Electrospinning or wet spinning are typically used to produce gelatin fibres (Stoessel et al., 2015b; Delyth et al., 2009; Hlavata et al., 2017; Tronci et al., 2015b). Electrospinning is a one-step process employing electrostatic voltage to achieve a mesh of submicron fibres. In light of the submicron fibre diameter, electrospun fibres are advantageous for mimicking fibres found in native tissue more closely and for realising 2D fabrics (overall thickness < 1 mm) with high total surface area. Wet-spinning is voltage-free and yields individual, dimensionally-controllable fibres that can be subsequently converted in to a wider range of textile formats, including nonwovens as well as knitted, woven, braided and hybrid structures.

Compared to electrospinning, wet-spun fibres assembled into nonwovens allow for increased customisation of liquid absorbency, porosity, mechanical properties, cell homing capability, and macroscopic shape (Kalaithong et al., 2017; Zeugolis, Dimitrios I. et al., 2008; Ghasemi-Mobarakeh et al., 2008; Khorshidi et al., 2016). Other major advantages of wet spinning are the ability to more readily control and predict molecular alignment and the fibre diameter distribution using fibre drawing, dope concentration alteration and spinneret size compared to electrospinning (Stepanyan et al., 2014; Zeugolis et al., 2009b; Cong et al., 2012). Consequently, wet spinning provides a more consistent, yet highly versatile route to industrial manufacture of fibre-based medical devices compared to a platform based on electrospinning.

The functionality of gelatin fibres in medical devices is impeded by gelatin's uncontrollable swelling at room temperature in aqueous environments, thermo-reversible dissolution at increased temperature and poor thermo-mechanical properties in physiological conditions. Taking inspiration from nature, covalent functionalisation and crosslinking of gelatin chains have been pursued to restore covalent crosslinks present in collagen fibres *in vivo* and ensure retention of fibrous architecture following material contact with water. Various approaches have therefore been reported in the literature based on either bifunctional reagents, e.g. diisocyanates, (Arafat et al., 2015)

and aldehydes (Bigi et al., 2001), or carbodiimide-induced intramolecular crosslinking (Stoessel et al., 2015a; Stoessel et al., 2015b).

Recent work on collagen-derived polypeptides has focused on the synthesis of covalently crosslinked networks as building blocks of water-insoluble wet-spun gelatin fibres, whose wet-state tensile properties were found to be directly related to the molecular weight of the fibre-forming polypeptide (Tronci et al., 2015b).

Photoinduced covalent networks have also been synthesised with either gelatin random coils or collagen triple helices (Shi et al., 2015; Tronci et al., 2013a). Once grafted onto the amino acid residues of the polypeptide, covalently-coupled photoactive moieties can induce the formation of covalent crosslinks when exposed to a photoinitiator and a specific wavelength of light. This photoinduced network formation approach enables *in situ* crosslinking to occur at a much faster rate than typical chemical crosslinking reactions (Tronci et al., 2015a; Shi et al., 2015; Yue et al., 2015; Zhao et al., 2016), combined with cellular tolerability. It also introduces additional precipitation steps to ensure that any cytotoxic, unreacted crosslinker has been removed from the material before processing. One of the most prevalent photoactive compounds is methacrylic anhydride (MA), which has been widely employed to obtain gelatin networks with varied macroscopic material formats (Shi et al., 2015; Yue et al., 2015; Akbari et al., 2014; Wang, Y. et al., 2019).

Despite extensive research on MA-functionalised gelatin (Gel-MA) hydrogels, relatively few investigations have been reported on the formation of Gel-MA hydrogel fibres, in part due to the poor mechanical properties and fibre-forming capability of the photoactive fibre precursor (Yue et al., 2015). Shi *et al.* (Shi et al., 2015) reported the formation of grooved Gel-MA fibres by microfluidic spinning of the polymer dope into an ethanol bath at -21°C, wherein the surface grooves were reported to encourage cell alignment. Control of phase separation and fibre formation was achieved by spinning mixtures of Gel-MA and alginate into $CaCl_2$, whereby the coagulation bath

was selected to induce crosslinking of the alginate chains enclosing the Gel-MA. The Gel-MA was subsequently crosslinked using UV irradiation (Tamayol et al., 2015). The sacrificial alginate component was removed using a calcium chelator leaving a hybrid hydrogel filament that could be subsequently assembled into woven and braided structures. Given the multiple steps required, a simpler route for delivering gelatin fibres is ideally required to accelerate scale-up.

Additionally, although photocured Gel-MA fibres proved to support cells, the mechanical stability of the material in clinically-relevant medical devices has been shown to be sub-optimal. Comparing the mechanical characteristics of collagen hydrogels crosslinked with different photoactive moieties, Tronci *et al.* found that UV-cured hydrogels made of MA-functionalised collagen to exhibit both lower water uptake and compressive modulus than UV-cured hydrogels made of 4-vinylbenzyl chloride (4VBC)-functionalised collagen (Tronci et al., 2015a). Rather than hydrogels, it was therefore of interest to determine if vinylbenzylation is capable of yielding mechanically-competent, wet spun gelatin fibres (Tronci et al., 2010), yet ensuring full cellular tolerability.

Accordingly, the present study focuses on the manufacture and physical properties of photoactive and UV-cured Gel-MA and Gel-4VBC wet spun fibres and compares their *in-vitro* biocompatibility. To mediate fibre-forming capability and minimise toxicity issues, wet-spinning of collagen-based polypeptides into polyethylene glycol (PEG)-supplemented aqueous solutions has been shown to enhance the thermal and mechanical properties of the fibres as well as cell infiltration and tissue in growth (Deible et al., 1999; Vasudev and Chandy, 1997; Zeugolis, D. I. et al., 2008b). PEG can be used as plasticiser and is widely accepted as an inert and safe polymer, with various PEG-conjugated drugs having been approved by the FDA (Alconcel et al., 2011). Therefore, an evaluation of wet-spun Gel-4VBC fibre properties was made using both PEG and aqueous coagulation media.

3.2 Experimental

3.2.1 Materials

Polysorbate 20, diethyl ether, HCl, and ethanol were purchased from VWR Prolabo Chemicals. Acetone was purchased from Fischer Chemicals. Acetic acid was purchased from Fluka Analytical. Dulbecco's PBS was purchased from Lonza Chemicals. High molecular weight gelatin type A (Bloom strength ~ 270), 4VBC, MA, Triethylamine (TEA), poly(ε-caprolactone) (PCL) (M_n: 80000 g·mol^{-1}), PEG (M_n: 8000 g·mol^{-1}), PBS (0.1 M, pH 7.4), 2-Hydroxy-4-(2-hydroxyethoxy)-2-methylpropiophenone (I2959), and all other reagents were purchased from Sigma Aldrich. LIVE/DEAD staining kits and cell culture plates were purchased from Thermofisher. Murine L929 fibroblasts were purchased from Sigma Aldrich.

3.2.2 Synthesis of Gel-4VBC and Gel-MA

Gelatin was dissolved in distilled water at 10% (w/v) at 37°C and neutralised to pH 7.4. Either 25× or 10× molar ratio (with respect to the lysine molar content in gelatin) of TEA and either 4VBC or MA ([monomer]=[TEA]) was added with 1 wt.% of polysorbate 20. Lysine molar content was quantified by 2,4,6-trinitrobenzenesulfonic acid (TNBS) assay and proved to be equal to 3.05×10^{-4} moles·g^{-1} of gelatin. The reaction of gelatin with either 4VBC or MA was carried out at 40 °C for 5 hours, then the reacting mixture was precipitated in a 10× volumetric ratio of pure ethanol and incubated for 24 hours to remove unreacted chemicals.

3.2.3 TNBS assay

The degree of gelatin functionalisation was quantified using the TNBS colorimetric assay as described by Bubnis *et al* (Bubnis and Ofner, 1992). Briefly, 1 ml 4 vol.% $NaHCO_3$ and 1 ml 0.5 vol.% TNBS was added to 11 mg of gelatin sample and shaken at 200 r·min^{-1} at 40 °C for 4 h. 3 ml of 6N HCl solution was added to each sample and 1-hour incubation at 70°C was performed. 5 ml distilled water was added and 20 ml diethyl ether (x3) was used to remove any unreacted TNBS. 5 ml of diethyl ether-extracted solution was collected and diluted with 15 ml H_2O. Resulting solution was analysed

via UV-Vis spectrophotometry (6315 UV/Visible Spectrophotometer, Jenway, UK) and the absorbance value recorded at 346 nm against a blank sample [39]. These absorbance values were used in conjunction with Equation 3.1 and 3.2 to determine the molar content of remaining lysines (per gram of gelatin) and the degree of gelatin functionalisation, respectively:

$$\frac{Moles\ (Lys)}{g\ (gelatin)} = \frac{2 \times Abs \times 0.02}{1.46 \times 10^4 \times p \times m}$$

Equation 3.1

$$\boldsymbol{F = \left(1 - \frac{Gel_F}{Gel_N}\right) \times 100}$$

Equation 3.2

In Equation 3.1, 1.46×10^4 is the molar absorptivity (in $M^{-1}cm^{-1}$) of trinitrophenly lysine, *p* is the spectrophotometer cell path length (1 cm), m is the sample weight (0.011 g), 0.02 is the total volume (in litres) of the diluted diethyl ether-extracted solution. In Equation 3.2, Gel_N and Gel_F are the molar lysine content in either native or functionalised gelatin, respectively. Three replicates were performed for each sample.

3.2.4 Viscometry

Wet spinning dopes were heated to 50 ºC to maintain the gelatin as a liquid and measured with a modular compact rotational rheometer (MCR 302, Anton Paar, Austria). Measurements were taken at 50 ºC using a 25 mm parallel plate with a 0.3 mm distance between it and the sample plate. An initial 60 s of rotation at a shear rate of 0.1 s^{-1} was performed to stabilise the sample, following which dope viscosity was recorded at shear rates of 0.1-1000 s^{-1} over 5 min.

3.2.5 Wet spinning

Preliminary wet spinning experiments were carried out manually with a syringe and blunt needle with a 0.8 mm internal diameter. 17.4 mM aqueous solution of acetic acid was used to prepare the wet spinning gelatin (native, Gel-MA, and Gel-4VBC) dopes (15 wt.% gelatin), due to the increased solubility of gelatin at acidic pH, aiming to minimising wet spinning-associated risks of needle blockage (Larson and Greenberg, 1933).

The native gelatin and Gel-4VBC wet spinning dopes (held at 50°C using a 10ml syringe heater, Warner, USA) were extruded into a coagulation bath consisting of 0.1 M PBS supplemented with 20% (w/v) PEG at 20ºC (room temperature). Following confirmation of the spinnability of functionalised gelatin systems, fibres were extruded using a syringe pump in contact with a rotating coagulant bath at a pump rate of 30 $ml \cdot hr^{-1}$. Spinning parameters for each sample can be seen in Table 3.1.

Gel-MA fibre controls could be wet spun using a wet spinning dope of 30% wt methacrylated gelatin in 17.4 mM acetic acid. A fibre coagulant consisting of 20% wt NaCl (20 ºC) in distilled water was initially used, in line with previous reports (Zeugolis, D. I. et al., 2008b; Zeugolis et al., 2009b; Cavallaro et al., 1994). Owing to the rapid solidification and poor fibre formation in the salt-supplemented bath, ethanol was employed as a suitable coagulation bath for wet spinning of Gel-MA.

Table 3.1: Experimental conditions investigated for the formation of wet spun gelatin fibres.

Sample ID	Wet spinning dope (% w/v)	Coagulating bath
Type A gelatin	15	PEG 20% (w/v), 0.1 M PBS
Gel-4VBC	15	NaCl 20% (w/v)
		PEG 20% (w/v), 0.1 M PBS
Gel-MA	30	EtOH

To enhance wet spinning compliance, ethanol was stored at -20 ºC prior to, and placed on an ice bath during, wet spinning (Shi et al., 2015). To reduce the potential for end-breaks during spinning, instead of conventional linear take-off, the dopes were extruded into a rotating coagulation bath (rotational circumference = 30 cm) with the needle placed eccentrically in the bath. The rotation speed was selected at 1.6 rpm, whilst the needle tip was 1 cm away from the bath bottom surface. The fibres were incubated in the coagulating bath for 1 hour at 5 ˚C to enhance phase separation of gelatin and promote fibre formation. Subsequently, fibres were transferred to distilled water for 1 hour to remove excess coagulant and solvent and then air dried.

3.2.6 Feasibility of scaled up wet-spinning

The feasibility of larger scale f-gelatin spinning was explored to produce longer fibres using a stable production platform. Here a 10% wt dope of native gelatin dissolved in 17.4mM of acetic acid was extruded at 50ºC into a 4L bath of 20ºC 20% wt PEG/ 0.1M PBS solution. A larger pump capable of holding up to 100ml of dope was utilized (Dienes Apparatebau GmbH, Germany). The dope was extruded through a 100x 100µm hole spinneret.

A lower concentration was used in this incidence to reduce the dope viscosity to prevent blockages of the machine tubing. The fibres were spun at a rate of 1ml min^{-1}, collected at a rate of 200 mm min^{-1}, washed in distilled water for 30 min, and air dried for 30 min.

3.2.7 UV-curing of wet spun fibres

After air drying for 30 min wet spun staple fibres were incubated in a 90 vol.% ethanol solution in distilled water supplemented with 1% (w/v) Irgacure 2925 for 30 min during UV exposure (λ: 365 nm, 8 $mW \cdot cm^{-2}$) with a sample-UV lamp distance of approximately 10 cm. Irradiation intensities were measured with an IL1400A radiometer equipped with a broadband silicon detector (model SEL033), a 10× attenuation neutral density filter (model QNDS1), and a quartz diffuser (model W) (International Light Technologies, USA).

Fibres were then incubated in pure ethanol for 1 hour and air dried on a polyethylene surface.

3.2.8 Manufacture of nonwoven fabrics

Samples intended for fibroblast attachment were directly spunlaid into the form of a nonwoven fabric by manually agitating the coagulation bath using a 20 mm wide implement placed eccentrically in the bath during rotation-assisted wet spinning. In this way, the fibre-forming wet spinning dope was displaced to enable merging of resulting fibres and nonwoven structure via hydrogen bonding formed at fibre junctions within the liquid. PCL scaffolds were wet-spun for use as a positive control during cytotoxicity screening using a 15 wt.% PCL dope dissolved in acetone at 40 ºC and spun into ethanol, following a previous report (Puppi et al., 2011).

3.2.9 Attenuated Total Resistance Fourier Transform Infrared (ATR-FTIR)

ATR-FTIR was performed to detect the presence of any PEG residue in wet spun fibres. Spectra were recorded on a Spectrum BX (Perkin-Elmer, USA) with a diamond ATR attachment at a resolution of 4.0 cm^{-1}, scanning intervals at 2.0 cm^{-1}. Scans were recorded from 600 to 4000 cm^{-1} and 64 repetitions were averaged for each spectrum. A blank sample was measured to remove unwanted noise from atmospheric organic compounds.

3.2.10 Scanning Electron Microscopy

A SU8230 FESEM (Hitachi, Japan) was used to study longitudinal and cross-sectional fibre morphology. Samples were gold-coated with at a beam intensity of 10 kV in vacuum using a JFC-1200 fine sputter coater and imaged at ×20-1500 magnification (working distance 38-14 mm). ImageJ software was used to analyse images and quantify fibre diameter distribution.

3.2.11 Mechanical testing

Samples were conditioned at 20 °C 65% r.h. for 24 h. Fibres were mechanically tested using a Titan Universal Strength Tester (James Heal, UK) with a 10 mm gauge length and 10 mm·min^{-1} extension rate following BS EN ISO 5079:1996 standards (n=10). Rubber pads were placed over the clamps to prevent breakage at the jaws. Any jaw breakages were discounted from results. Optical microscopy at ×4 magnification was used in conjunction with ImageJ analysis software to approximate the cross-sectional diameter of fibres to enable fibre stress calculations assuming a circular fibre shape.

3.2.12 Differential Scanning Calorimetry

Thermal characterisation was performed using differential scanning calorimetry (DSC, Q20 V24.11 Build 124, TA Instruments, USA). Dry samples (11 mg) were hermetically sealed in aluminium pans and thermograms recorded with a nitrogen purge gas flow with a ramp of 0-200 °C and incremental rate of 10 °C·min^{-1}. OriginPro was used to plot DSC thermograms, whereby the denaturation temperature and enthalpy were quantified as the endothermic peak and integration of corresponding thermal transition area, respectively.

3.2.13 Fibre and nonwoven scaffold swelling

Swelling of individual fibres was measured by imaging 10 mm length of fibres using optical microscopy before and after 24 h incubation in PBS at 37ºC (n=4). Image analysis was used to calculate fibre diameters at a minimum of ten points along the fibre length. These diameters were used to calculate the fibre cross-sectional area based on a cylindrical shape (A= π·r^2), so that dry- (X_d) and swollen- (X_s) state cross-sectional areas were obtained. The fibre swelling index (*SI*) was calculated as percent change in cross-sectional area following sample equilibration with water (Equation 3.3):

$$SI = 100 \times \frac{X_s - X_d}{X_d}$$

Equation 3.3

Other than fibre swelling, weight-based water uptake (*WU*) of nonwoven fabrics was quantified according to Equation 3.4:

$$WU = 100 \times \frac{m_s - m_d}{m_d}$$

Equation 3.4

whereby m_d and m_s are the sample weights before and after 24 h incubation in PBS at 37ºC (n=6), as described previously (Holmes et al., 2017).

3.2.14 Cytotoxicity testing

Samples of 100 mg of dry nonwoven fabric were individually placed in non-tissue culture treated 24-well plates and incubated overnight in a 70 vol.% ethanol solution in water. Retrieved samples were washed in sterile PBS three times under UV light, prior to cell seeding. L929 murine fibroblasts were grown in a Dulbecco's Modified Eagles Medium (DMEM) of 10 vol. % FBS and 1% (w/v) Penicillin Streptomycin and 1% (w/v) Glutamine. Cells were seeded (cell density: 8×10^4 cells in 100 µl cell culture medium) on each nonwoven scaffold and incubated for 8 h to allow the cells to adhere to the scaffold.

Cell-seeded nonwoven scaffolds were transferred to a newly sterilised 24-well plate and incubated for 7 days at 37˚C. After incubation, the nonwoven scaffolds were washed with sterilised PBS (×3) before cell staining with Calcein AM and ethidium homodimer 1 (ThermoFisher Scientific, UK), according to manufacture instructions. The samples were then incubated for 40 min in the dark and imaged by fluorescence microscopy (DMI6000 B, Leica Microsystems, Germany). The cell viability/proliferation assay was assessed using an alamarBlue metabolic assay at days 1, 4, and 7. The alamarBlue working solution was measured at an excitation wavelength of 560nm and emission wavelength of 590nm using a fluorescence plate reader (Varioscan, ThermoScientific, USA).

3.2.15 Statistical analysis

OriginPro software was used for Normality tests, means comparisons using Tukey testing, and One-Way ANOVA providing normal distribution was observed. Data are presented as average ± standard deviation.

3.3 Results and Discussion

In the following, the design of photoactive and UV-cured gelatin fibres is presented and characterised from the molecular up to the macroscopic scale. The degree of gelatin functionalisation, the morphology, swelling and mechanical properties of wet spun fibres, as well as the manufacture and cellular tolerability of UV-cured gelatin nonwovens is reported. Following synthesis of the photoactive gelatin building blocks, wet spun fibres and nonwovens were prepared using different coagulation conditions. The reacted wet spun gelatin product was collected and air dried prior to UV curing, as illustrated in Figure 3.1.

Functionalised gelatin samples are coded as “XXXXYY”, whereby “XXXX” identifies the monomer, either MA or 4VBC. “YY” indicates the monomer/lysine molar ratio used during the functionalisation reaction (either 10 or 25). Sample nomenclature for the wet spun and UV cured fibre samples is as follows: ‘4VBC-PEG’ indicates fibres whereby 4VBC-functionalised gelatin was dissolved in 17.4 mM acetic acid (15 wt.% gelatin) and wet spun into 0.1 M PBS supplemented with 20% w/v PEG. ‘4VBC-NaCl’ indicates fibres prepared by dissolving 4VBC-functionalised gelatin (15 wt. %) in 17.4 mM acetic acid followed by wet spinning into an aqueous solution containing 20% w/v NaCl. ‘MA-EtOH’ identifies fibres prepared with 30 wt. % dope of MA-functionalised gelatin in acetic acid and wet spun into ethanol at -20ºC; ‘Native-PEG’ is the fibre control made of 15 wt. % native gelatin in 17.4mmol acetic acid and wet spun into PEG-supplemented PBS bath; ‘Native-NaCl’ is the fibre control prepared by wet spinning the native gelatin dope into the aqueous solution containing 20 % w/v NaCl.

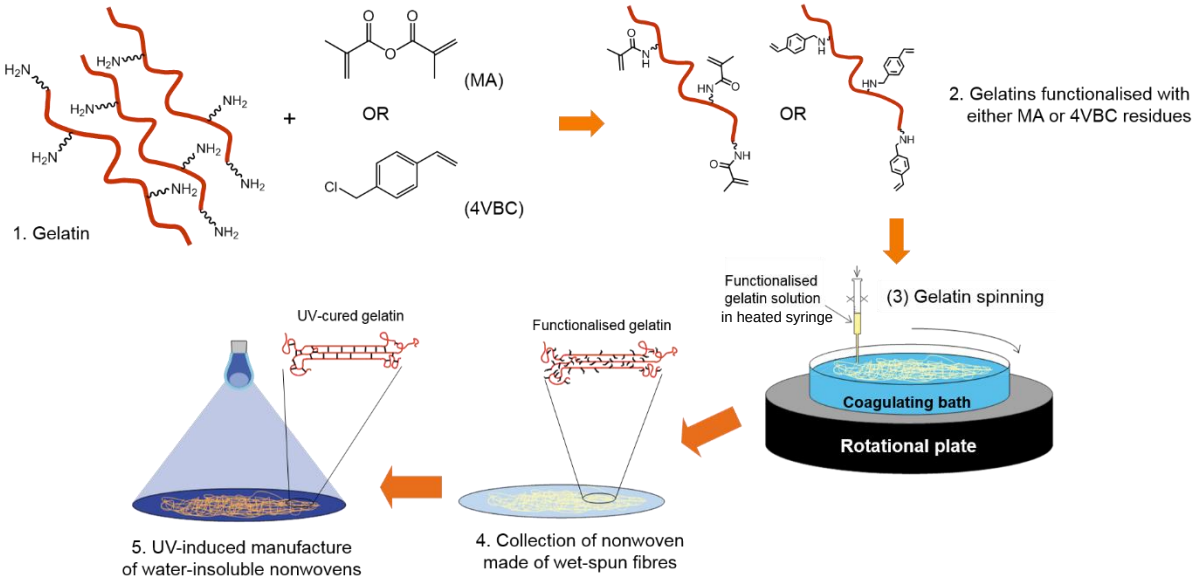

Figure 3.1: Rotation-assisted wet spinning of UV-cured gelatin fibres and nonwovens. Gelatin is reacted with either MA or 4VBC (1) to achieve a photoactive fibre-forming building block (2). The functionalised gelatin product is dissolved in aqueous environment, heated to 50 ºC, and wet spun into a rotating coagulating bath (3). Either the individual fibres or nonwovens are withdrawn from the bath and incubated in a photoinitiator-supplemented ethanol dope (4). UV curing leads to water-insoluble fibres and nonwovens made of a covalently-crosslinked gelatin network (5).

3.3.1 Synthesis of functionalised gelatin

TNBS colorimetric assay was employed in reacted gelatin products to indirectly assess the derivatisation of lysine amino groups of gelatin with either 4-vinylbenzyl or methacrylamide adducts. Reaction products indicated that both 4VBC- and MA-mediated functionalisation were achieved, with degree of functionalisation (*F*) equalling to 66±4 and 97±2 mol.%, respectively (Table 3.2). The consumption of amino groups measured by TNBS was found to increase when gelatin was reacted with MA rather than 4VBC, despite the same monomer/Lys ratio being used during the reaction.

In an effort to achieve building blocks with equivalent molar content of 4-vinylbenzyl and methacrylamide adducts, both MA/Lys molar ratio (25→10 mol.%) and reaction time (5→3 hours) were reduced during the functionalisation reaction, although insignificant variations (p=0.99) in values of *F* were observed with reacted products (F_{MA}= 99±0 mol.%). These results are in line with previous reports (Hoch et al., 2012; Tronci et al., 2015a) and reflect the higher reactivity of MA towards lysine-induced nucleophilic substitution compared to 4VBC.

Table 3.2: Degree of functionalisation (F) determined via TNBS assay on gelatin products reacted with either 4VBC or MA at varied monomer/Lys molar ratio. (a-c): p <0.05.

Sample ID	*F* /mol.%
MA10	97±2 [(a)]
MA25	99±0 [(b)]
4VBC10	47±4 [(b) (c)]
4VBC25	66±4 [(a) (c)]

Interestingly, the *F* values observed with MA- and 4VBC-reacted gelatin were higher than those previously reported with 4VBC-reacted type I rat tail collagen, when the same reaction conditions were applied (Tronci et al., 2015a). Despite collagen and gelatin sharing the same primary protein structure, the reversible helix-to-coil thermal transition of gelatin allows for increased chemical accessibility in the selected reaction conditions, with regards to the steric hindrance effects expected when the same reaction is carried out with collagen triple helices (Okamoto and Saeki, 2013).

In comparison to commercially-available Gel-MA products (F_{MA}= 40-80%), the values of F_{MA} measured on in-house-reacted gelatin products proved to be increased. This finding is potentially due to an increased molar content of either MA or TEA, or to an increased reaction time being used for the synthesis in-house of Gel-MA product, as reported previously (Liang et al., 2018). This suggests that the developed reaction conditions used herein may

enable increased tunability of macroscopic properties and fibre-forming capability in resulting products. In light of the presented results, samples MA10 and 4VBC25 were selected for the preparation of wet-spinning dopes and respective fibres, as reported in the following sections.

3.3.2 Characterisation of wet-spinning dopes

The viscosity of the wet spinning dopes was measured to assess the levels of shear force being exerted upon the spinning dopes during extrusion, aiming to draw relationships between solution characteristics and fibre dimensions and morphology. From Figure 3.2, it is apparent that all gelatin dopes behave as a non-Newtonian fluid, whereby an increase in shear rate is corelated with a decrease in shear viscosity (η), in line with previous studies (Hoch et al., 2012; Lee et al., 2016). When the shear rate is increased, gelatin chains disentangle since molecular interactions are attenuated, and the corresponding dope viscosity is reduced. As expected, an increase in Gel-MA concentration resulted in an increase in viscosity, due

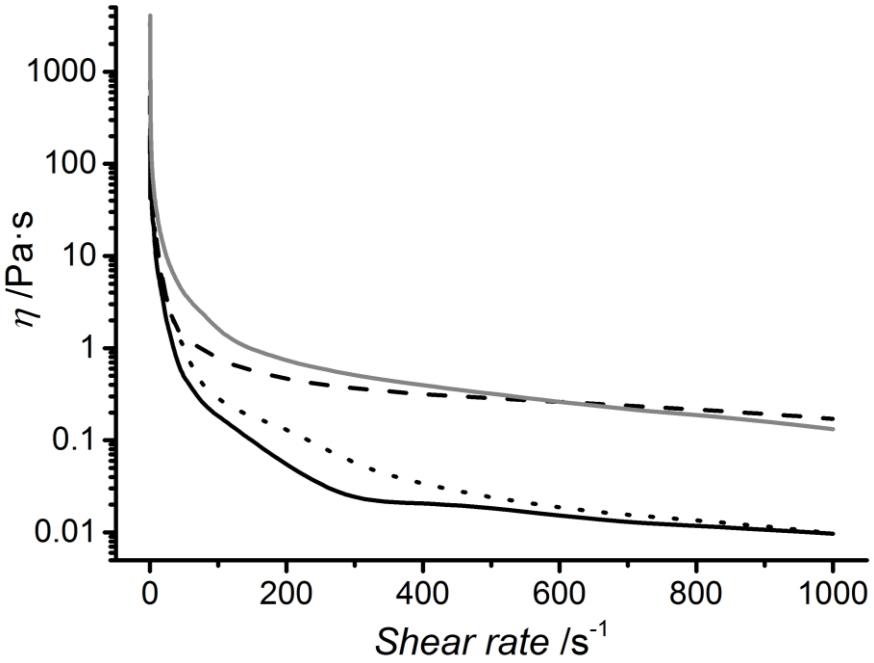

to the increased chain entanglements and intermolecular interactions (Hoch et al., 2012; Lee et al., 2016).

Figure 3.2. Viscosity curves of wet spinning dopes prepared in 17.4 mM acetic acid solution with varying gelatin building blocks. (—):

Native gelatin (15 wt. %). (⋯): Gel-4VBC (15 wt. %). (– – –): Gel-MA (15 wt. %). (—): Gel-MA (30 wt. %).

With respect to the native polypeptide, functionalisation of gelatin was found to lead to an increased viscosity when dopes with the same gelatin concentration were measured. This observation is likely due to an increase in lysine side chain length in functionalised gelatin, causing more entanglement and interaction between polypeptide chains. Similar trends were also observed when considering dopes of Gel-4VBC, in light of the presence of 4VBC aromatic rings and pi-pi interactions between lysine residues (Tronci et al., 2015a) (Tronci et al., 2016a).

Other than Gel-Native, the wet spinning dopes of Gel-MA were considerably more viscous than the ones containing Gel-4VBC, when the same concentration of polypeptide was considered. This is likely to reflect the increased level of functionalisation in Gel-MA with respect to Gel-4VBC.

Although the original intention was to compare wet spun fibre produced with wet spinning dopes of similar polymer concentrations, it was not possible to continuously wet spin fibres from dopes of Gel-MA with 15 wt.% concentration (as in the case of dopes of Gel-4VBC) due to dispersion of the wet spinning dope in the coagulating bath. Therefore a dope of 30 wt.% Gel-MA was selected, in agreement with previous literature (Shi et al., 2015).

Such an increase in polypeptide concentration, dope viscosity and internal shear stress during wet spinning was likely to result in reduced alignment of the polypeptide chains in respective wet spun fibres (Wang, Y. et al., 2019). These considerations were experimentally supported by the fact that needle blockages as well as difficulties in achieving continuous fibre formation were encountered during wet spinning of dopes with increased polypeptide concentration.

Subsequent literature has addressed the viscosity of Gel-MA solutions by co-extruding the polypeptide with native gelatin (Wang, Y. et al., 2019).

Wang *et al* produced hollow porous fibres by mixing 8 wt. % Gel-MA and 8 wt. % gelatin solutions together and spinning with a PVA core. This modulated the dope viscosity allowing for the solution to be readily spun. The tubular fibres were then heated to above the gelation point, removing the uncrosslinked native gelatin.

3.3.3 Chemical characterisation of wet spun gelatin fibres

Dried wet spun fibres were analysed via ATR-FTIR spectroscopy to detect the presence of any chemical residues, e.g. PEG. Figure 3.3A compares the spectra of fibres spun into PEG-supplemented PBS solution with the ones of gelatin and PEG raw materials. The gelatin spectra show a major peak at 3600-2700 cm^{-1} (Amide A) as well as peaks at roughly 1630 (Amide I) and 1550 cm^{-1} (Amide II). An additional peak at 1230 cm^{-1} (Amide III) was also observed in accordance with previous literature (Muyonga et al., 2004; Aloglu and Harrington, 2018; Cebi et al., 2016; Gunzler, 2002).

Other than the gelatin peaks, the ATR-FTIR spectra was enlarged close to the fingerprint area to further elucidate the presence of PEG in the fibres (Figure 3.3B). The spectra showed clear disparity between the gelatin fibres spun in to PEG-supplemented coagulant and the native gelatin raw material. Clear peaks related to ether bonds (at 1100 cm^{-1}) were observed in the spectra of both PEG raw material and gelatin fibres spun into the PEG-supplemented bath.

Although this peak was slightly shifted towards reduced wavenumbers due to the interference of gelatin amide bonds, the result confirms the presence of PEG in the wet spun fibres, as reported previously (Kew et al., 2011; Kew et al., 2012).

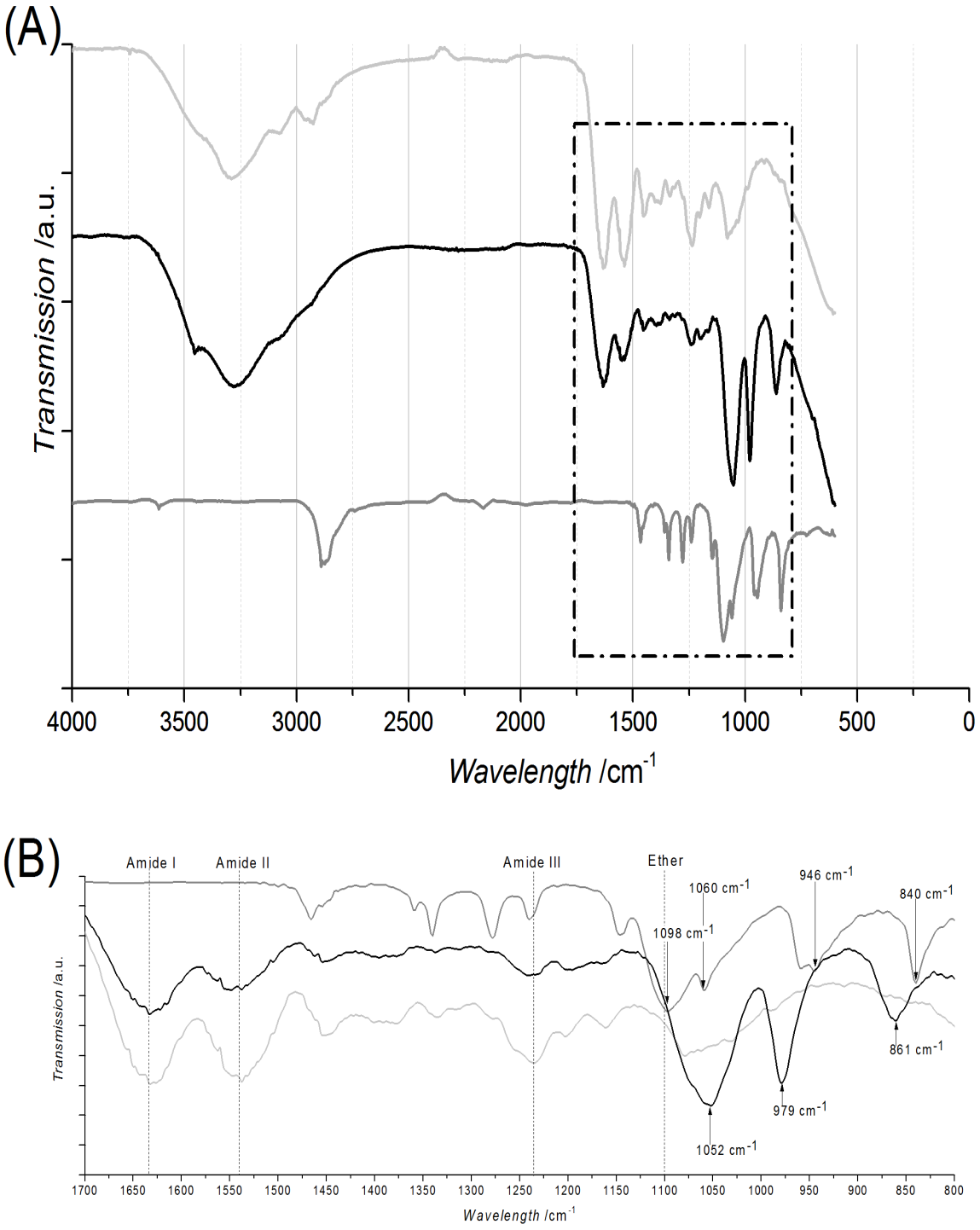

Figure 3.3. ATR-FTIR spectra of fibres made of native gelatin wet spun in PEG-supplemented PBS coagulation bath (—) as well as PEG (—) and gelatin (—) raw materials. Both full (A) and zoomed-in (B) spectra are reported.

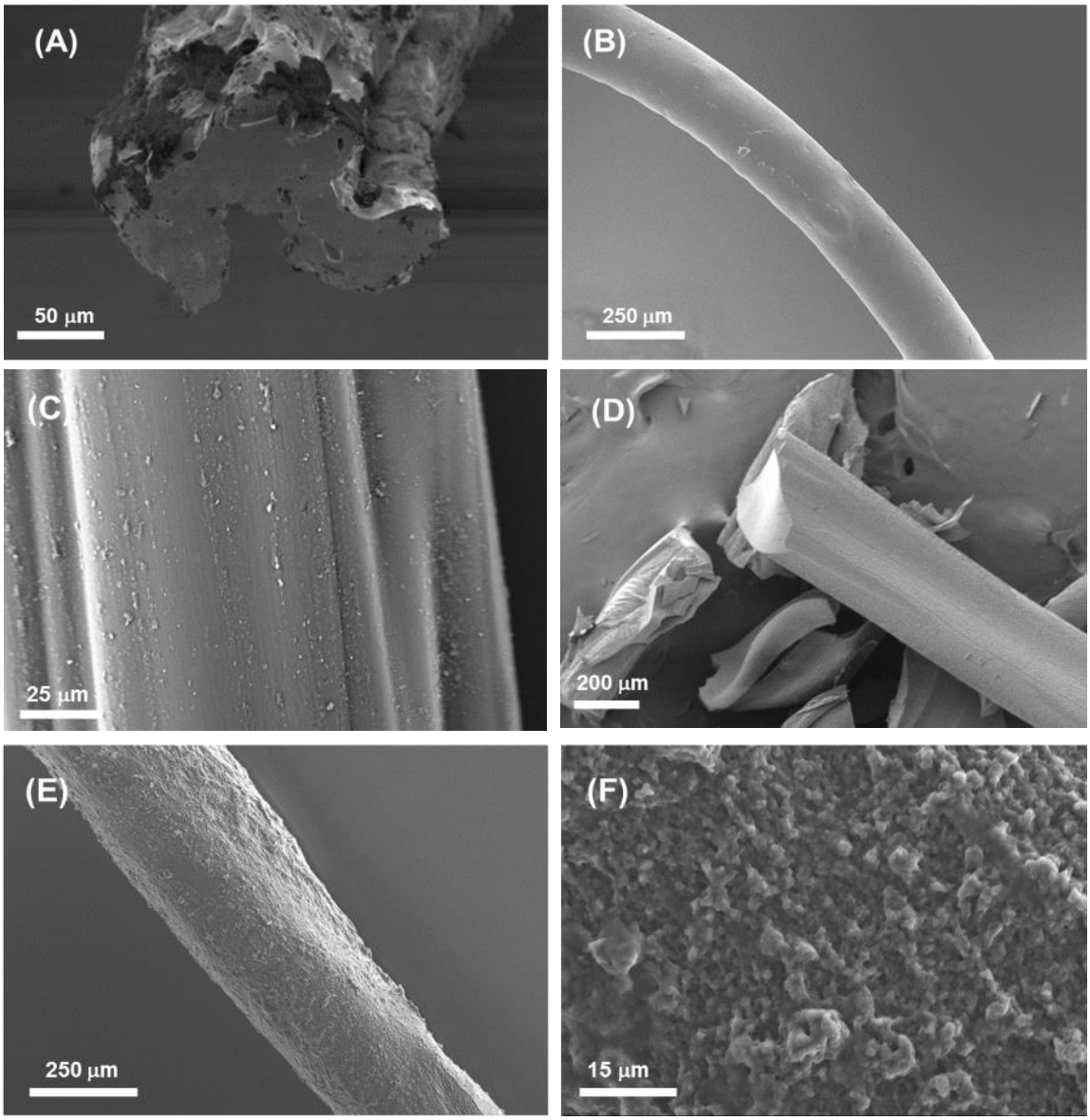

Figure 3.4. SEM images of wet spun gelatin fibres. (A): 4VBC-PEG. (B-C): 4VBC-PEG. (D): MA-EtOH. (E-F): 4VBC-NaCl. Image (A) refers to a sample wet-spun in a static coagulating bath. All other images refer to samples wet spun in a rotating coagulating bath

3.3.4 Fibre morphology

Other than the chemical composition, collected wet spun fibres were inspected by SEM to gather qualitative and quantitative information on the fibre morphology. As expected, the employment of a static coagulating bath during wet spinning process led to decreased fibre uniformity (Figure 3.4A), as compared to samples wet spun into rotating coagulation bath (Figure 3.4B).

Although low (~ 1.6 rpm), the rotation of the coagulating bath was expected to induce a degree of fibre drawing and increased molecular chain alignment of the fibre-forming polymer, resulting in fibres with increased surface homogeneity, thermal stability and tensile modulus (Midorikawa et al., 2012; Haynl et al., 2016).

In contrast to statically wet spun fibres (Figure 3.4A), the rotary wet spinning process clearly enabled the formation of fibres with smooth surface morphology and few cross sectional cavities (Figure 3.4B-C). Although surface roughness may aid cellular attachment and alignment, they are known to induce variation in fibre strength, and undesirable variation in mechanical properties (Bota et al., 2010; Chen et al., 2012; Teo et al., 2013; Shi et al., 2015).

Other than the effect of the coagulating bath rotation, the selection of specific non-solvents for the wet spinning gelatin solutions also proved to markedly affect resultant fibre morphology. Although fibre diameters were comparable, fibres (*d*: 336 ± 5 µm) spun in the sodium chloride-supplemented coagulating bath appeared less regular and more opaque than fibres (*d*: 370 ± 4 µm) spun using PEG-supplemented PBS (**Error! Reference source not found.**), suggesting differences in crystallinity between the two groups. With respect to the salt-supplemented solution, the increased translucency observed in the latter samples could be due to a PEG-induced reduction in crystallinity caused by the long PEG chains (M_n: 8000 g·mol^{-1}) intertwining within the gelatin polypeptides. In light of the
well-known miscibility with gelatin solutions, PEG chains could impede the spinning-induced alignment of gelatin chains, so that the formation of amorphous materials with increased light transmission capability could be explained.

In comparison to fibres made of Gel-4VBC, MA-EtOH fibres proved to display slightly decreased mean diameter (*d*: 322 ± 14 µm) and smooth surface

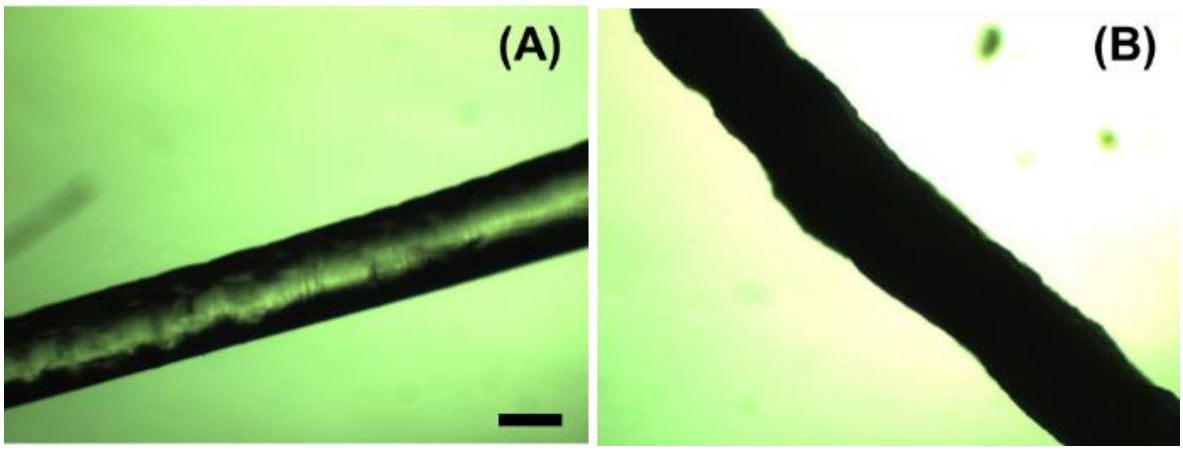

Figure 3.5. Optical microscopy images of UV-cured wet-spun fibres made of 4VBC-functionalised gelatin following 24-hour conditioning at 20 °C and 65% r.h. (A): 4VBC-PEG; (B): 4VBC-NaCl. Scale bar (200 μm) applies to both images.

morphologies, although they were found to be extremely brittle, as evidenced by top surface SEM (Figure 3.4 D-E). The large diameters of the fibres can be explained considering that a spinneret needle with an 800 μm internal diameter was employed during wet spinning. It is expected that decreased fibre diameters can be obtained via fibre drawing during or following wet-spinning.

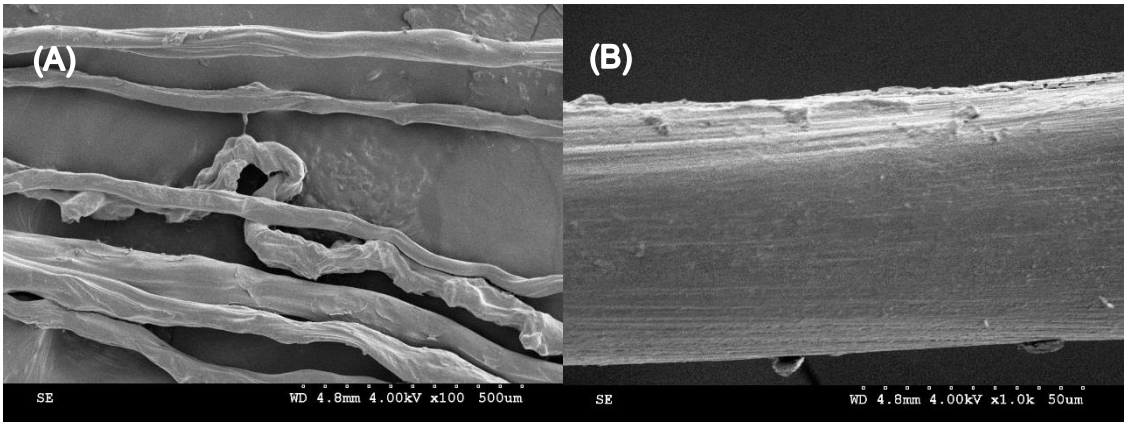

Figure 3.6: SEM micrographs of Gelatin fibres spun into PEG supplemented FFB using 10 wt. % dope and large scale Dienes wet-spinning machine. (A) x100; (B) x 1000

It is not thought that diameter or translucency levels would significantly affect the level of UV crosslinking induced. This is due to the inherent high surface area to volume ratio of fibres allowing for high levels of surface access over which photoinitiator incursion into the fibres can occur. In addition the relative low diameter of fibres would give UV light very little distance over which to penetrate when compared to studies creating larger hydrogels with lower surface areas where this issue was not raised (Tronci et al., 2015a; Liang et al., 2018).

Attempts at spinning and drawing native gelatin using a large scale Dienes pump and collector yielded some long fibres (Figure 3.6A and B). However the system was not stably balanced leading to either system blockages, or lack of fibre coagulation within the coagulant. Therefore the more basic, reliable syringe pump system was concentrated upon for these studies.

Fibres produced had an average diameter of 54 µm ±16. The morphology of the surface appeared smooth and homogenous with striations along the fibre axis likely caused by drawing during fibre collection. Figure 3.6A shows a central curling fibre which likely was broken off and not exposed to the same level of drawing.

3.3.5 Fibre swelling and nonwoven liquid uptake

Following characterisation of fibre morphology, the attention moved to the quantification of fibre properties in a hydrated near-physiological environment. Wet-spun fibres were UV-cured and characterised with regards to their liquid uptake capability. This is relevant for applications in medical devices such as wound dressings, where production of wound exudate can reach 4000-12000 $g \cdot m^{-2} \cdot day^{-1}$ (Cutting, 2003; Lamke et al., 1977)), and for tissue scaffolds, where nutrient and waste exchange is mediated by the physiological medium (Haslauer, 2014).

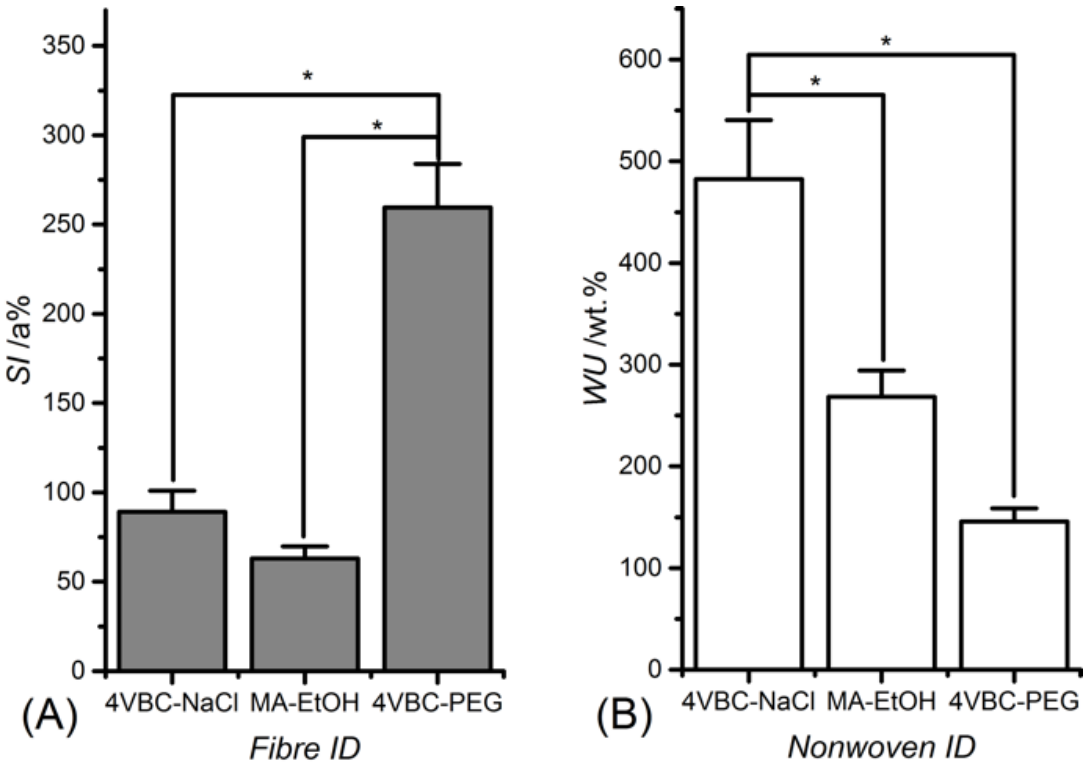

Figure 3.7. Swelling index (*SI*, A) of individual UV-cured wet spun fibres as well as water uptake (*WU*, B) of UV-cured nonwovens, following 24-hour incubation in PBS. (*: $p<0.05$, n=4).

The liquid uptake capability, hereby measured in terms of gravimetric and dimensional change, is also affected by the degree of covalent crosslinking achieved during fibre UV curing as well as molecular alignment and degree of crystallinity.

Fibre swelling and water uptake were measured for individual fibres and for nonwoven webs, respectively. For nonwovens, the liquid uptake also depends on liquid sorption of free liquid between the fibres, which is governed by the architecture of the structure. Liquid is then held at regions of close fibre proximity by capillary pressure (Junker et al. 2002). This leads to marked differences in water uptake as indicated in Figure 3.7A and B.

Photoinduced crosslinking was confirmed by investigating the macroscopic properties of UV-cured as well as wet spun Gel-4VBC fibres in near-physiologic conditions. UV-cured fibres proved to display significant swelling following 37 ºC incubation in aqueous environment (Figure 3.7A), In contrast

to the prompt dissolution observed in the case of the wet spun, non-UV-cured fibres. This observation therefore supports the fact that selected gelatin functionalisation and UV-curing route was key to enabling the synthesis of a covalent gelatin network at the molecular scale, and the manufacture of water-insoluble, mechanically-competent wet spun fibres at the microscale.

This confirmation was further obtained at room temperature, whereby significantly lower swelling index was measured in wet-spun, non-UV-crosslinked fibres 4VBC-PEG (SI= 234 ± 43 a.%) and 4VBC-NaCl (SI= 153 ± 28 a.%, p= 0.04), in contrast to the UV-cured fibres 4VBC-PEG (SI= 184 ± 12 a.%, p= 0.046) and 4VBC-NaCl (SI= 71 ± 18 a.%, p= 0.04).

Individual 4VBC-PEG fibres showed a significantly higher (p=0) level of swelling index (*SI*= 260±24 a%) than fibres 4VBC-NaCl (*SI*= 89±12 a% p=0) and MA-EtOH (*SI*= 64±7 a%). This is likely due to the hygroscopic nature of PEG present within the fibres, promoting an amorphous fibre morphology, allowing for liquid to move into the regions between the polypeptide chains. Other than the presence of PEG in 4VBC-PEG fibres, the reduced liquid uptake capability of MA-EtOH fibres is also in agreement with the increased degree of functionalisation found in MA- with respect to the 4VBC-reacted gelatin fibre building block.

With regards to the swelling trends observed with fibres, an almost inverse relationship was observed when quantifying the water uptake of corresponding gelatin nonwovens. Nonwoven samples made of 4VBC-NaCl fibres displayed the highest water uptake (*WU*: 482±58 wt. %), which was significantly higher than the one measured in nonwovens of either 4VBC-PEG (*WU*: 146±13 wt. %, $p=4\times10^{-5}$) or MA-EtOH (*WU*: 268±26 wt. %, p=0.003) fibres. Given that the SEM images of respective nonwovens appeared similar among the different sample groups (, A-D); the most likely explanation for the above observation is that the water-induced swelling of the individual fibres leads to reduced porosity in the corresponding water-equilibrated nonwoven. Consequently, decreased water content is expected

within the pores of the nonwoven structure, when fibres with increased swelling capability are employed.

3.3.6 Thermal characterisation

Thermal properties of native gelatin as previously reported in the literature indicate a glass transition temperature of 80-90ºC and a triple helix-related denaturation temperature of 110-115ºC (Marshall and Petrie, 1980). In the present study, no defined glass transition was detected in the DSC thermograms of the UV-cured fibres (Figure 3.8), which may be due to the presence of free water residues in the tested samples (Mukherjee and Rosolen, 2013; Luescher et al., 1974).

UV-cured 4VBC-PEG fibres were associated with the highest denaturation temperature (T_m =108 ºC), whilst a denaturation enthalpy of 106 $J \cdot g^{-1}$ was measured (Table 3.3). In comparison, UV-cured 4VBC-NaCl fibres displayed the lowest denaturation temperature (T_m = 84ºC), and a slightly higher enthalpy (ΔH= 125 $J \cdot g^{-1}$). The denaturation enthalpy indicates the heat energy required to break the crystalline-like triple helical junctions within the gelatin material (Skrzyński et al., 2009; Gabbott, 2008).

During the wet spinning of 4VBC-PEG fibres, PEG is known to act as a “reptating agent” during fibre formation (Zeugolis, D. I. et al., 2008b), intertwining with the fibre-forming polypeptide chains and leading to an increased melting point. In this instance, the presence of PEG within the polypeptide chains is expected to inhibit the renaturation of gelatin molecules into collagen-like triple helices, leading to decreased fibre denaturation enthalpy.

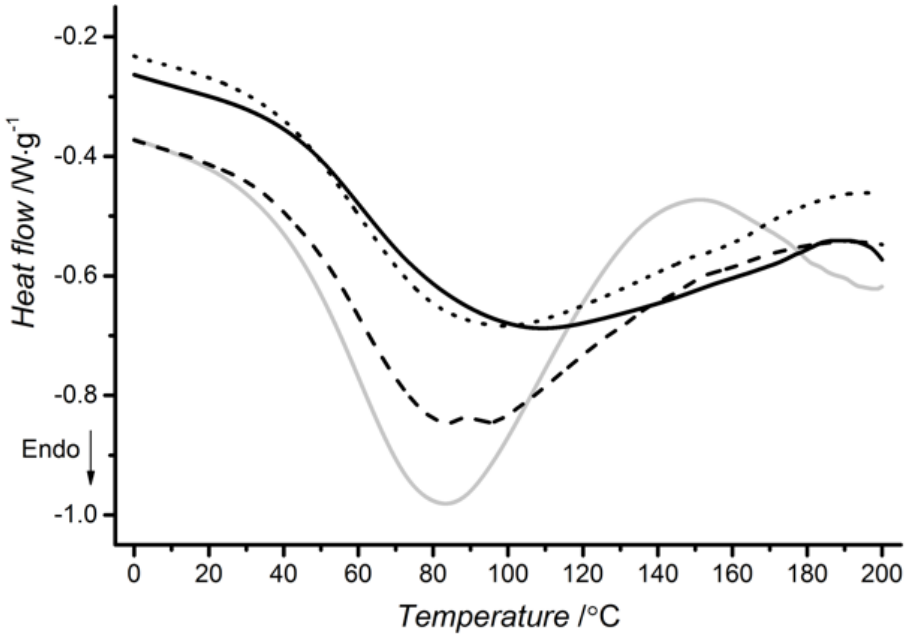

Figure 3.8. DSC curves of UV-cured wet spun fibres MA-EtOH (– – –), 4VBC-NaCl (—) and 4VBC-PEG (—) as well as fibre control Native-PEG (···).

This molecular organisation mechanism is likely missing in the case of fibres 4VBC-NaCl wet spun in PEG-free coagulants. Here, the absence of PEG in the coagulant enables chain alignment and renaturation of collagen-like triple helix to occur unperturbed, so that an increased fibre denaturation enthalpy can be measured with respect to fibres 4VBC-PEG. This mechanism is supported by both the observed morphology, swelling, and mechanical properties of the fibres.

3.3.7 Tensile properties

Together with the evaluation of liquid uptake and thermal properties, tensile measurements were also carried out on individual UV-cured and native gelatin fibres. The ultimate tensile strength (*UTS*) was significantly higher in the UV-cured 4VBC-PEG fibres (*UTS*: 74±3 MPa) with respect to samples MA-EtOH (p=0), 4VBC-NaCl ($p=8\times10^{-9}$) and Native-PEG ($p=9\times10^{-7}$) (Figure 3.9**Error! Reference source not found.**). Remarkably, the tensile strength of water-equilibrated 4VBC-PEG samples was also sufficiently high to permit

knotted and twisted fibre conformations to be generated by hand (Figure 3.10), providing further evidence of the mechanical stability of these fibres and their potential applicability as materials for medical device manufacture.

The increased values of tensile strength and elastic modulus measured with fibres made of 4VBC-PEG and 4VBC-NaCl with regards to fibre MA-EtOH, reflect molecular scale considerations regarding the UV-induced 4VBC-based crosslinking segment as well as the nature of the wet spinning

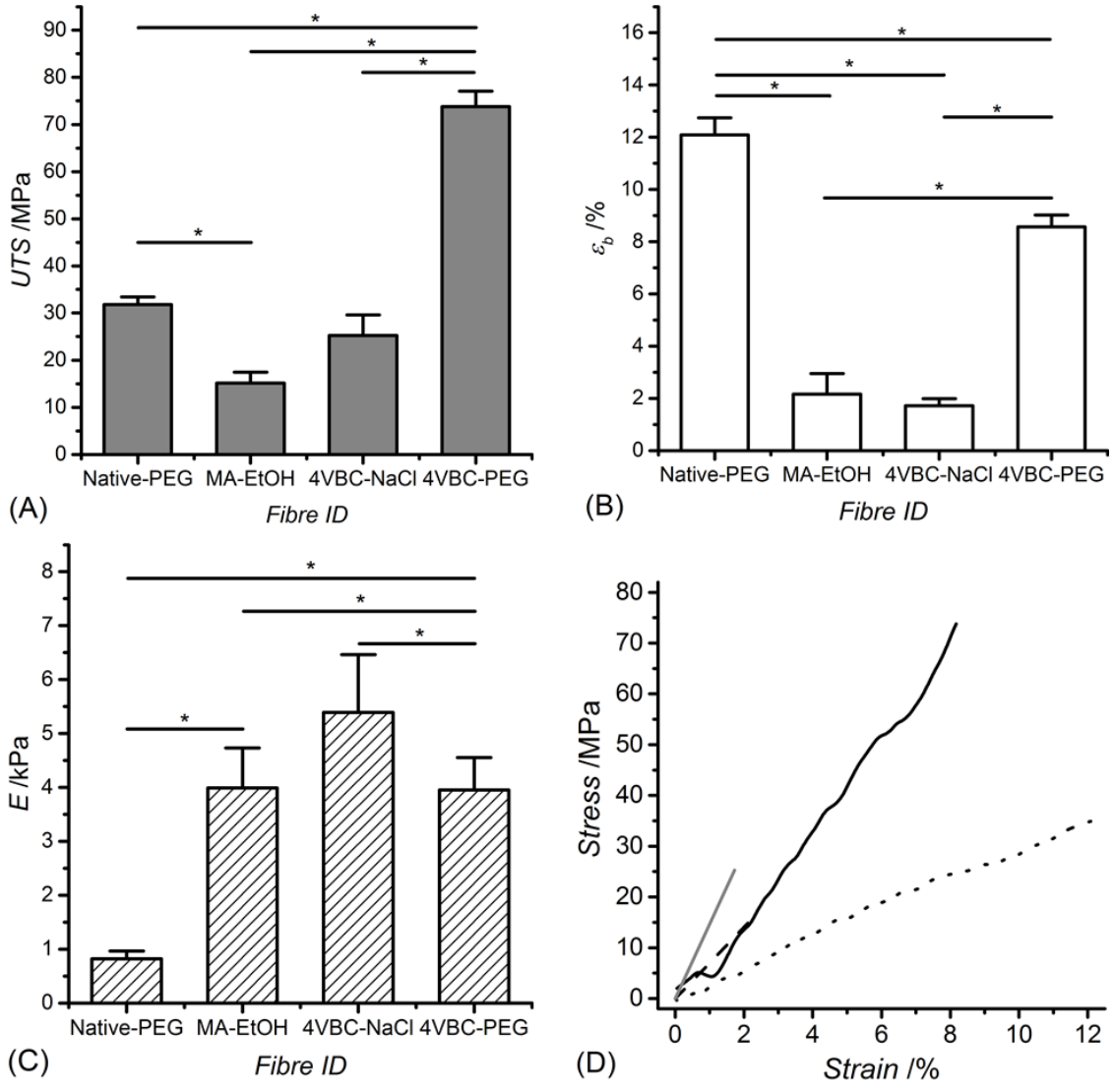

Figure 3.9. Tensile properties of individual wet-spun fibres made of either native or UV-cured gelatin. (A): Ultimate tensile stress (*UTS*); (B): extension at break (ε_b); (C): Tensile modulus (*E*); (D): Averaged stress-strain curves of UV-cured wet spun fibres MA-EtOH (– – –), 4VBC-NaCl (—), and 4VBC-PEG (—) as well as fibre control Native-PEG (···).*: $p<0.05$.

coagulating bath. UV-curing of 4VBC-functionalised gelatin chains leads to the formation of an aromatic crosslinking segment, with increased molecular rigidity with respect to the methacrylate segment obtained via UV-curing of MA-functionalised gelatin chains.

Besides the inherent molecular rigidity of the UV-induced crosslinking segment, the size of the photoactive moiety covalently-coupled to the gelatin backbone is also expected to impact on the yield of the free-radical crosslinking reaction.

Methacrylamide residues in MA-functionalised gelatin are indeed shorter than the 4-vinylbenzyl moieties present along the 4VBC-functionalised gelatin backbone, so that so that steric effects potentially hindering the free-radical crosslinking reaction are likely. These observations may count for the trends observed in tensile strength and tensile modulus with respect to the UV-cured fibres MA-EtOH and 4VBC-NaCl (Table 3.3).

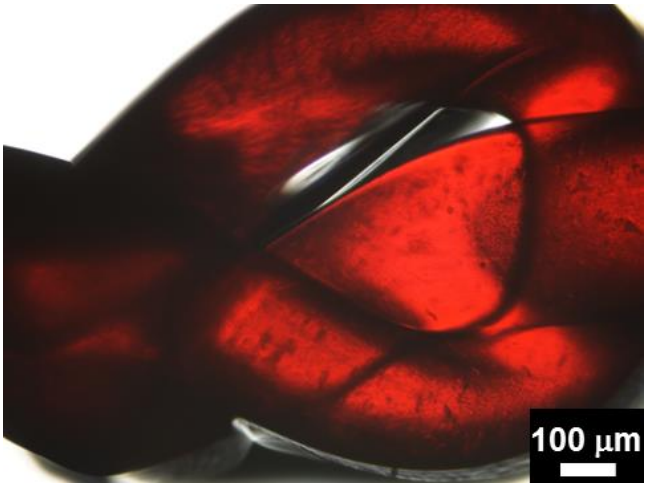

Figure 3.10 Optical microscopy image of a stained knotted sample of UV-cured gelatin fibre 4VBC-PEG following PBS equilibration

Other than that, it is likely that the plasticising effect of PEG coagulant contributed to the increase in strength of the UV-cured 4VBC-PEG fibres. Not only does PEG provide a more viscous coagulant in which diffusional

exchange during the wet-spinning process can occur more slowly preventing the formation of voids within the fibres (Tronci et al., 2015b), but the confirmed presence of PEG in the fibres is also expected to increase the tensile strength via hydrogen bonding between the polymer and gelatin hydroxyl groups (Luescher et al., 1974; Zeugolis, D. I. et al., 2008b).

The PEG polymer chains have previously been reported to act as a reptating agent, entangling within the chain structure and sliding parallel to gelatin chains when withstanding tensile forces (Zeugolis, D. I. et al., 2008b; Baker et al., 2004).

Table 3.3: Thermo-mechanical properties of gelatin fibres. UTS: Ultimate tensile strength; E: Young's modulus, Tm: melting temperature; ΔH: melting enthalpy

Sample ID	*UTS* /MPa	*Strain* /%	*E* /kPa	T_d /ºC	*ΔH* /W·g^{-1}
4VBC-NaCl	25±4	1.7±0.3	5000±1000	84	125
4VBC-PEG	74±3	8.6±0.5	4000±1000	108	106
Native-PEG	9±1	12.1±0.7	300±40	99	101
MA-EtOH	15±2	2.2±0.8	4000±1000	89	102

In contrast to PEG-containing fibres, wet spinning in the NaCl-supplemented coagulating bath resulted in extremely weak and brittle fibres. In the case of MA-functionalised gelatin, resulting wet spun fibres were too fragile to handle and so no mechanical data could be obtained. Likewise, 4VBC-NaCl samples were very brittle and, despite their increased Young's modulus (*E*: 5000 ± 1000 kPa), they could be uniaxially extended only up to about 2% of their initial length prior to fibre break.

The observed reduction in extension at break in samples 4VBC-NaCl with respect to 4VBC-PEG samples is in agreement with the fact that no gelatin plasticiser, i.e. PEG, was present. This tensile data also suggest that the

coagulating bath was not sufficiently viscous to support the diffusional exchange occurring during fibre formation, therefore resulting in the rapid diffusion of solvent away from the fibre-forming gelatin chains and the creation of weak fibres with irregular internal structure.

This is reflected by the morphological characterisation (E and F), which revealed fibres with a rough surface and low uniformity. The presence of PEG-induced plasticising effect in fibres with increased elongation at break agrees with previously discussed fibre thermal properties, whereby a corresponding decrease in denaturation enthalpy was recorded (Table 3.3).

The decreased denaturation enthalpy measured in both samples Native-PEG and 4VBC-PEG correlates with a decrease in fibre crystallinity, whereby resulting amorphous regions mediate fibre elongation during the tensile test. During stretching, fibre elongation is indeed mainly attributed to the straightening of amorphous regions, whilst the presence of chemical bonds fixes gelatin chains in a molecular network (Mackley, 2010).

Other than the UV-cured fibres, it was interesting to note that the native gelatin control fibres were significantly more extensible with respect to samples MA-EtOH (p=8×10^{-9}), 4VBC-NaCl (p=0), and 4VBC-PEG (p=2×10^{-4}). This was found to correlate with the fact that no covalent crosslinking was introduced between the fibre-forming gelatin chains, therefore allowing for parallel chain slippage to occur during uniaxial tension.

3.3.8 Morphology and cytotoxicity of f-gelatin nonwovens

To determine the feasibility of forming fabrics directly during the wet spinning process, nonwoven webs were spunlaid from wet spun f-gelatin fibres, using a rotary deposition system and slight agitation of the coagulating liquid. Agitation of the coagulation bath allowed displacement and crossing of proximal fibres to produce a self-supporting fibrous network that could be manually manipulated after drying. The fibre morphology in the nonwoven

assembly varied considerably depending upon the fibre building block and the selection of the coagulating liquid.

Unlike the case of the individual wet spun fibres, respective nonwovens 4VBC-NaCl exhibited irregular fibre morphology (A-B). This observation is likely due to merging of fibres during wet spinning and prior to drying, leading to surface buckling and collapse and explaining the morphology variation between the nonwoven and single fibre (Adanur, 1995). MA-EtOH fibres (C) exhibited flattened or ribbon-like morphologies, again suggesting rapid diffusion of the dope solvent from the fibre-forming gelatin solution.

By contrast, 4VBC-PEG fibres (D) were characterised by a smooth and rounded morphology with negligible fibre merging, indicating coagulating bath conditions consistent with enhanced diffusional exchange in light of the increased viscosity of the coagulating bath.

The cellular tolerability of the nonwoven structures containing gelatin was assessed with L929 murine fibroblasts following 7-day cell culture via both an alamarBlue assay and Live/Dead cell staining, whereby a PCL nonwoven control was also tested (Figure 3.12).

All gelatin nonwovens showed significantly higher ability to support cell survival than the PCL control, following both 4- and 7-day cell culture. These results confirm that the increased cellular tolerability of gelatin with respect to PCL is maintained even though chemical functionalisation, fibre spinning and UV-induced network formation were applied to the native polypeptide (Puppi et al., 2011).

Within the two gelatin groups, a significant difference in metabolic activity was observed in cells cultured on fibres made of 4VBC-functionalised gelatin when compared to cells cultured on fibres made of MA-functionalised, following 7-day cell culture. This could be due to multiple factors such as the increased degree of functionalisation and corresponding crosslink density

measured in methacrylated gelatin fibre, which may mask the cell-binding sites present in native gelatin.

Within the 4VBC-functionalised gelatin groups, an insignificant decrease in metabolic activity was recorded in cells following 7-day culture on sample 4VBC-PEG compared to cells cultured on sample 4VBC-NaCl, suggesting that the presence of PEG within the fibre did not induce any detectable change in cell response. Overall, confocal images from the Live/Dead staining supported previous results, whereby substantial cellular viability was observed within the nonwoven gelatin fibres (Figure 3.13A-D).

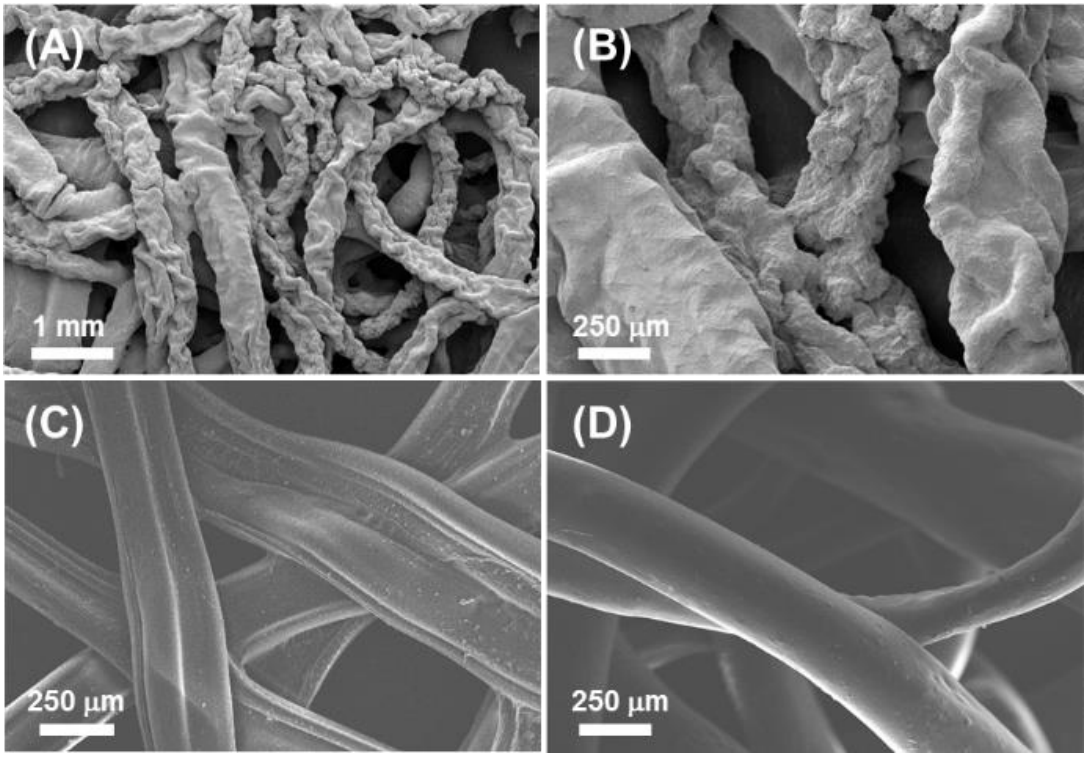

Figure 3.11. SEM micrographs of UV-cured gelatin nonwovens prepared during wet-spinning in one step. (A-B): 4VBC-NaCl; (C): MA-EtOH; (D): 4VBC-PEG

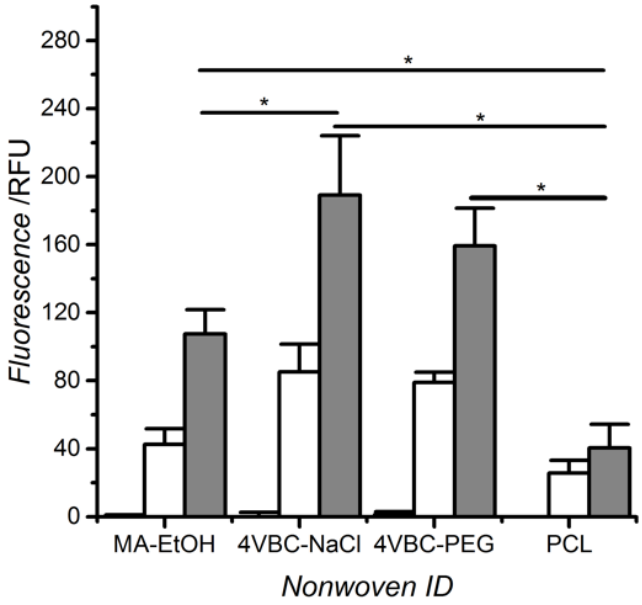

Figure 3.12. alamarBlue assay following L929 cell culture on both UV-cured gelatin nonwovens and PCL controls at day 1 (black columns), 4 (white columns), 7 (grey columns). *: p< 0.05.

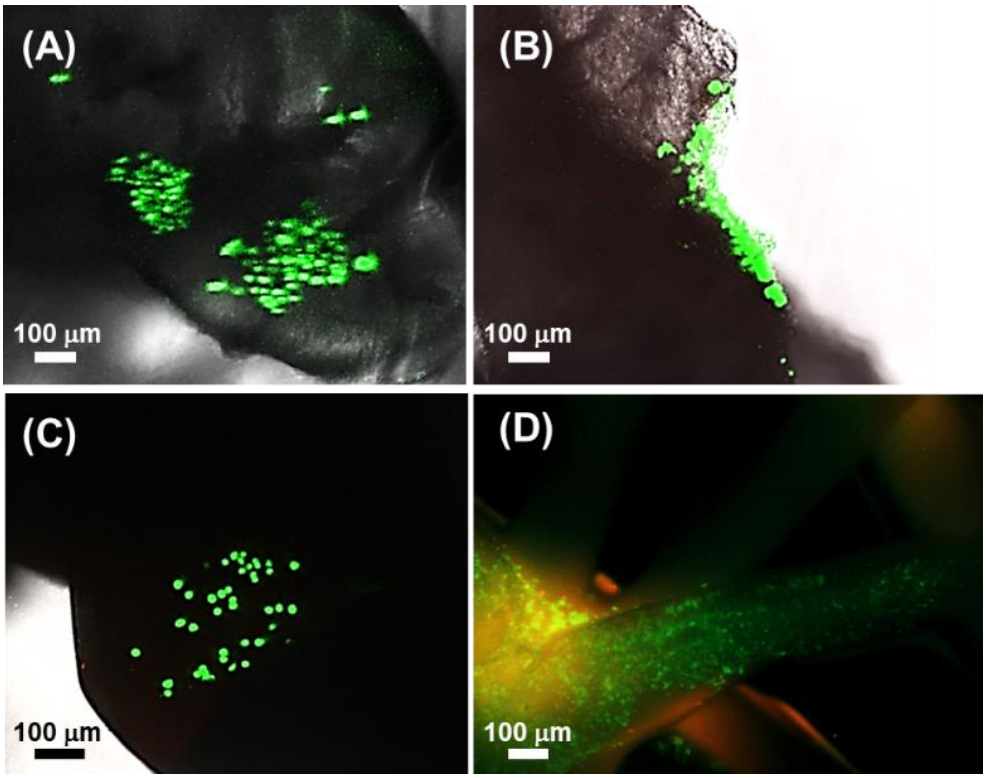

Figure 3.13. (A-C): Confocal images obtained following Live/Dead staining of L929 fibroblasts cultured on to UV-cured gelatin nonwovens for 7 days. (A): 4VBC-PEG; (B): 4VBC-NaCl; (C): MA-EtOH. (D): Fluorescence microscopy image of UV-cured gelatin nonwoven MA-EtOH following 7-day culture with L929 fibroblasts and Live/Dead staining.

3.4. Conclusions

Both 4VBC- and MA-functionalised gelatin precursors were successfully wet spun and UV-cured in both the fibre and nonwoven state, demonstrating the formation of mechanically-competent building materials for use in medical devices. The type of photoactive monomer proved to impact on the degree of gelatin functionalisation, so that solubility and spinnability of the resulting product were affected. Solutions of 4VBC-functionalised gelatin (15 wt. %) were readily spun at room temperature into a non-volatile aqueous coagulating bath supplemented with either NaCl or PEG.

On the other hand, wet dopes of MA-functionalised gelatin required a two-fold increase in gelatin concentration and a -20 ºC ethanol-based coagulating bath for fibres to be successfully formed. Regardless of the coagulating parameters, 4VBC-based wet spun fibres compared favourably with respect to MA-based fibres in terms of biocompatibility when tested with murine fibroblasts for up to 7 days.

These data indicate that the photoactive gelatin precursor functionalised with 4-vinylbenzyl residues enables enhanced fibre spinnability and cellular tolerability, which is key to enable further development for use in medical device manufacture spinning on a full scale set up, using a spinneret, and whilst fully controlling parameters such as draw ratio. Both the spinning process and gelatin building block developed in this study present wide applicability in bioprinting, whereby a computer-controlled extrusion device could be employed to deposit and UV-cure layers of gelatin fibres aiming to achieve precise 3D architecture of fibres (Di Giuseppe et al., 2018; Wang, X.H. et al., 2017; Roseti et al., 2018).

Variation in wet spinning coagulating bath conditions was shown to produce a significant difference in the morphology and mechanical properties of the fibres. 4VBC-functionalised gelatin solutions spun into a PEG-supplemented PBS coagulant generated fibres with increased ultimate tensile strength (*UTS*= 74±3MPa) and strain at break (ε_b= 8.6±0.5 %) compared to fibres

spun into a sodium chloride-supplemented aqueous solution (*UTS*= 25±4 MPa; ε_b= 1.7±0.3 %). As confirmed by ATR-FTIR, this variation of mechanical properties was likely due to the uptake of PEG molecules into the forming wet spun fibres, acting as a reptating agent within the polypeptide chains of the fibre. This PEG-induced effect also explains the homogenous morphology observed in fibres spun against the PEG-supplemented coagulant with respect to the case of PEG-free spinning.

Chapter 4

Preparation and Characterisation of Functionalised Collagen Fibres

4.1 Introduction

Type I collagen is abundant within the human body, being the predominant connective tissue in bone, skin, tendon, and ligament (Gelse et al., 2003; Shoulders and Raines, 2009). Its valuable properties of biocompatibility, mechanical strength, and collagenase and cell adhesion motifs, have made it a sought after biomaterial for use in medical devices aiming to biomimic human tissue to encourage healing and regeneration.

Although recent progress has been made on triple helical conservation during electrospinning using a collagen core and a sacrificial polyvinylpyrrolidone sheath to protect the material (Wakuda et al., 2018), the technique of wet-spinning remains the pragmatist's choice for collagen spinning. This is due to the ability to minimise denaturing of the triple helix structure because of the absence of voltage or highly polar solvents used during the process (Zeugolis, Dimitrios I. et al., 2008; Zeugolis et al., 2009a; Zeugolis, D. I. et al., 2008a; Zeugolis, D. I. et al., 2008b; Zeugolis et al., 2009b; Caves et al., 2010; Siriwardane et al., 2014; Haynl et al., 2016; Yaari et al., 2016; Arafat et al., 2015).

Wet-spun fibres have the ability to be incorporated into three-dimensional textile assemblies, such as nonwovens, braids, woven and knitted fabrics, as opposed to the 2D, membrane-like meshes produced by electrospinning, which can impede cellular infiltration due to the small pore sizes (Kalaithong et al., 2017).

Wet-spinning has been shown to allow control of fibre diameter, morphology, and alignment by varying drawing levels, coagulant selection,

dope concentration, and die size thereby affecting the mechanical and thermal resistance of the fabric, as well as cellular alignment, swelling properties, and collagenase susceptibility (Zeugolis, Dimitrios I. et al., 2008; Zeugolis et al., 2009a; Zeugolis, D. I. et al., 2008a; Zeugolis, D. I. et al., 2008b; Zeugolis et al., 2009b; Caves et al., 2010; Siriwardane et al., 2014; Haynl et al., 2016; Yaari et al., 2016; Arafat et al., 2015).

In short, wet spinning permits the production of fibres that can be tailored to the requirements of the specific end-use more reproducibly than is possible with other methods such as electrospinning. For example a chronic wound producing exudate at a typical rate of 1.3g/cm^2/24 h or more, could be managed with a wound dressing produced from collagen fibres arranged in a near random orientation with a high porosity (>0.9) to yield a highly liquid absorbent structure. By contrast a collagen scaffold required to mimic neural tissue would require high uniaxial alignment of fibres similar to the surrounding tissue's architecture.

Previously, drawing of fibres during the wet spinning process to elongate the initial polymer stream is known to have a significant effect on molecular alignment of fibre-forming molecules and fibre mechanical properties, as well bulk dimensions, specifically fibre diameter. Drawing within a coagulation bath has been shown to lead to a significant increase in fibrillar alignment and strength up to a draw ratio (DR) of 1:8.1, but with a decrease in strength attributed to overdrawing observed at higher DRs (Yaari et al., 2016). Following cross-linking, a remarkably high tensile strength of 150 MPa in the hydrated state, was reported, together with a dry tensile strength of 378 MPa. However these results were obtained using fibres crosslinked with glutaraldehyde (GT), a cytotoxic reagent that can compromise applications in medical devices (Zeugolis et al., 2009a).

The application of microfluidics is an interesting new avenue of research for collagen wet-spinning (Lu et al., 2020; Haynl et al., 2016; Hiramatsu et al., 2016; Bai et al., 2014; Shi et al., 2015). Here, coagulant and collagen solution are simultaneously pumped through a capillary wherein the collagen solution

is stretched out in the flowing solution and then solidifies to form fibrils. This technique has been shown to produce fibres of very small diameter (3.7µm), the smallest reported in literature using a wet-spinning technique. The small diameter is also accompanied by a high tensile strength without the need for crosslinking (Haynl et al., 2016). The main drawback is the relatively low rates of production that are possible using this approach, and the need for a complex microfluidic circuit.

In general the wet-spinning of collagen has addressed the initial critical hurdle of preventing denaturation of the material (Arafat et al., 2015; Zeugolis, D. I. et al., 2008a), but the process still has many limitations that have prevented it from becoming more widely used by the industry to prepare collagen fibre-based products.

Many of the existing processes have extremely low yields and produce discontinuous fibres ranging from 50-150 cm in length (Siriwardane et al., 2014; Haynl et al., 2016). Whilst this is adequate for the preparation of nonwoven webs and fabrics, it limits the use of collagen fibre materials in knitting and weaving, which require continuous filaments or staple spun yarns to be prepared. Very low production rates are also frequently reported, in the range 0.1-4.8 m h^{-1} (Haynl et al., 2016; Kato and Silver, 1990).

Many previous research articles report the production of fibres without chemically crosslinking to ensure the material is as biologically similar to the native biomaterial as possible. This has been shown to increase collagenase susceptibility and lead to rapid collagen degradation (Helling et al., 2017; Vasudev and Chandy, 1997; Caves et al., 2010). Caves *et al.* compared crosslinked and uncrosslinked bundles of collagen by subcutaneous implantation in mice over six weeks. After that period crosslinked fibres showed little change in length whereas uncrosslinked showed a 70% reduction (Caves et al., 2010).

Eventual degradation and resorption of collagen fibres is advantageous from a clinical standpoint, as an implant remaining intact for too long leads to encapsulation and rejection by the recipient's immune system. However, rapid breakdown of the material can compromise the intended functions of the material, and this is also undesirable leading to no benefit and repeated operations which adversely affect patient health and consume valuable time for medical practitioners. Few previous studies have taken into account the effects of collagenase upon fibres and so ignore an important question over the material's adequacy following implantation.

Many different modes of crosslinking have been experimented with in relation to collagen, all of which serve to improve wet-strength and reduce collagenase susceptibility. A review into the effects of crosslinking modes upon mechanical and thermal properties of fibres reveal certain chemical crosslinkers that have been particularly successful at stabilising the fibre, but which are also cytotoxic for example, formaldehyde, and glutaraldehyde (Zeugolis et al., 2009a). Glutaraldehyde is one of the most widely used crosslinkers as it reacts rapidly with collagen and produces strong fibres (Yaari et al., 2016; Siriwardane et al., 2014). However, it has been shown in multiple studies to induce apoptosis if present due to residues in the material, unstable side chains and leaching (Salgaller and Bajpai, 1985; Gough et al., 2002; Sung et al., 1999).

In investigations of different crosslinkers, which do not produce cytotoxic effects riboflavin (RF) a photoactivating vitamin has been used to induce crosslinking (Tonndorf et al., 2019). UV exposure of RF causes the molecule to absorb energy and transition into an excited riboflavin triplet which induces covalent crosslinking between amino acids (Raiskup and Spoerl, 2013).

Tonndorf *et al.* compared crosslinking methods and confirmed that the resulting RF collagen fibres showed better biocompatibility than GTA due to the cytotoxic side chains produced using the latter. They also discovered that

RF induced crosslinking, increases the fibre strength when hydrated. However, they also found that RF decreased the strength of the fibre compared to the non-crosslinked version when dry. This was thought to be due to structural flaws but would also likely be exacerbated by the zero-length crosslinking induced within the fibre. This is problematic due to the necessity for a level of tensile strength consistent with the needs of subsequent textile processing, including nonwoven manufacture, braiding or knitting.

An alternative use of UV for photoinduced crosslinking within collagen networks which has not shown evidence of cytotoxicity is by pre-functionalising the protein prior to spinning with molecules such as GMA, MA, and 4VBC (Tronci et al., 2015a). This method includes a precipitation stage to remove any unreacted chemicals from the material prior to spinning, thereby reducing chemical leaching. Furthermore when used in the preparation of collagen hydrogels, these modes were shown to conserve triple helical structure whilst maintaining the gel swelling properties, as well as endowing the materials with high compressive moduli. This method also has the potential to increase fibre yields and processing times, as a one-step spin and photoactivation step could be possible preventing fibres from breaking during spinning.

For these reasons, the present study focuses on transferring this technique of pre-functionalisation and post-spinning photo-activation into collagen wet-spinning, with the aim of determining the feasibility of spinning RTC-4VBC into continuous filaments. Following wet-spinning the objective was to characterise resulting physical properties and compare results with those reported for fibres produced by alternative methods, in terms of water interaction, mechanical strength, resistance to collagenase, and cytotoxicity.

Finally, a one-step spin and crosslinking process is explored with respect to achieving crosslinked RTC-4VBC fibres using a shorter manufacture process, requiring no handling of the uncrosslinked fibres.

4.2 Experimental

4.2.1 Materials

Sprague-Dawley rat tails were provided by the University of Leeds, Faculty of Biological Sciences. Polysorbate 20, diethyl ether, HCl, and ethanol were purchased from VWR Prolab Chemicals. Acetone was purchased from Fischer Chemicals. Acetic acid was purchased from Fluka Analytical. Dulbecco's PBS was purchased from Lonza Chemicals. 4VBC, Triethylamine (TEA), poly (ε-caprolactone) (PCL), PEG (M_n: 8000 g·mol^{-1}), PBS tablets, 2-Hydroxy-4-(2-hydroxyethoxy)-2-methylpropiophenone (I2959), and all other reagents were purchased from Sigma Aldrich.

4.2.2 Collagen Extraction

Frozen Sprague-Dawley rat tails were defrosted in 70% vol. ethanol, skinned and left to dry. The tail tendons were extracted and dissolved in 17.4 mM acetic acid (50ml/tail) for 48 h at 4ºC. The collagen solution was subsequently centrifuged at 10,000 rpm for 40 min to remove the tendon pellet. The remaining collagen solution was frozen at -80 °C and freeze dried to form a sponge like collagen material (Holmes et al., 2017).

4.2.3 Collagen functionalisation

Collagen was functionalised with 4VBC by dissolving at 1 wt. % in 10mmol HCl and adding 1 wt. % Polysorbate 20 surfactant. A 25x molar excess of 4VBC to lysine concentration (3.24 x 10^{-4} mol) was added, followed by a 25x molar excess of TEA catalyst (Tronci et al., 2015a). The reaction was left for 24 h at 20ºC before precipitating for 24 h in ethanol and centrifuging at 10,000 rpm for 40 min and retaining the collagen pellet. Collagen

functionalisation was characterised using the TNBS method outlined in Section 3.2.3. (n=3)

4.2.4 Filament spinning

RTC-4VBC was dissolved at 1.2 wt. % in 17.4mM acetic acid and extruded from a 1 ml syringe through a 0.8 mm or 0.6 mm diameter blunt headed needle at rates of 11.4 ml/hr, 7.6 ml/hr, and 3.6 ml/hr into the coagulant of either 20% (w/v) PEG/ 0.1M PBS or 100 vol. % ethanol (Zeugolis et al., 2008b, Arafat et al., 2015).

To enable continuous filament spinning, the coagulant container was placed upon a rotating plate, which allowed for single filaments emerging from the needle tip (spinneret) to be deposited at a regular rate into the coagulant. The rotational speeds of the ARDS were varied from 1.6rpm (29m hr^{-1}) to 2rpm (36 m hr^{-1}). Table 4.1 shows the different combinations of extrusion and collection rates with respect to given sample IDs. The needle was positioned on the outer edge, 1cm from the bottom of the container which had a circumference of 30cm. Initial spinning attempts were performed using syringe pump but by rotating the bath manually. This lead to irregular disturbance in the buffer liquid dynamics and so the ARDS system was utilized to improve spinning rerproducability.

Filaments were then hung, air dried and transferred into 90 vol. % ethanol for 10 min, then into 90 vol. % ethanol with 1 wt. % I2925 and exposed to UV for 30 min (λ: 365 nm, 8 $mW \cdot cm^{-2}$) with a sample to UV lamp distance of approximately 10 cm. The fibres were then washed for 1 h in ethanol, removed, and left to dry at 20ºC.

4.2.5 Two-step fibre spinning and crosslinking

The 1.2% RTC-4VBC solution was extruded directly into 90 vol. % EtOH, 1 wt. % I2925 in a dark room. The fibre bath and nascent fibres were then

exposed to UV light (specification indicated in Section 3.2.7) for 30 min, washed for 1 h in EtOH, and hung up to air dry.

Table 4.1: Sample IDs with respect to extrusion and collection rates

Sample ID	Extrusion/ ml hr^{-1}	Rotation/ m hr^{-1}
EtOH-10	3.6	36
EtOH-8	3.6	29
EtOH-4	7.6	29
EtOH-3	11.4	29
EtOH-m	3.6	manual
PEG-10	3.6	36
PEG-8	3.6	29

4.2.6 Circular Dichroism

Collagen materials (Native collagen sponge, RTC-4VBC, uncrosslinked RTC-4VBC fibre, and Type A porcine gelatin) were dissolved at 0.2 mg ml^{-1} in 17.4mM acetic acid. Far-UV CD spectroscopy was used to observe the tertiary protein structure using a ChirascanCD spectrometer (Applied Photophysics Ltd, UK). Sample solutions were collected in quartz cells of 1.0 mm path length, CD spectra were obtained between 180-260 nm with a band width of 2 nm and scanning speed of 2 nm s^{-1} (n=2). Backgrounds were taken of no cuvette and 17.4 mM acetic acid and subtracted from the collagen solution samples. CD molar ellipticity (corrected for concentration) was calculated using Equation 4.1,

$$\theta = m^o \times \frac{M}{10} \times L \times C$$

Equation 4.1

where, θ= molar ellipticity/ deg*cm^2*dmol^{-1}, m^o=absorbance/ mdeg. L= path length/ cm and MR= mean residual weight (average molecular weight of amino acids within collagen protein)/ g mol^{-1} (Sutherland, J.C., 1996).

4.2.7 Fibre density

Fibre segments of 1 m were weighed and the mean fibre density (g cm^{-3}) was calculated by dividing the mass by the total volume of the fibre (mean diameter transformed to cross sectional area assuming circular cross section, and then volume by multiplying by fibre length (100 cm)), with n=3 replicates.

4.2.8 Optical microscopy and image analysis

Filaments were imaged using optical microscopy and analysed using ImageJ. Diameter measurements (n= 10 minimum) were taken randomly every 1 mm along the length of 10 x 1cm sections of fibre.

4.2.9 SEM

SEM imaging was used to study the morphology of fibre samples, details of which are given in Section 3.2.9. For cross-sections, fibres were set in bundles using clear nitrocellulose (Rimmel Int Ltd, UK) and prepared using a 0.1mm microtome (MIECO, US).

4.2.10 Filament liquid uptake

Volumetric swelling ratio was measured by using optical microscopy and image analysis to determine dimensional changes based on 10mm lengths of fibres, with n=10 replicates. Diameter and longitudinal dimensions were recorded to ascertain the dry volume of the filaments assuming a cylindrical cross-section, using Equation 4.2

$$V = (\pi r^2) \times l.$$

Equation 4.2

where V= fibre volume, r=diameter cross sectional radius, l=fibre length.

The fibres were measured in their dry state, incubated in 2 ml PBS at 37°C for 24 h and measured again.

The swelling index was calculated using Equation 4.3, wherein Vd= dry volume, Vs=swollen volume, and SI =swelling index.

$$SI\ (vol\ \%) = \frac{Vs - Vd}{Vd} \times 100$$

Equation 4.3

To provide further information on the physical stability, a gravimetric technique was employed, as discussed in Section 3.2.12, which involved treatment of samples for 24 h at 37 °C as part of a hydrolytic degradation study (Siriwardane et al., 2014).

4.2.11 Filament hydrolytic degradation

Samples of 3 - 5 mg of dry collagen fibres were incubated in 2 ml of PBS at 37 ºC for 4 d (n=5). The fibres were retrieved, rinsed with 2 x 2 ml clean PBS and dried. The fibres were weighed in their dry state and their dry degraded state after 24 h of conditioning (20 ºC and 65% humidity). The mass change ratio (MR) was calculated using Equation 4.4 wherein Md=non-degraded dry fibre mass and Mh=hydrolytically degraded fibre mass.

$$MR = \frac{Md - Mh}{Md} \times 100$$

Equation 4.4

4.2.12 Filament collagenase degradation

RTC-4VBC fibres were weighed and incubated for 4 days in 1 ml of 50 mM TES buffer, 0.36 mM CaCl2, 5 collagen digestive units (CDU) (*Clostridium* collagenase, Sigma Aldrich). The enzyme was inhibited using 0.25 M EDTA and centrifuged at 1000 rpm for 10 min and the supernatant discarded. The pellet was washed twice using 3 ml distilled water and twice using 3 ml ethanol then frozen at -80ºC and lyophilised before measuring the degraded weight (Ward et al., 2010). For a positive control RTC fibres spun in EtOH at an extrusion rate of 3.6 ml hr^{-1} and collection rate of 29 m hr^{-1} were used. Weight loss by collagenase degradation was calculated using Equation 4.5, wherein D=% mass loss, Md= dry mass, and Mc= collagenase degraded mass.

$$D = \frac{Md - Mc}{Md} \times 100$$

Equation 4.5

4.2.13 Differential Scanning Calorimetry

Thermal characterisation was performed using differential scanning calorimetry (DSC, Q20 V24.11 Build 124, TA Instruments, USA). Dry samples (5-10 mg, n=3) were hermetically sealed in aluminium pans and thermograms recorded with a nitrogen purge gas flow with a ramp of 10-200 $^{\circ}C$ and incremental rate of 10 $^{\circ}C \cdot min^{-1}$. OriginPro was used to plot DSC thermograms, whereby the denaturation temperature and enthalpy were quantified as the endothermic peak and integration of corresponding thermal transition area, respectively.

4.2.14 Filament tensile properties

An Instron (3340 Series Universal Testing Systems) single filament uniaxial tensile tester was used. Filaments were first conditioned for 24 h at 65% humidity and 20ºC, glued onto 20 mm cardboard frames and imaged under

an optical microscope to ascertain the mean fibre diameter based on a minimum of 15 fibre diameter measurements taken using ImageJ. From that data the mean fibre cross-sectional area was calculated. The frame was placed within the jaws of the machine, cut at both sides and extended at a rate of 20mm/min with a load cell of 2.5N. The initial gauge length was 20 mm.

A total of 20 samples were tested, rejecting any samples which broke within 5mm of the jaws in accordance with BS EN ISO 5079:1996 (BSI, 1996). The yield point was calculated using Meredith's Construction, where a line parallel to the straight line joining the stress-strain curve's point of origin (0,0) to the break point is tangential to the stress strain curve itself (Elmogahzy, 2018). The work of rupture (WOR), defined as the modulus of toughness, or the energy required to break the fibre was calculated using integration software on OriginPro 9.1.

Wet strength of the fibres was also measured. Here, samples were immersed in PBS for 24 hrs at 20ºC and diameters were measured at minimum 10 points along the length of the sample. The filaments were fixed within a frame and measured using the Instron.

4.2.15 Statistical analysis

OriginPro software was used for Normality tests, means comparisons using Tukey testing, and One-Way ANOVA providing normal distribution was observed. Data are presented as average ± standard deviation.

4.3 Results and Discussion

This section details the results from the manufacture and characterisation of spun collagen fibres. For clarity, fibre samples are identified in terms of their composition and spinning conditions used in manufacture according to Table 4.2: Wet-spinning variables used during production of collagen fibres RTC =

Rat tail collagen, 4VBC=4VBC functionalised RTC. Ethanol coagulated fibre=EtOH, PEG/PBS coagulated fibres=PEG.XL=Crosslinked, NXL=Not crosslinked.

Table 4.2: Wet-spinning variables used during production of collagen fibres RTC = Rat tail collagen, 4VBC=4VBC functionalised RTC. Ethanol coagulated fibre=EtOH, PEG/PBS coagulated fibres=PEG.XL=Crosslinked, NXL=Not crosslinked.

Fibre variables					
Material	**Needle diameter mm**	**Extrusion rate $ml \cdot h^{-1}$**	**Rotation rate $m \cdot h^{-1}$**	**Coagulant**	**State of XL**
RTC	0.6	3.6	2.9	EtOH	XL
4VBC	0.8	7.6	3.6	PEG/PBS	NXL
		11.4			

4.3.1 Chemical characterisation of collagen

Following collagen sample preparation the TNBS calorimetric assay indicated 38% ±0.6 functionalisation. This is slightly higher than figures reported by previous researchers using the same method, potentially due to variations in the collagen raw material or slight variances in the temperature (Tronci et al., 2015a). This level of functionalisation is also consistent with the hypothesis proposed in Section 3.3.1 Synthesis of functionalised gelatin that gelatin functionalises more readily than collagen due to fully accessible lysine residues on the randomly organised polypeptide chains (Okamoto and Saeki, 2013).

CD was performed to determine triple helical preservation within spun RTC-4VBC fibres. Typically collagen triple helices exhibit a small positive peak at around 220 nm and a larger negative peak around 197 nm, which correspond to the presence of triple helices and polyproline chains respectively (Hashimoto et al., 2016; Cheng et al., 2011; Tronci et al., 2015a). This is clearly in evidence in Figure 4.1 for all three of the collagen materials, indicating that functionalisation and spinning of the collagen did not disrupt collagen triple helices preservation. By contrast, the negative control, gelatin, showed no positive peak at the 220 nm site (y= -3), which is indicative of denaturation of the secondary protein structure and a lack of polypeptide chain organisation when dissolved.

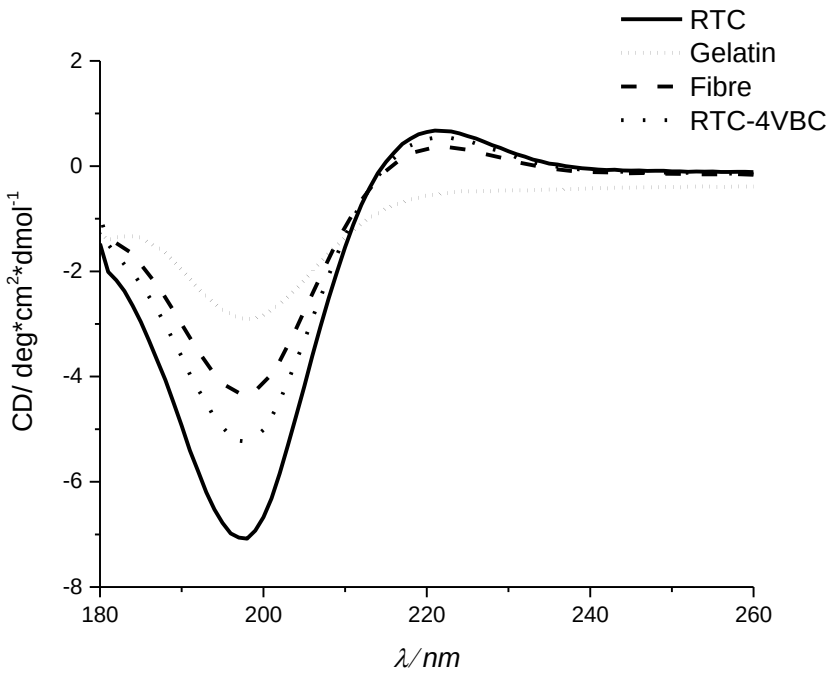

Figure 4.1: Circular Dichroism of gelatin, native RTC, RTC-4VBC, and RTC-4VBC spun fibre

The ratio of positive to negative peak magnitudes (RPN) can be used to compare levels of triple helix preservation within collagen materials once normalised against the RTC RPN (0.103). Fibre triple helical retention (RPN=0.077) was found to be 82%, which is considerably higher than has been reported previously for electrospun fibres (Zeugolis, Dimitrios I. et al., 2008). It is also comparable to previous studies, which reported preservation levels of 79% when RTC was functionalised with 4VBC (Tronci et al., 2015a).

Previous literature has cited a 94% retention of collagen triple helices when spinning a native collagen dope into ethanol, as measured using CD (Arafat et al., 2015). Reduced levels of triple helices in the fibre when compared to this figure is likely due to the functionalisation of the material with the bulky benzyl material. This does not facilitate H-bonding required for triple helical stabilisation and sterically hinders the formation of stable triple helices causing denaturation (Hodges and Raines, 2005; Sakakibara et al., 1973). It could also relate to ethanol precipitation stages undergone by the material which has been shown to cause denaturation (Engel and Bachinger, 2005; Wakuda et al., 2018; Gopinath et al., 2014).

Viscometry of the collagen dope (Figure 4.2A) indicated that the solution was highly viscous relative to the Gel-4VBC solutions reported in Section 3.3.2 Characterisation of wet-spinning dopes. Indeed, it would be more correct to refer to the dope as a suspension of collagen triple helices as opposed to a solution, with the collagen helices existing as a solid dispersion throughout the liquid (Arafat et al., 2015). This is unlike gelatin, which dissolves due to its shorter chain length. This would account for the increased viscosity of the suspension as compared to the gelatin solution, despite the considerably lower concentration. A lower spinning temperature (50 ºC vs 20 ºC) is also likely to contribute to the increase.

ATR-FTIR spectrometry was used to analyse fibres spun into PEG solutions to determine the presence of residual PEG after the washing process (Figure 4.2B). As with the gelatin fibres, residual PEG was found to be present within the fibre samples. This contradicts other literature wherein PEG was claimed to have been removed from the material by a washing process (Shepherd, D.V. et al., 2015). It suggests that an improved washing regime must be incorporated in to the post-processing of as-spun fibres to effectively remove the PEG, or that the PEG polymer chains are integrated within the fibres as seen in the gelatin fibres formed in Section 3.3.2 Characterisation of wet-spinning dopes

The viscosity of the wet spinning dopes was measured to assess the levels of shear force being exerted upon the spinning dopes during extrusion, aiming to draw relationships between solution characteristics and fibre dimensions and morphology. From Figure 3.2, it is apparent that all gelatin dopes behave as a non-Newtonian fluid, whereby an increase in shear rate is corelated with a decrease in shear viscosity (η), in line with previous studies (Hoch et al., 2012; Lee et al., 2016). When the shear rate is increased, gelatin chains disentangle since molecular interactions are attenuated, and the corresponding dope viscosity is reduced. As expected, an increase in Gel-MA concentration resulted in an increase in viscosity, due to the increased chain entanglements and intermolecular interactions (Hoch et al., 2012; Lee et al., 2016).

Figure 3.2. Viscosity curves of wet spinning dopes prepared in 17.4 mM acetic acid solution with varying gelatin building blocks. (—): Native gelatin (15 wt. %). (···): Gel-4VBC (15 wt. %). (– – –): Gel-MA (15 wt. %). (—): Gel-MA (30 wt. %).

With respect to the native polypeptide, functionalisation of gelatin was found to lead to an increased viscosity when dopes with the same gelatin concentration were measured. This observation is likely due to an increase in lysine side chain length in functionalised gelatin, causing more entanglement and interaction between polypeptide chains. Similar trends were also observed when considering dopes of Gel-4VBC, in light of the presence of 4VBC aromatic rings and pi-pi interactions between lysine residues (Tronci et al., 2015a) (Tronci et al., 2016a).

Other than Gel-Native, the wet spinning dopes of Gel-MA were considerably more viscous than the ones containing Gel-4VBC, when the same concentration of polypeptide was considered. This is likely to reflect the increased level of functionalisation in Gel-MA with respect to Gel-4VBC.

Although the original intention was to compare wet spun fibre produced with wet spinning dopes of similar polymer concentrations, it was not possible to

continuously wet spin fibres from dopes of Gel-MA with 15 wt.% concentration (as in the case of dopes of Gel-4VBC) due to dispersion of the wet spinning dope in the coagulating bath. Therefore a dope of 30 wt.% Gel-MA was selected, in agreement with previous literature (Shi et al., 2015).

Such an increase in polypeptide concentration, dope viscosity and internal shear stress during wet spinning was likely to result in reduced alignment of the polypeptide chains in respective wet spun fibres (Wang, Y. et al., 2019). These considerations were experimentally supported by the fact that needle blockages as well as difficulties in achieving continuous fibre formation were encountered during wet spinning of dopes with increased polypeptide concentration.

Subsequent literature has addressed the viscosity of Gel-MA solutions by co-extruding the polypeptide with native gelatin (Wang, Y. et al., 2019). Wang *et al* produced hollow porous fibres by mixing 8 wt. % Gel-MA and 8 wt. % gelatin solutions together and spinning with a PVA core. This modulated the dope viscosity allowing for the solution to be readily spun. The tubular fibres were then heated to above the gelation point, removing the uncrosslinked native gelatin.

3.3.3 Chemical characterisation of wet spun gelatin fibres(Zeugolis, D. I. et al., 2008b).

PEG is biodegradable via molecular hydrolysis and has been FDA approved suggesting that it is suitable for use in medical devices. However, it has been found to stimulate hypersensitivity in a small proportion of the population (Alconcel et al., 2011; Patterson and Hubbell, 2010; Wenande and Garvey, 2016).

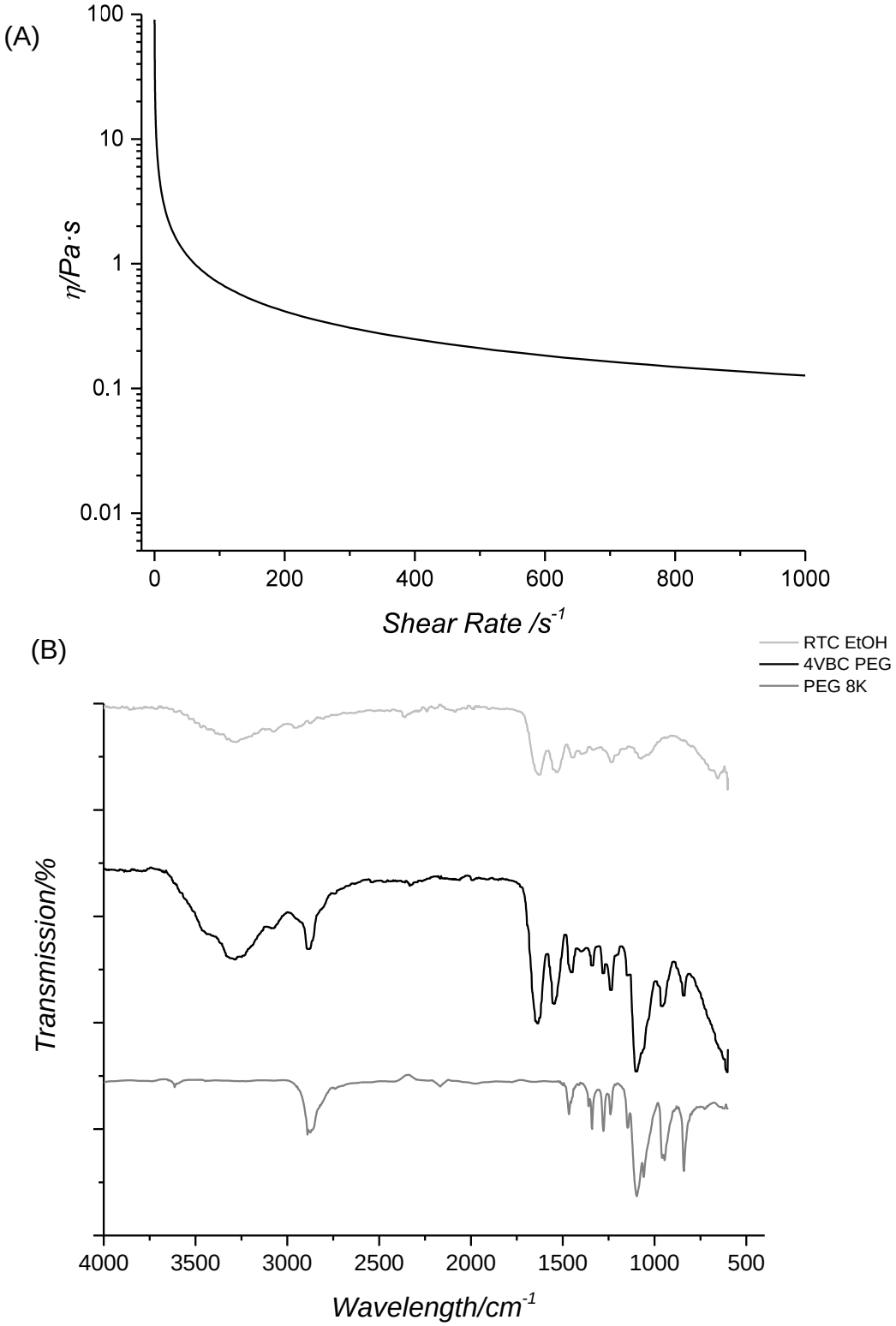

Figure 4.2: A) Viscometry of 1.2 wt. % RTC-4VBC solution; B) FTIR of RTC-4VBC fibres coagulated in EtOH and PEG/PBS compared to PEG 8K

4.3.2 Manufacturing of samples using the ARDS rig and evaluation of resulting fibre morphology

Manufacture of continuous collagen filaments was found to be challenging using conventional wet spinning techniques because of the relatively low coherency and strength of filaments in the coagulation bath, leading to frequent breakages during manufacture. Similarly, use of a syringe and manual wet spinning was not consistent with the ability to scale-up or with the production of uniform fibre morphologies.

To address this, it was hypothesised that an automated rotary deposition system (ARDS) (Figure 4.4) could increase the homogeneity of the fibre morphology by reducing the variations in the rate of rotation that occur when manually spinning. It was also reasoned that it could provide potential to introduce a small degree of fibre drawing, by exploiting drag forces between the polymer liquid and the coagulant without inducing filament breakage. Finally, it was also thought to be a potential basis for in-situ nonwoven fabric formation, by allowing fibres to be deposited on others within the coagulation bath, providing a route for web formation.

Each sample set formed by different conformations of extrusion rate and rotation rate was given a specific “Stretch Factor” (sf) in $m \cdot ml^{-1}$ determined by the rotation rate ($m \cdot hr^{-1}$) divided by the extrusion rate ($ml \cdot hr^{-1}$).

Fibres of different extrusion to collection ratios and manual collections coagulated in EtOH and PEG were collected and analysed to determine the degree to which fibre diameter varied between manually collected fibres and those produced by the ARDS. The results are reported in

The rate of fibre extrusion can be expected to affect the fibre diameter and morphology because of a changes in the shear rate as the dope passes

Table 4.3 and visualised in Figure 4.3

Overall, manually collected fibres produced the highest standard deviation indicating that the manual collection method created fibres with the least uniformity in fibre diameter compared to the ARDS system (Figure 4.3) . Process variables also influenced the resulting fibre diameters, particularly the rates of extrusion and collection in the coagulating bath.

The rate of fibre extrusion can be expected to affect the fibre diameter and morphology because of a changes in the shear rate as the dope passes

Table 4.3: Diameters of manually collected f-collagen fibres and automated ARDS collected fibres SD= standard deviation.

Sample ID	Extrusion/ ml · hr^{-1}	Rotation/ m · hr^{-1}	N	Mean/µm	SD
EtOH 10	**3.6**	**36**	169	**43**	19
EtOH 8	**3.6**	**29**	334	**49**	17
EtOH 4	**7.6**	**29**	104	**56**	29
EtOH 3	**11.4**	**29**	226	**80**	30
EtOH m	**3.6**	**manual**	166	**60**	37
PEG 10	**3.6**	**36**	100	**87**	25
PEG 8	**3.6**	**29**	393	**109**	28

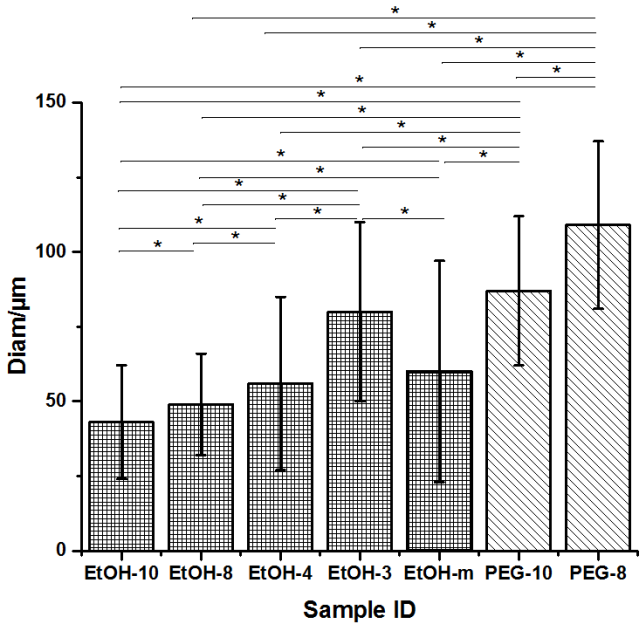

Figure 4.3. F-collagen fibre diameters spun at different extrusion:rotation ratios into either ethanol (EtOH), or PEG/PBS buffer (PEG)

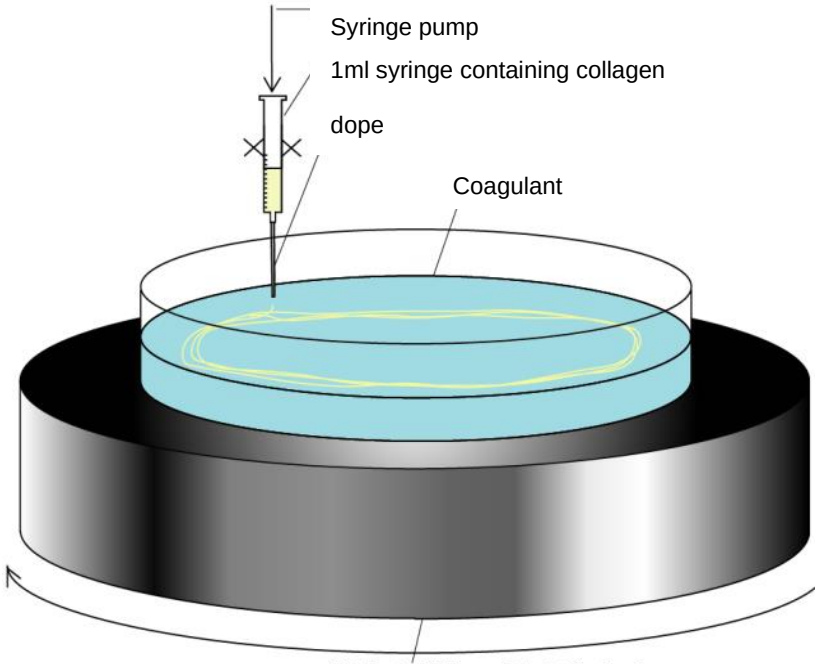

Figure 4.4: Schematic of the ARDS wet-spinning rig

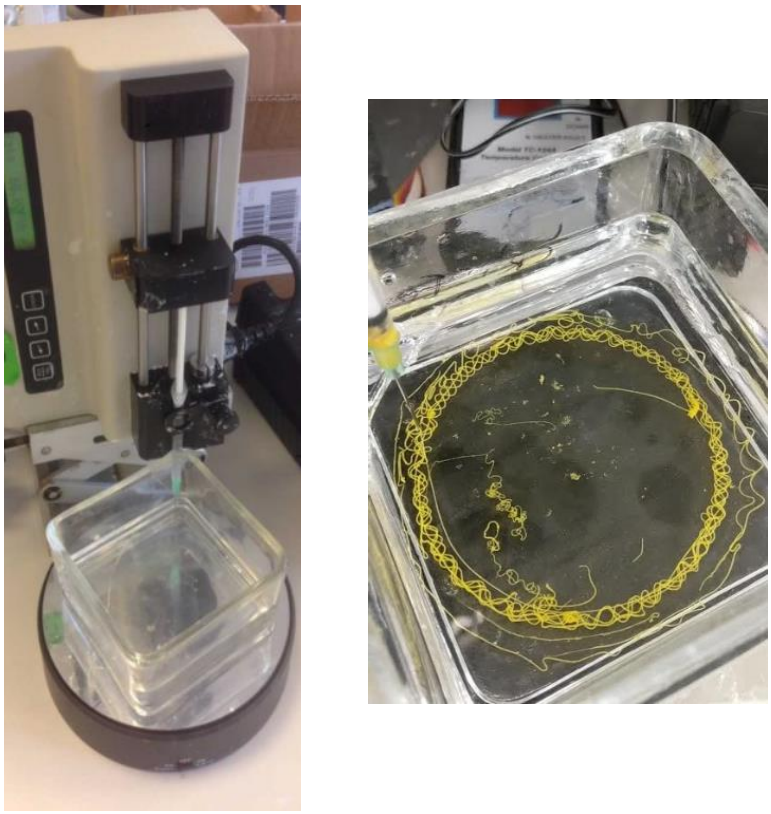

Figure 4.5: Photos of ARDS spinning rig. Dope in right image loaded with yellow pigment to aid fibre visualisation

through the needle, leading fibres spun at a higher extrusion rate to have a larger cross sectional area, due in part to an increase in die swelling (Peng et al., 2009; Wang, K., 2012).

Die swelling, or the Barus effect, occurs when a long chain polymer in the form of liquid (or dope) such as a polypeptide solution is forced through a narrow opening or die, in this case a needle. Within the syringe, molecular chains take up a spherical formation which minimises entropy. When pushed through the narrow die the flow rate is significantly increased causing the conformation to lengthen and the chains to untangle due to the shear stress imparted by the inner surface of the die. After leaving the die, the flow rate slows and the

chains attempt to regain their spherical organisation once again causing a swelling of the dope (Wang, K., 2012). As the flow rate increases more shear force is experienced by the dope and an increase in swelling occurs leading to fibres with larger diameters.

The ARDS collection plate effectively serves as a circular conveyor belt to collect the fibres upon. With the ethanol coagulant the fibres sunk and lightly adhered to the bottom of the collector allowing for some fibre stretching to occur, causing the change in diameter between the EtOH-10 and EtOH-8 fibres (Yaari et al., 2016). The fibres spun into the PEG coagulant floated due to the increased density of the coagulant. This meant that there was negligible stretching and only the shear friction of the rotating liquid served to elongate the fibres. This explains the relatively large diameter and the irregular fibre morphology of these fibres (PEG-10: 87 µm ± 25 vs ETOH-10: 43 µm ± 19 p=0; PEG-8 109 µm ± 28 vs EtOH-8 49 µm ± 17, p=0) (

The rate of fibre extrusion can be expected to affect the fibre diameter and morphology because of a changes in the shear rate as the dope passes

Table 4.3: Diameters of manually collected f-collagen fibres and automated ARDS collected fibres SD= standard deviation.). The increase in rotational

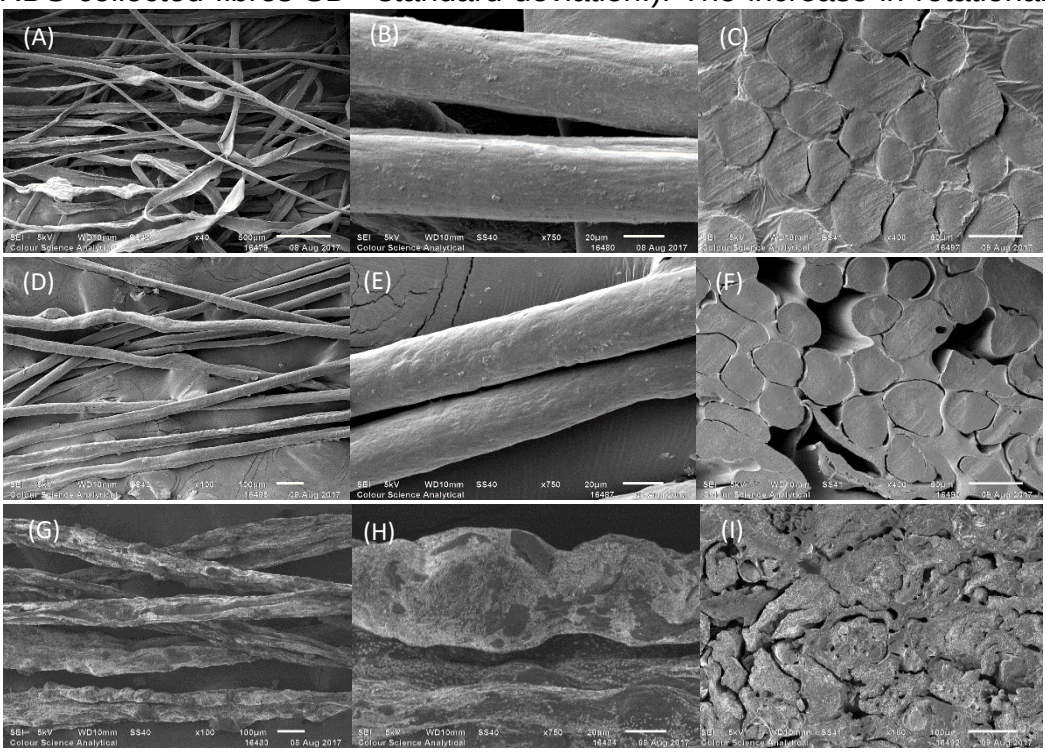

Figure 4.6: SEM micrographs of RTC-4VBC fibres (f-collagen). A-B: EtOH-8; C: cross section of EtOH-8; D-E: EtOH-10; F: cross section of EtOH-10; G-H: PEG-8; I: cross section of PEG-8

speed did affect the PEG-10 and PEG-8 fibre diameters significantly with higher velocities of collection forming finer fibres due to increased coagulant to fibre shear friction (p=0).

SEM imaging revealed a marked contrast in the fibre morphologies in relation to coagulant. EtOH-produced fibres were characterised by a smooth and homogenous surface structure whereas PEG-produced fibres had a more irregular surface and larger diameter variations along their length (Figure 4.6). This is due to the differential viscosities and polarities of the coagulants which will affect the rate of diffusional exchange (Table 4.4: Viscosities of coagulants) (Tronci et al., 2015b). The EtOH-produced fibres were precipitated at a rate preventing core sheath formation. This heterogeneous structure occurs when the diffusional exchange rate is too rapid, resulting in the formation of an outer solid sheath around a porous inner core and an approximately circular fibre cross section.

Cross sectional images of the PEG-produced fibres were difficult to evaluate due to the large voids in the fibres (Figure 4.6I). Initially PEG fibres appeared to have a granular substance on the fibre surfaces, which is likely to be a result of PEG precipitation.

Once washed, the extraneous granular material was removed revealing a highly porous fibre surface suggesting that the relatively high viscosity of the coagulant prevented full diffusional exchange from occurring (Figure 4.7) (Paul, 1968). The discontinuities in the fibre resulting from the pores could

lead to an irregular distribution of stress across the fibre cross section during uniaxial tension resulting in low tensile strength.

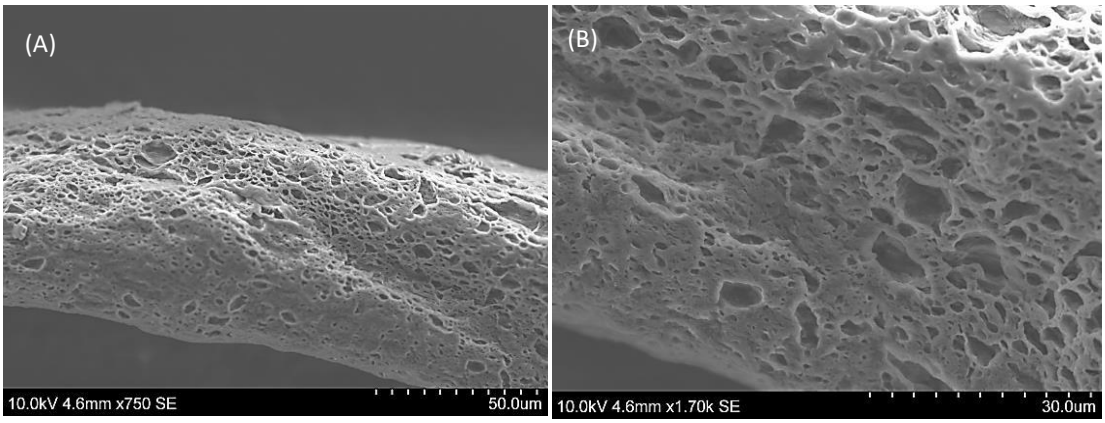

Figure 4.7: SEM micrographs showing morphology of washed PEG-produced f-collagen fibre; A) x750; B) x1.7k

Fibres were found to have a density range of 0.77-2.1 g cm^{-3} (Figure 4.8). Use of a PEG coagulant was shown to significantly reduce the density of the fibres, as suggested by the porous structures in SEM micrographs (PEG-8= 0.77 g cm^{-3} ±0.3 ; EtOH-8= 2.1 g cm^{-3} ±0.4, p=0.001). Altering the extrusion rate also significantly reduced the fibre density between 7.6 and 11.4 ml h^{-1} (EtOH-8:EtOH-4 and EtOH-4:EtOH-3 p=0.02). Although there was likely to be a higher shear stress within the die when spinning the EtOH-3 samples, the collection speed was at its lowest setting, resulting in an overfeed of fibre in to the rotating collector. Under these circumstances, reduced elongation of the polymer stream was expected, and therefore reduced alignment of the protein chains. The effects of overfeed are illustrated in Figure 4.9.

Table 4.4: Viscosities of coagulants

Coagulant	Viscosity / Pa·s
PEG 8k 20 wt. %, 0.1M PBS	0.020
Ethanol	0.001

With reference to Figure 4.8, there was no significant difference between EtOH-10 and EtOH-8 produced fibres, produced using two different collection rates. This may be that the collection rate differences were insufficiently high using the ARDS system to produce a marked change in diameter for this particular dope. In terms of processing stability and homogeneity of fibre morphology, it was established that the most promising collagen fibres were produced using ethanol as a coagulant

Using EtOH as a coagulant wet spun functionalised collagen fibres with uniform morphologies were produced with diameters ranging from 5-200 µm depending on processing conditions. This provides a basis to create fibrous networks with a large surface area over which cells can attach whilst maintaining adequate mechanical strength (Vogt, 2015). The resulting fibres

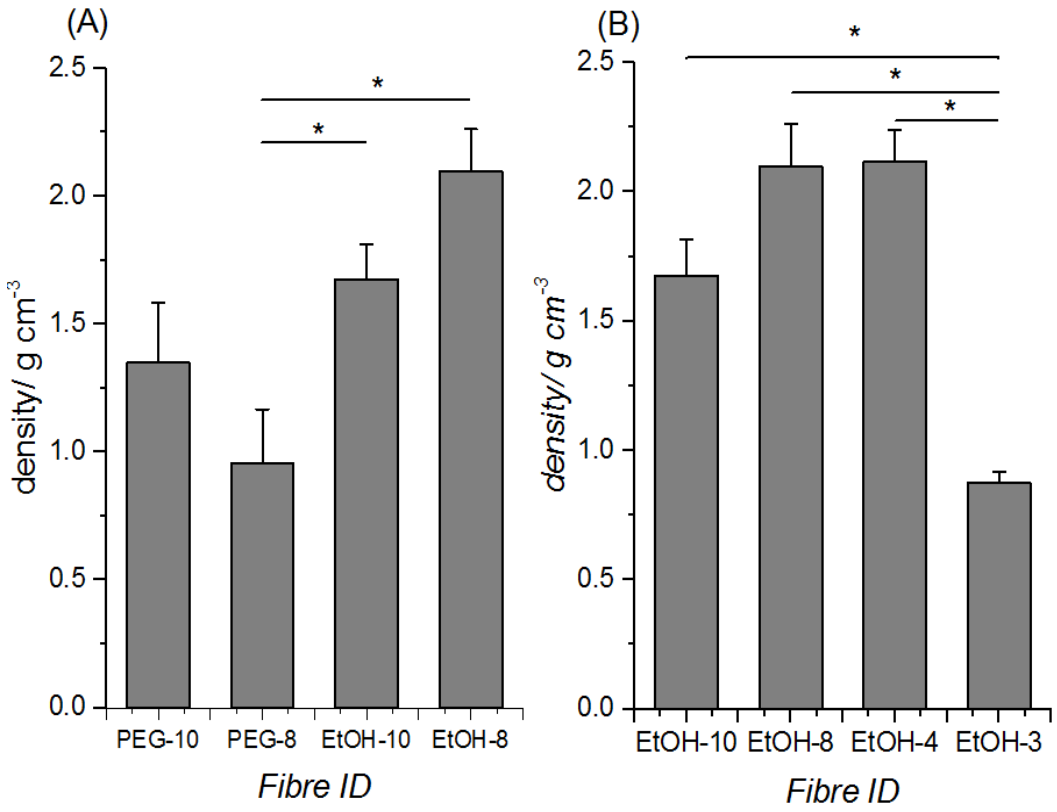

Figure 4.8: F-Collagen fibre densities spun using A) Different coagulants; B) Different extrusion and collection conditions

are free of residual solvent, unlike the PEG coagulated fibres, obviating the potential for cytotoxic or sensitisation responses.

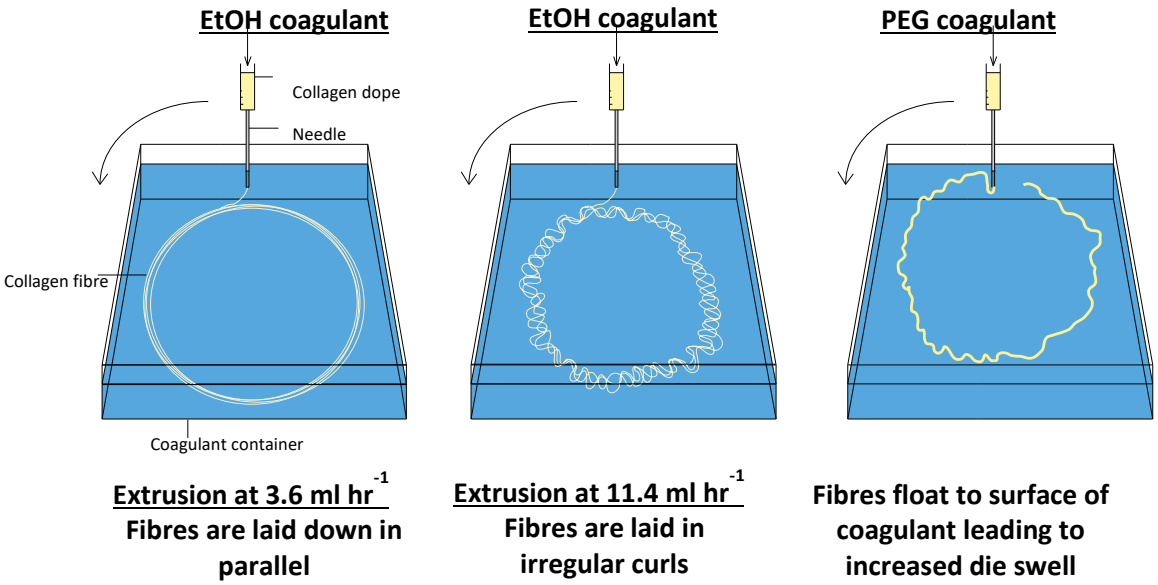

Figure 4.9: Diagram of fibre behaviour during spinning with varied extrusion rates and coagulants.

4.3.3 F-collagen fibre swelling

As an initial step to confirm crosslinking, manually collected fibre segments were exposed to UV light and photoinitiator. Control segments that were not UV-exposed were left to swell for 24 h at room temperature. As expected, fibres which were not exposed to UV exhibited higher swelling that those which did, although this difference was only significant between EtOH coagulated fibres ($p=0$) (Figure 4.1). This may be due to the relatively short incubation time and wet spinning-induced molecular alignment of, and packing between, collagen triple helixes, delaying liquid absorption (Arafat et al., 2015).

There was a significant difference between PEG and EtOH spun non crosslinked fibres observed at room temperature (A) (p=0) and this was also repeated in crosslinked fibres incubated at 37 ºC (p=0.009).

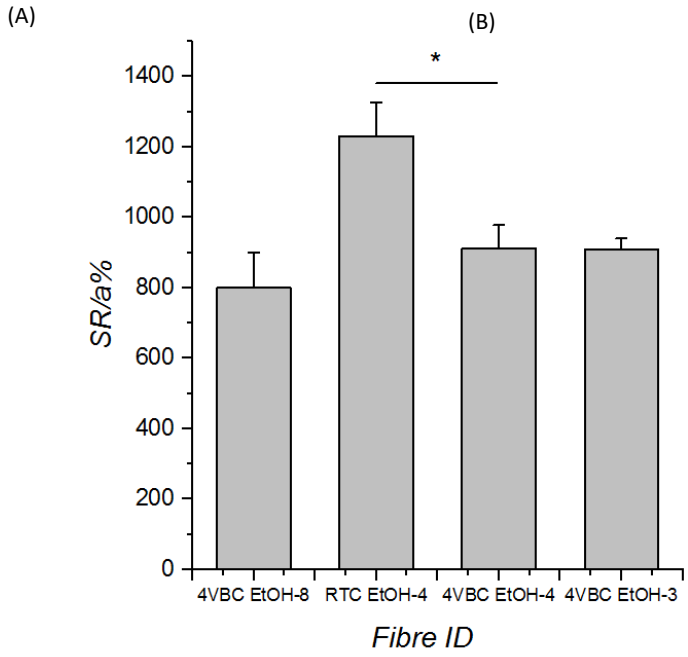

Figure 4.10: Physiological swelling of RTC-4VBC fibres spun at varied stretch factors with RTC control

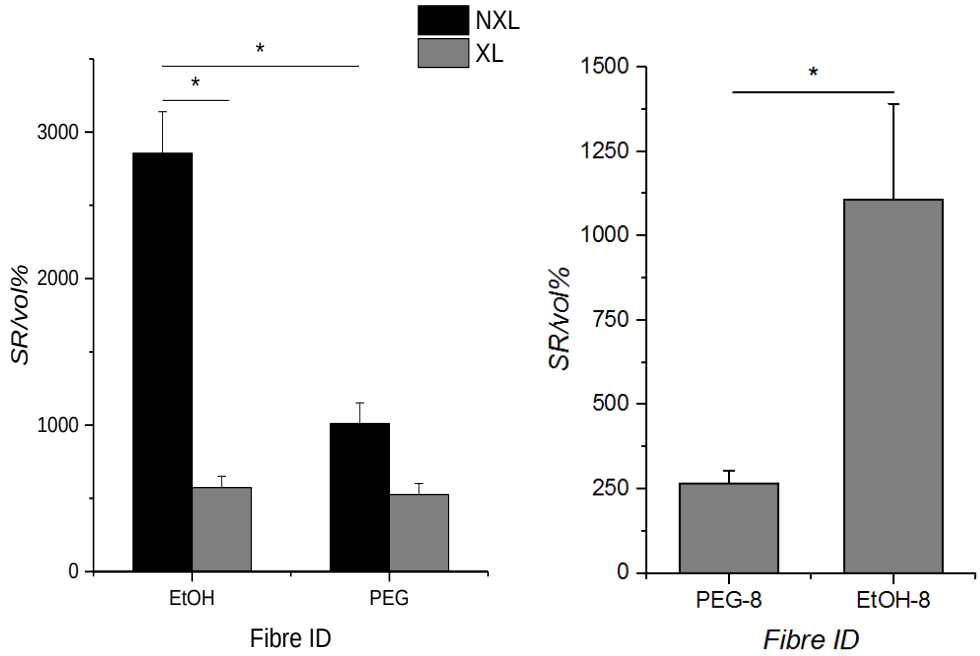

Figure 4.10: A) swelling of crosslinked and non-crosslinked manually spun f-collagen fibres precipitated in PEG and EtOH coagulant at 20ºC for 24 h; B) swelling of crosslinked fibres precipitated in PEG and EtOH coagulant at 37ºC for 24 h

This was unexpected as PEG is a hygroscopic polymer and so was expected to increase the liquid absorbency. Interestingly, the swelling for PEG-coagulated fibres reached 267 vol. % ± 38 compared to that of the EtOH-produced fibres: 1107 vol. % ± 284. This may be related to the lower density and porosity of the PEG-coagulated fibres. Higher porosity could lead to liquid absorption associated increases in fibre volume being accommodated for within the pores of the fibre, thereby not increasing the outer diameter of the fibre. An alternative measurement of swelling could be made by measuring fibre mass before and after equilibration in liquid. However, this process requires a high mass of material for improved accuracy, and risks erroneous measurement of surface liquid mass.

Extrusion and collection rates did not markedly effect swelling of the fibres in simulated physiological conditions (Figure 4.1). Native RTC fibres did exhibit significantly higher swelling ($p=0.049$) compared to its 4VBC crosslinked counterparts. This is likely due to the obstruction of water binding sites by crosslinking moieties as previously discussed in Section 3.3.5 Fibre swelling and nonwoven liquid uptake. Overall, the crosslinked fibres coagulated in EtOH showed excellent swelling capability, which is important for applications such as wound healing, and other clinical uses where fluid management is important.

4.3.4 Fibre tensile testing

Tensile testing was performed on fibres spun with native RTC and UV crosslinked RTC-4VBC fibres spun with different extrusion and ARDS rotation rates to observe any changes in mechanical properties caused by spinning variables. Crosslinked fibres had significantly higher Ultimate Tensile Strength (UTS) ($p=7\times10^{-8}$), modulus ($p=0.002$), strain ($p=0.03$), and work of rupture (WOR) (1×10^{-7}) compared to non-crosslinked RTC fibres recorded in previous literature (Figure 4.11, Table 4.5) (Arafat et al., 2015;

Pins et al., 1997b). This can be attributed to the effects of crosslinking in the functionalised collagen.

Coagulating collagen into ethanol markedly increased the UTS, modulus and WOR with respect to PEG coagulated fibres despite previous reports of PEG acting as a reptating agent, leading to increases fibre strength (Figure 4.11C and D) (Zeugolis, D. I. et al., 2008b). As shown in SEM images (Figure 4.7)

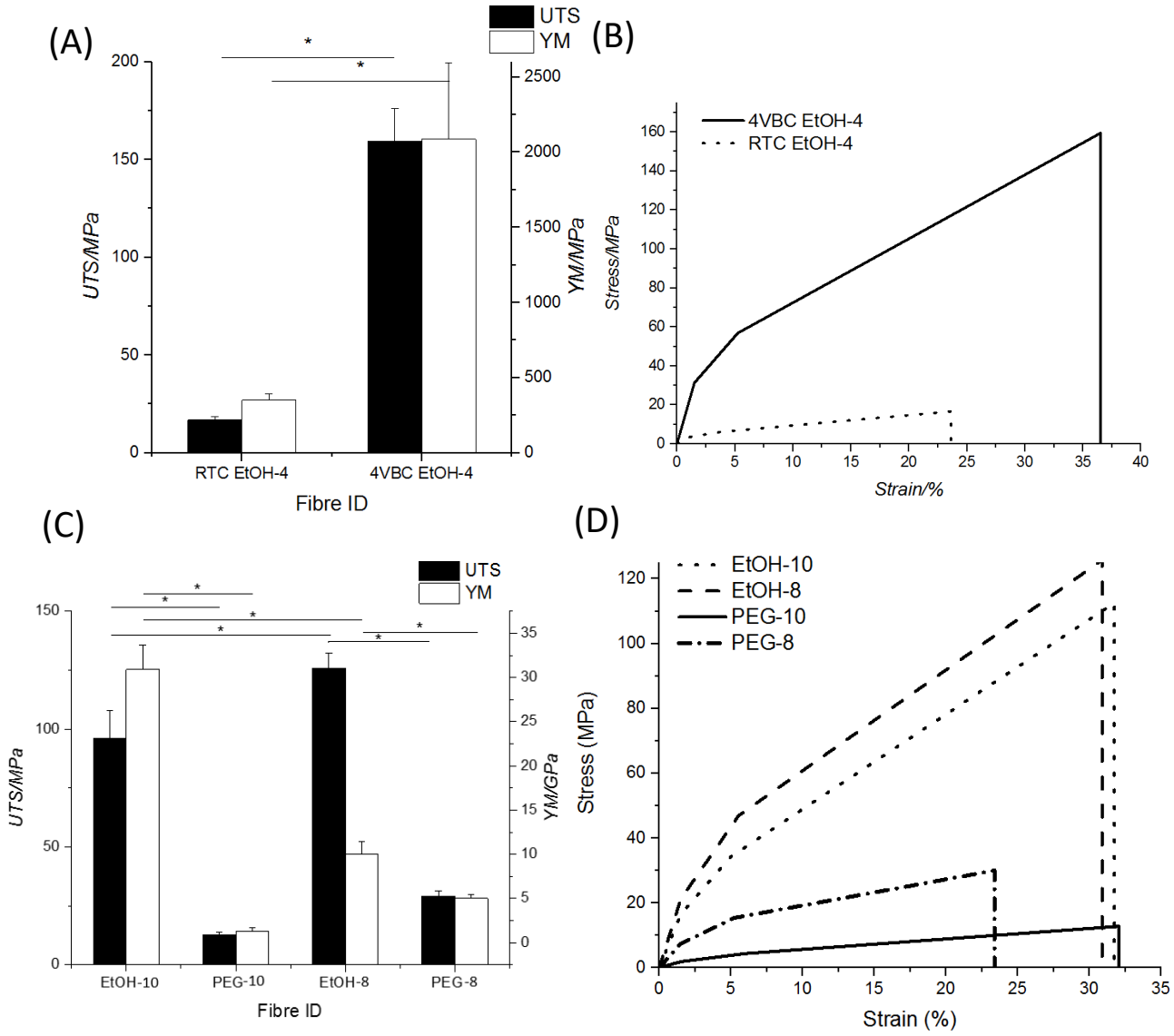

Figure 4.11: A) Tensile strength and moduli and B) Stress strain curves of fibres spun with 4VBC functionalised and native RTC; C) Tensile strength and moduli and D) Stress strain curves of f-collagen fibres spun with PEG and EtOH coagulants.

PEG fibres were extremely porous leading to heterogeneities sufficient to adversely affect breaking strength. The potential for tensioning of the polymer stream between the needle tip and coagulation bath during spinning was not possible due to the low density of fibres and floatation on the surface of the coagulant.

By contrast EtOH coagulated fibres were fully immersed by the coagulant, in some cases to the bottom of the coagulation bath, such that they partially adhered and allowing greater elongation of the filament. Such uniaxial tension would be expected to contribute to molecular alignment of the collagen subunits and lead to an increase in fibre crystallinity (Pins et al.,

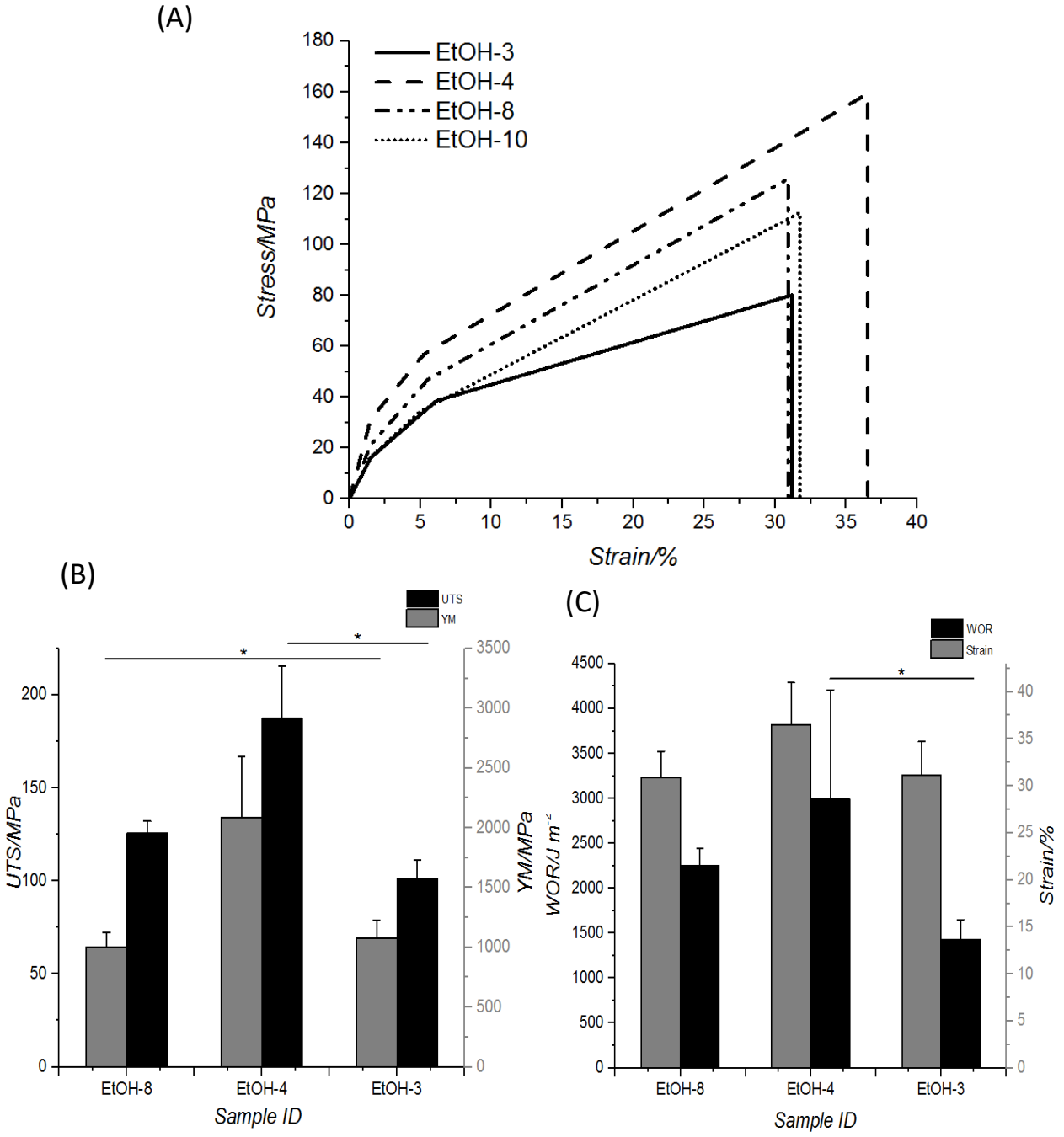

Figure 4.12: A) stress strain curves; B) UTS and YM; C) WOR and strain of f-collagen fibres spun in EtOH with varied extrusion and collection rates

1997b; Yaari et al., 2016). Accordingly, it was concluded that the use of PEG

as a coagulating medium was not appropriate for the ARDS method of spinning.

Fibres spun into EtOH using a high collection rate of 36 m hr^{-1}(EtOH-10) were significantly weaker than those collected at 29 m hr^{-1} (EtOH-8),UTS of 96 MPa ±12 vs 126 MPa ±6 . This is surprising given that elongation of the fibre would be expected to increase intermolecular alignment (Haynl et al.,

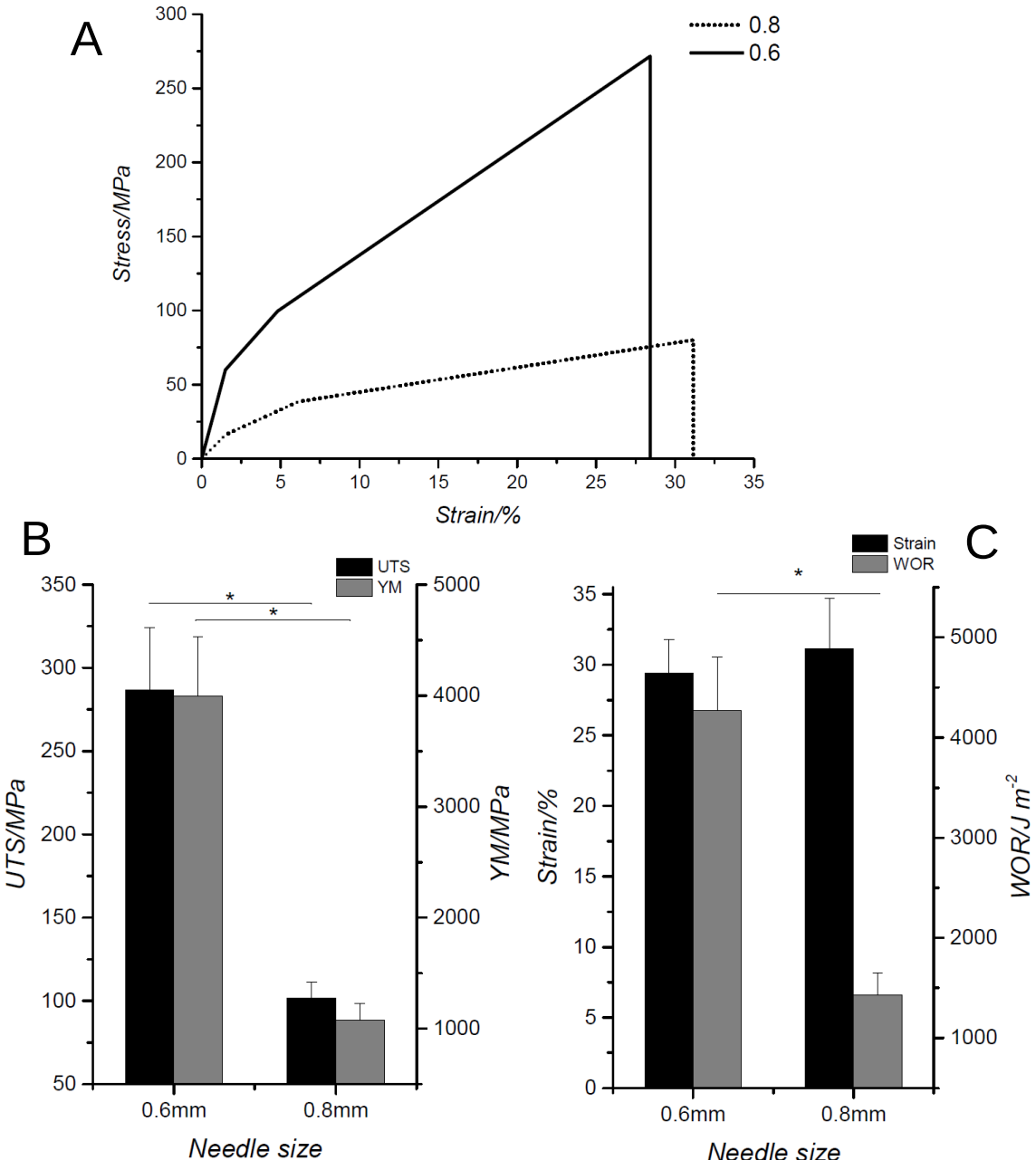

Figure 4.13: A) Stress-strain curves; B) UTS and YM; C) WOR and strain of f-collagen fibres spun using 0.6mm and 0.8mm needle diameters

2016). However, as reported by Yaari *et al*, over a certain range of elongations, microscopic imperfections can start to emerge (Yaari et al., 2016), which can reduce the overall strength of the fibre. It is possible that the level of stretching exerted by the faster collection rate introduced structural defects. However, these were insufficient to prevent an increase in Young's Modulus. The rate of dope extrusion also affected the mechanical properties of the fibres (Figure 4.12).

Increasing the extrusion rate is known to be capable of increasing molecular alignment due to an increase in the shear stress within the die. However, as the collection rate was constant for all three extrusion rates this meant that the relative flow rate was lower for fibres extruded at higher rates thereby potentially inducing die swelling and a low level of fibre elongation. The highest UTS was observed for sample EtOH-4 with a UTS, YM, strain at break, and WOR of 187 MPa ±28, 2.1 GPa ±0.5, 37% ±5, and 2998 J m^{-2} ±1208 respectively. Here there was a balance between extrusion and collection rate; a higher extrusion rate than EtOH-8 creating higher shear force on the dope causing increased fibrillary alignment, and a relative collection rate higher than EtOH-3 allowing for adequate flow rate to attenuate die swelling (Peng et al., 2009). An overview of mechanical properties of fibres in dry and hydrated forms are given in Table 4.6.

For future experimentation increasing the rotation speed of the ARDS system would allow higher extrusion rates to be used without inducing die swelling associated reductions in strength. This would hypothetically permit the production of stronger fibres at higher extrusion rates.

4.3.5 Effects of needle diameter on f-collagen fibre properties

Needle diameter was reduced from 0.8mm to 0.6mm for one set of drawn fibres (EtOH-8) to study any differences in mechanical properties. As the needle diameter decreased, there was an increase in the UTS ($p=1\times10^{-7}$), YM ($p=6\times10^{-5}$) and WOR ($p=1\times10^{-4}$) of the fibres as shown in Figure 4.13.

The change of UTS from 126 MPa ± 6 to 286 MPa ± 38, was a 227% increase, suggesting an increase in the crystallinity of the fibre. Decreasing the internal diameter of the extrusion nozzle reduces the cross-sectional area through which the dope flows thereby increasing the internal die pressure. This would result in higher shear forces on the extruded dope. This in turn can be expected to lead to an increase in molecular chain alignment as well as a reduction in fibre diameter which was observed here (Peng et al., 2009).

The mechanical properties observed herein were higher than others observed in previous reports on wet spun collagen fibres (Arafat et al., 2015; Zeugolis, D. I. et al., 2008b; Zeugolis et al., 2009b; Siriwardane et al., 2014). It is also worth noting that this was achieved without optimisation of filament elongation or drawing. Further increases in strength could therefore reasonably be expected by modulation of the collection rate, post-drawing or the use of even smaller nozzle diameters to achieve values similar to those reported by other literature(Haynl et al., 2016; Yaari et al., 2016). A comparison of the mechanical properties of collagen fibres reported in the literature is given in Table 4.6.

With respect to the tensile properties of other fibres utilized for medical device purposes the collagen fibres spun with the 0.6mm diameter needle are comparable. Polylactic acid, frequently used for medical implants due to its biodegradability has had a reported UTS of 48 MPa, and YM of 3100 MPa (Ovlaque et al., 2019). Thermoplastic polypropylene (PP) is stronger, however has none of the biocompatible qualities which makes collagen so attractive. Research has reported PP to have a UTS of 370 MPa and YM of 3250 MPa (Juhar et al., 2001). Finally, Bombyx mori silk, an increasingly popular fibre for tissue regenerative scaffolds has extremely high tensile properties of 650 MPa UTS and 16000 MPa YM (Poza et al., 2002).

Though it is important for fibres to have adequate mechanical strength to be able to be processed on machinery for knitting or braiding, for example, It should be noted that the differentiation of cells is significantly affected by the mechanical properties of their surrounding scaffolds. Therefore, though silk may be of superior mechanical strength compared to a collagen fibre, it may not be the best material for forming scaffolds to biomimick elastic, or soft tissue such as neural matter or skin.

Table 4.5: Ultimate tensile strength (UTS), Young's modulus (YM), Strain (%), and Work of Rupture (WOR) of dry wet-spun f-collagen fibres

Fibre ID	UTS MPa	YM GPa	Strain %	WOR $J \cdot m^{-2}$
EtOH-10	96 ± 12	3.1 ± 0.1	32 ± 2	1914 ± 165
EtOH-8	126 ± 6	1.0 ± 0.1	31 ± 3	2254 ± 192
EtOH-4	187 ± 28	2.1 ± 0.5	37 ± 5	2998 ± 1208
EtOH-3	102 ± 10	1.1 ± 0.2	31 ± 4	1432 ± 217
EtOH-8 (0.6mm needle)	286 ± 38	4.0 ± 0.5	29 ± 2	4267 ± 537
PEG-10	13 ± 1	0.1 ± 0.03	32 ± 3	217 ± 28
PEG-8	29 ± 5	0.5 ± 0.04	23 ± 2	437 ± 43
RTC EtOH-4	17 ± 2	0.4 ± 0.04	25 ± 8	267 ± 144

The tensile strength of the fibres once hydrated which should be taken into account. Although the fibres in this study exhibited excellent dry strength, in physiological conditions fibres are swollen with liquid, which is likely to negatively impact UTS and Young's modulus. A human patellar tendon has a UTS and YM of 60 MPa and 513 MPa respectively with a strain of 18% and achilles tendons have a stress at break of 81 MPa, YM of 550 MPa, and strain of 21% (Hashemi et al., 2005; Shaw and Lewis, 1997).

Hydration significantly decreases their tensile strength so it is vital to ascertain the fibre wet strength with further experimentation (Yaari et al.,

2016; Zeugolis et al., 2009a). Failure to do so can lead to inadequate mechanical stability being available during clinical applications. For certain potential applications of collagen filaments, such as in tendon and ligament replacement, the high mechanical forces that are required could otherwise lead to total device failure (Shaw and Lewis, 1997; Hashemi et al., 2005).

4.3.6 Hydrated tensile properties

Tensile testing of hydrated crosslinked fibres (n=13) showed a UTS of 3.3 ± 0.6 MPa and Young's Modulus of 0.6 ± 0.3 MPa (). This was significantly higher when compared to the non-crosslinked samples due to the absence of stabilising covalent bonds between the collagen chains in the non-crosslinked samples (UTS of 0.62 ± 0.3 MPa, p=0.002; YM of 0.4 ± 0.2 MPa, p=0.01, n=10).

The non-crosslinked samples did have a higher water content than the crosslinked fibres, directly affecting the UTS results due to the higher cross sectional area used to calculate tensile strength. However, the crosslinked samples showed a significantly higher force was required to break the fibres (3.9 ± 3.4 cN vs 1.8 ± 0.5 cN, p=0.048). This indicates that, when normalized for varied water content levels, crosslinked fibres were still stronger than non-crosslinked fibres.

Fibre strain was significantly higher in the non-crosslinked samples (6.1 ± 2.4 %, vs 8.1 ± 5.8, p=0.02), likely due to the reduced resistance to chain slippage within the non-crosslinked material.

As expected, the hydrated fibres exhibited lower mechanical property values compared to their dry-state due to fibre swelling. This increases the space between collagen chains and replaces inter-chain H-bonding with water to collagen H-bonding. These factors allow chains to more readily slide over one another and break under a lower stress. This is reflected in the stress-

strain curves in . These show a j-shaped curve for the hydrated fibre, contrasting to the s-shaped curve seen in the dry fibre tensile testing. This is consistent with findings in previous literature, using different cross-linking strategies (Zeugolis et al., 2009a; Lu et al., 2020).

Relative to previous wet-strength testing of collagen fibres, as reported in Table 4.6, these fibres were weaker and more easily deformed. The low tensile strength of the hydrated fibres is likely due to low levels of 4VBC crosslinking with two potential causes at the root. Firstly, low levels of collagen-4VBC functionalisation resulting in fewer covalent crosslinks. As indicated in Section 4.3.1, TNBS characterisation showed a 38% lysine functionalisation level. This level is considerably lower than literature reported methacrylation levels (91%±7) and so would lead to a lower crosslinking density (Tronci et al., 2015a).

Table 4.6: Ultimate dry tensile strength and Young's Modulus of wet spun f-collagen fibres reported in the literature in dry and hydrated states (nr= not reported)

Paper	Spinning parameters	Dry UTS (MPa)	Dry YM (GPa)	Hydrated UTS (MPa)	Hydrated YM (MPa)	Hydrated Strain (%)
(Yaari et al., 2016)	GT XL	nr	nr	378 (±nr)	3.5 (±nr)	138 (±nr)
(Yaari et al., 2016)	EDC/NHS	nr	nr	40 (±nr)	nr	nr
(Haynl et al., 2016)	Phosphate, TES, NaCl, PEG microfluidics	383 ± 85	4.1 ± 0.5	nr	nr	nr
(Caves et al., 2010)	GT XL; Phosphate TES, NaCl, PEG spun	94 ± 19	0.8 ± 0.2	nr	nr	nr
(Siriwardane et al., 2014)	Genipin and GT XL; NH_4OH, Acetone spun	262 ± 62	1.3 ± 0.2	nr	nr	nr
(Lu et al., 2020)	EDC/NHS	nr	nr	26 (±nr)	0.1 (±nr)	nr
(Zeugolis et al., 2009a)	GT	32 ± 10	34 ± 19	11 ± 3	7 ± 3	43 ± 4
(Zeugolis et al., 2009a)	EDC/NHS	126 ± 39	58 ± 25	3 ± 0.6	2 ± 0.3	54 ± 11
(Zeugolis, D. I. et al., 2008b)	Native collagen fibres	255 ± 89	3.3 ± 1.1	nr	nr	Nr
(Zeugolis, D. I. et al., 2008b)	PEG spun	136 ± 57	0.9 ± 0.7	nr	nr	nr
Current study	4VBC XL; EtOH spun	286 ± 38	4.3 ± 0.5	3 ± 0.6	0.6 ± 0.3	6 ± 2

This could be addressed by increasing the molar excess of 4VBC during the collagen functionalisation reaction. However, as also shown in CD testing in Section 4.3.1 the bulky aromatic ring within the 4VBC molecule disrupts the helical organisation of the collagen chains, causing denaturation. Therefore, a balance would need to be found between increasing crosslinking density, and preventing denaturation thereby altering the native material organisation.

Other potential causes could be that the penetration of the photoinitiator into the collagen fibres was not enough to reach internal 4VBC moieties, or that the I2925 photoinitiator was not effective enough at the 365nm wavelength. In this scenario, levels of functionalisation are adequate to form a stable collagen fibre upon crosslinking. However, the grafted moieties within the centre of the circular fibre are not activated by the UV light, leading to unreacted 4VBC moieties and a low density of crosslinks within the core of the fibre. This could be improved by utilizing other photoinitiators such as lithium acylphosphinate

(LAP) which have been shown to have faster reaction kinetics and from more stable collagen based materials (Tigner et al., 2020).

Additionally, an extra step could be incorporated whereby the fibres are equilibrated in water to induce swelling prior to photoactivation. This would improve the access of the aqueous solution carrying the photoinitiator into the fibre, the higher levels of fibre translucency would allow improved UV penetration. A disadvantage of this step would be that the swelling of the fibres would increase the distance between collagen polypeptide chains. This may cause more intra-chain bonding than inter-chain bonding which could attenuate the strength of the fibre.

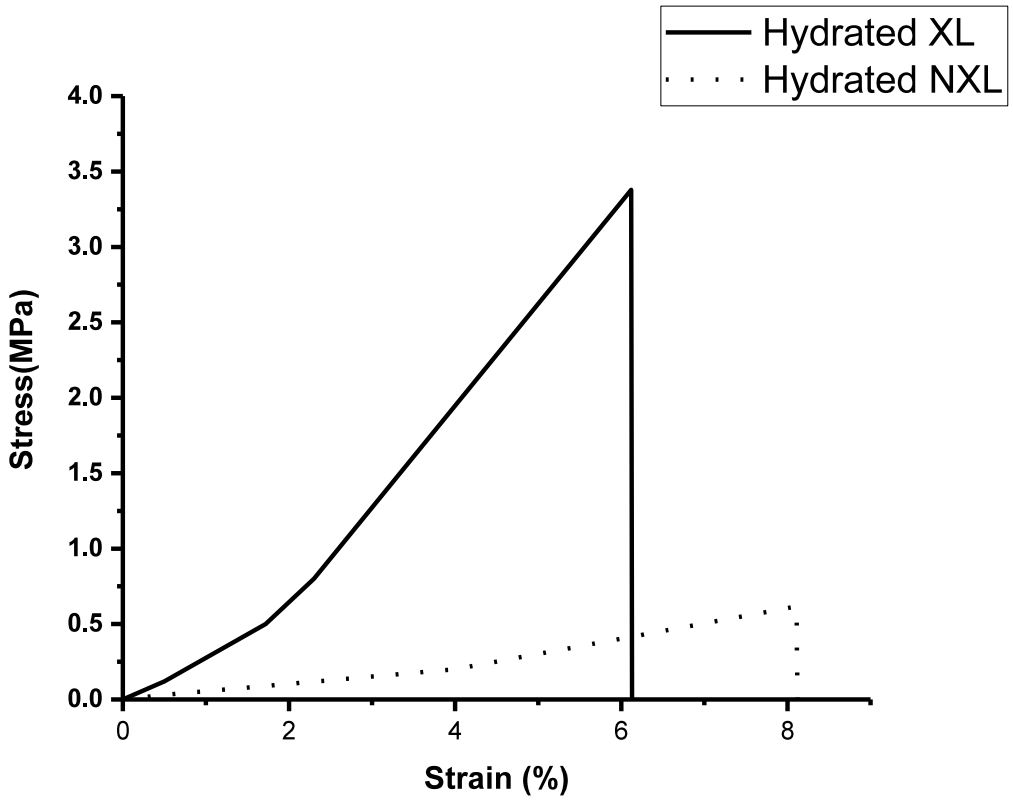

Figure 4.14: Stress-strain average curve of hydrated crosslinked (XL) and non-crosslinked (NXL) f-collagen 4VBC fibres

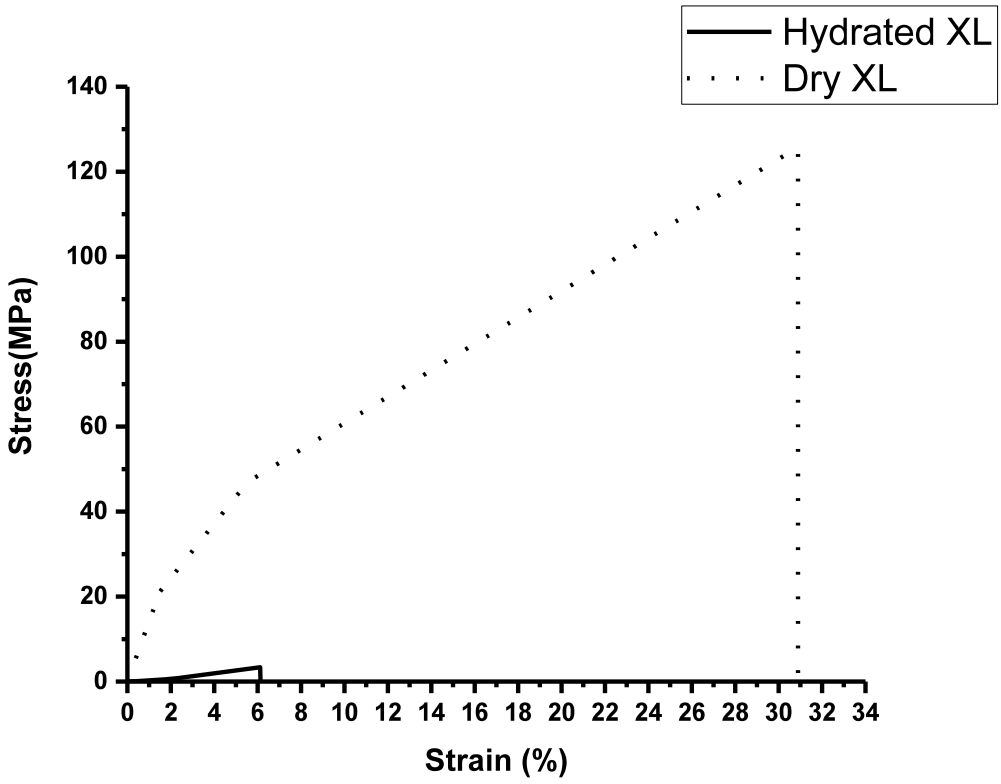

Figure 4.15: Stress-strain average curve of hydrated and dry RTC-4VBC EtOH-8 f-collagen fibres

4.3.7 Thermal characterisation

DSC was performed to define the thermal resistance of the as-spun regenerated functionalised collagen fibres (Table 4.7). Previous literature has reported the thermal denaturation temperature of collagen (T_d), the point where collagen helices begin to unfold, as 55-67ºC (Arafat et al., 2015; Tronci et al., 2015a; Miles, C.A. and Ghelashvili, 1999). Thermal enthalpy, or the amount of energy required to break intermolecular bonds, has been reported as significantly higher than most proteins at roughly 70 J/g due to the high levels of energy needed to uncouple the α chains in the triple helix (Miles, A.C. and Bailey, 1999; Skrzyński et al., 2009). Enthalpy is generally associated with the level of fibre crystallinity (Mai et al., 2015). Needle diameter, collection and extrusion rates were varied to determine any corresponding changes in enthalpy or denaturation temperature. Results can be seen in Table 4.7.

Table 4.7: Denaturation temperature (Td) and enthalpy (ΔH) of f-collagen fibres spun under different conditions (nozzle diameter shown in brackets)

Sample ID	T_d/ ºC	ΔH/ J g^{-1}
EtOH-10	77	306
EtOH-8	69	256
EtOH-4 (0.8mm)	82	316
EtOH-3	78	414
EtOH-4 (0.6mm)	69	260

No overall trends were observed with respect to needle diameter, or extrusion rates. This was likely due to the lack of sensitivity of the machine. Denaturation temperatures ranged from 69-82ºC, comparable to literature . Enthalpies varied from 260-414 J g^{-1} (Skrzyński et al., 2009; Gabbott, 2008). The relatively large enthalpies reported are in likely due to limitations in the pan crimping mechanism. Literature shows that using a

pan which is not fully sealed leads to a broad thermal peak resulting in large enthalpies (Mukherjee and Rosolen, 2013).

4.3.8 Hydrolytic degradation by water and collagenase

Hydrolytic degradation refers to the breakdown of materials due to immersion in liquid causing breakage of amide bonds by the addition of water. Assessing these material properties are vital in the context of its potential end use in a medical device. For instance, if the material is used as a wound dressing it will have to maintain its mechanical efficiency *in situ,* withstanding high levels of liquid wound exudate and body temperatures. If the dressing dissolves or deteriorates under these circumstances then it is not fit for purpose.

In the first of these studies collagen fibres were incubated in PBS at pH 7.4 at 37 °C to observe their mass loss over a week. Results showed no significant difference between crosslinked fibres of varied extrusion rates. However, a significant increase in mass loss in uncrosslinked RTC fibres (35

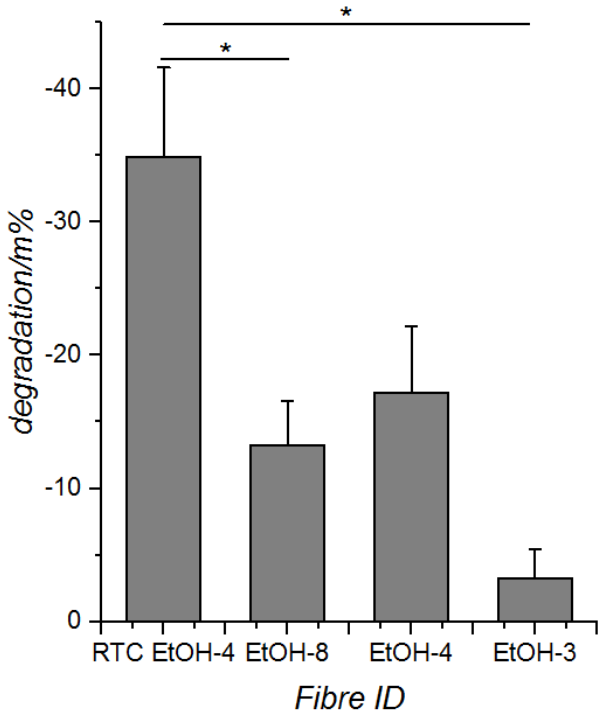

Figure 4.16: Hydrolytic degradation of f-collagen fibres after 4 days of incubation in PBS at 37 ºC

± 7 %) when compared to crosslinked fibres ($p<0.05$) (Figure 4.16). This is due to lack of stabilising crosslinks which improve wet stability.

This trend be seen in work by Lu *et al* where rapid native collagen degradation was observed. After 55 hours uncrosslinked collagen was significantly more degraded than collagen fibres in their crosslinked form (Lu et al., 2020).

The second study observed the degradation levels of collagen fibres when incubated in collagenase solutions (5 CDU of Clostridium collagenase). Degradation by collagenase for 4 days showed almost complete degradation levels for uncrosslinked, native collagen fibres due to lack of stabilisation by

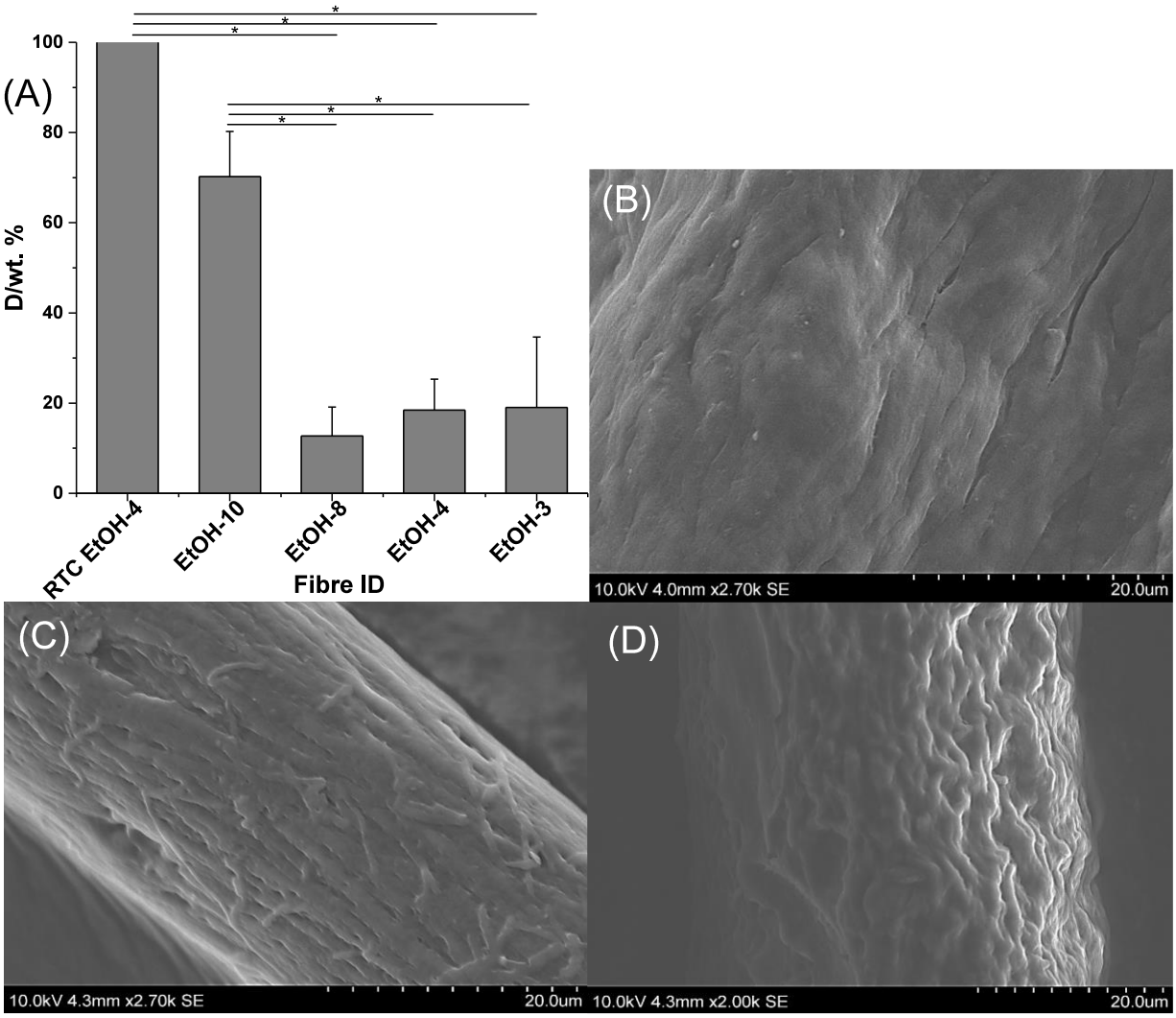

Figure 4.17: A) % mass loss of collagenase degraded f-collagen fibre; SEM micrographs post degradation of B) EtOH-4; C) EtOH-8; D) EtOH-10

crosslinks. This allows for the collagen to be easily degraded (Figure 4.17A). Other significant differences were seen between EtOH-10, a fibre spun with the highest levels of fibre stretching, (70% ±10) and all other fibres (EtOH-8 p=0.01; EtOH-4 and EtOH-3 p=0.02).

Figure 4.17B clearly shows this disparity, with relatively little degradation being shown in EtOH-4 fibres increasing to large grooves formed by degradation in EtOH-10. These images can be compared to those in Figure 4.6A-F where the fibre surface is smooth and absent of ridges to show the extent of degradation.

This higher level of mass seen in EtOH-10 samples loss is likely due overstretching within the fibre (as seen during tensile testing) leading to faults within the structure. These would act as toe holds for collagenase degradation. The EtOH-10 fibres also have a lower fibre diameter, and so a higher surface area to volume ratio. Therefore there is a larger area over which collagenase can catalyse the breakdown of collagen.

In other, non-overstretched samples it seems that the increase in the collagen alignment offsets the effects of the high surface area to volume ratio of a smaller diameter fibre. This explains why EtOH-8 fibres do not show a significantly different mass loss to EtOH-3 and EtOH-4. Interestingly EtOH-8 (Figure 4.17C) image shows some fibrillation, possibly caused where the collagenase has acted to almost strip fibrils off the fibre. A similar pattern is seen in native collagen fibres when degraded with cysteine proteases (Panwar et al., 2013).

This experiment serves to show the rate of degradation of the material when exposed to collagenase enzymes such as MMPs which are present physiologically. Considering the potential end use of this fibre as a wound dressing or implant this is crucial to quantify. With many collagen implants

and dressings biodegradation and resorption is intended. The rate of this process should ensure the product has time to take the crucial steps of wound healing before being degraded. However it should also not remain whole in the insertion site for too long, a possibility which risks encapsulation and rejection from the body.

Collagenase acts by targeting specific sequences in the collagen peptide chain cleaving the peptide bond by insertion of a water molecule. This serves to break the chains down into smaller segments increasing the surface area of the substrate as a whole. Clostridium collagenase, as used in this experiment, cleaves collagen at all 3 helical domains within the collagen chain forming 4 products. Mammalian collagenase is less potent cleaving the molecule at one site to make one quarter and three quarter collagen fragments. Therefore the rate of degradation in this *in vitro* will be significantly higher than the *in vivo* degradation (Gorgieva, 2011; Agren et al., 1992).

Although the *in vitro* conditions of this experiment do not relate directly to the *in vivo* this work does serve to show the importance of crosslinking within collagen materials. It is vital to control collagen degradation within implants as otherwise rapid *in situ* degradation due to lack of chemical stabilisation can occur (Enea et al., 2013). This causes the device to fail.

4.3.9 Feasibility of one-step manufacturing of f-collagen crosslinked fibres

To investigate whether a new, one-step wet spinning and crosslinking manufacturing process was feasible a truncated two-step technique was performed. F-collagen fibres were spun directly into a 90 vol. % EtOH, 1 wt. % photoinitiator solution and then exposed to UV light, as shown in Figure 4.18. The fibres were spun at a Stretch Factor of 8 m · ml^{-1} This approach prevented the need for a third step involving transferring as-spun and dried fibres to another bath between spinning and crosslinking, as done in Section 4.2.4, such that only crosslinked fibres were manually handled leading to fewer breakages.

To determine if crosslinking had occurred using this procedure, the swelling of fibres was compared after incubation in PBS at 37 ºC for 24 h (n=5). Crosslinking was successfully confirmed, with statistically lower swelling in the two step formation process as compared to swelling of fibres formed into the photoinitiator solution and not exposed to UV (p=0) as seen in Figure

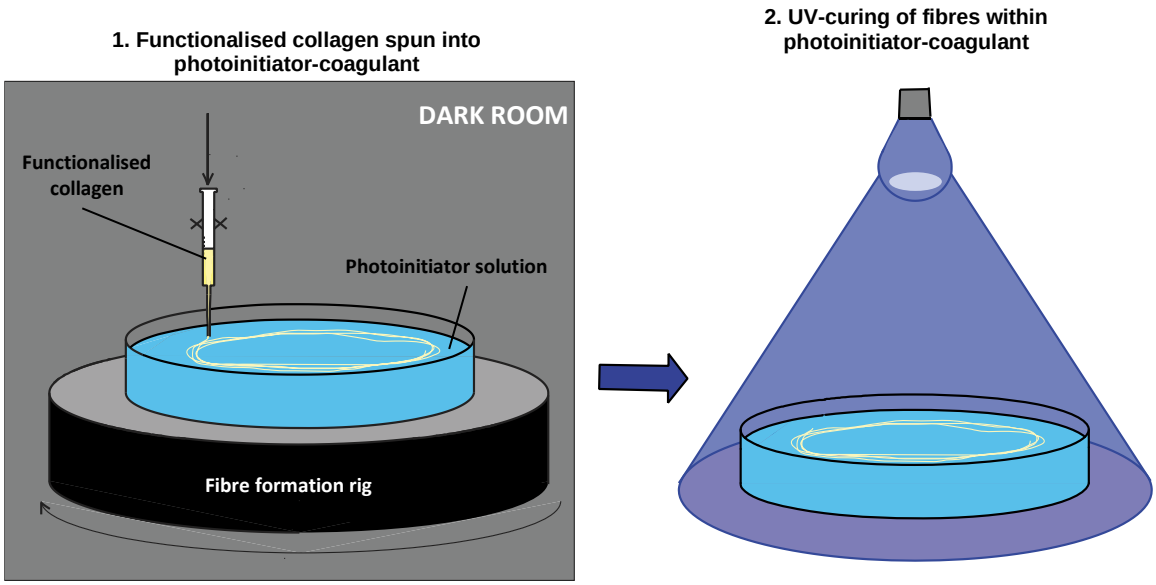

Figure 4.18: Two-step formation of crosslinked f-collagen fibres assessing the feasibility of one-step spin and crosslink manufacturing

4.19.

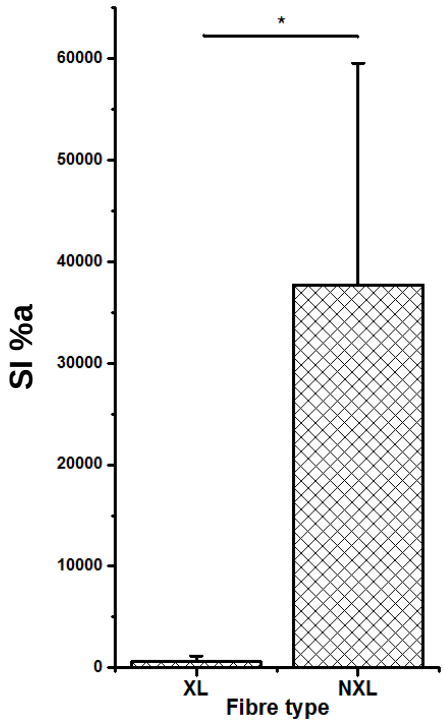

Figure 4.19: Swelling Index (a%) of crosslinked (XL) RTC-4VBC f-collagen fibres spun utilising the intermediate 2-step spin and crosslink manufacturing technique as shown in Figure 4.18. Non-crosslinked (NXL) fibres were spun as shown, but not UV-irradiated. Fibres incubated in PBS for 24hr at 37º C

Fibres spun and crosslinked in the two step process showed significantly lower swelling (589 a % ± 578) than the fibres spun, dried, and then UV irradiated in the 3 step process as described in Section 4.2.4 (1033 a % ± 617), shown in Figure 4.20 (p=0.001). This indicates that crosslinking levels were higher in the two step manufactured fibres likely due to a higher penetration of the photoinitiator into the material, ensuring crosslinking was achieved throughout the fibre cross section. Mechanical testing of hydrated fibres showed no significant difference between the original three step manufactured fibres and the two step manufactured fibres, which had a UTS of 3.3 MPa (n=19).

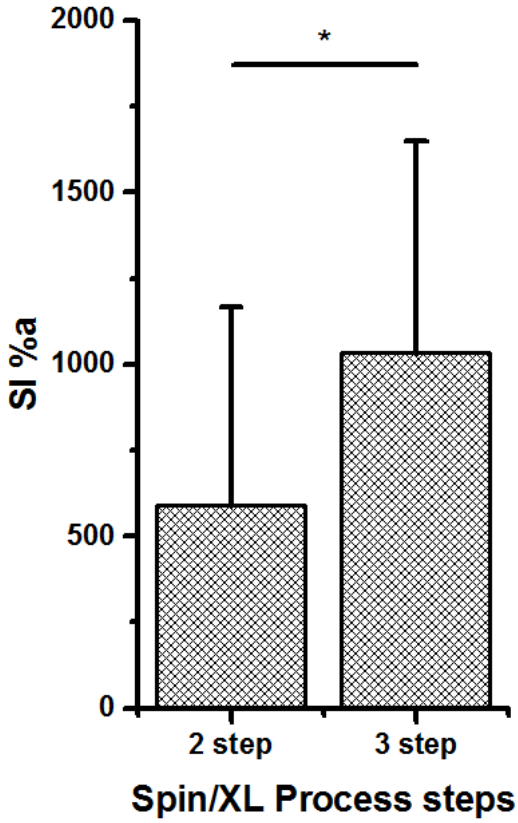

Figure 4.20: Swelling Index (a%) of crosslinked RTC-4VBC f-collagen fibres spun utilising the intermediate 2-step spin and crosslink manufacturing technique as shown in Figure 4.18, and the 3-step process including an intermediary drying stage. Fibres incubated in PBS for 24hr at 37º C

The development of a full one-step process, as schematically outlined in Figure 4.21, in which UV exposure occurs during fibre spinning, and not directly afterwards, is therefore possible and is likely to be scalable as an approach. As outlined in Chapter 3, single step spinning and crosslinking of methacrylated gelatin (Gel-MA) has been achieved in previous literature (Wang, X.H. et al., 2017; Shi et al., 2015). However, simultaneous spinning and crosslinking could potentially interfere with the more complex collagen's molecular alignment, control of the fibre's crystallinity, mechanical properties, and degradation profile.

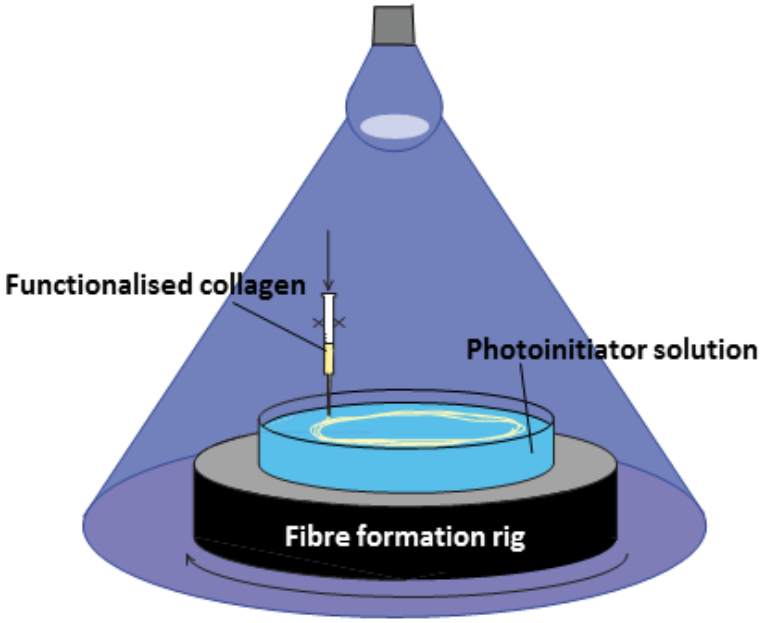

Figure 4.21: Proposed set up for one-step collagen-4VBC fibre spinning combined with UV crosslinking

4.4 Conclusions

A new spinning and crosslinking process is established for producing photoactive RTC-4VBC f-collagen fibres. Fibres coagulated in PEG exhibited lower mechanical strength, moduli, and WOR than those spun in ethanol due to the lack of complete diffusional exchange producing a porous material. Fibres spun into ethanol were stronger and more homogenous with a circular cross section devoid of pores and abnormalities.

Decreasing the Stretch Factor of the fibres (extrusion rate/collection rate) significantly increased the diameter of the fibres. Varied Stretch Factors were also observed to alter the mechanical properties of the fibres due to alterations in extension of the coagulating collagen dope, serving to align the collagen chains producing a denser, more crystalline material.

An increased in UTS and modulus was observed up to an SF of 4. Over this range, a decrease in UTS was observed due to overdrawing, wherein increased stretching caused microimperfections within the fibre structure.

A significantly stronger fibre could be produced using a smaller needle diameter through which to extrude the collagen. A change from 0.8mm to 0.6mm needle led to a 227% increase in UTS to 286 ± 38 MPa with a YM of 4.0 ± 0.5 GPa, comparable to many current pieces of literature. Further work focussed on the drawing of these finer fibres could increase these already excellent dry tensile properties.

Hydrated crosslinked fibres were shown to have a significantly higher UTS than uncrosslinked RTC-4VBC fibres with a UTS of 3.3 MPa compared to 0.6MPa due to the presence of stabilising covalent crosslinks. Although weak this is comparable to previous literature. Fibre strain was statistically lower than the uncrosslinked samples (6.1% vs 8.1%). This is hypothesised to be due to the reduced resistance to chain slippage in the uncrosslinked material.

The feasibility of one step spin and crosslink production was proven. This combined approach, decreases manufacturing time and complexity as well as prevented the need for handling the weaker uncrosslinked fibres. Fibre swelling was used to confirm crosslinking within these fibres. These fibres exhibited a lower swelling level than the longer three step process, likely due to increased photoinitiator penetration into the coagulating fibre.

Overall, this work has demonstrated a plausible route for vinylbenzylated collagen spinning for the production of wet stable collagen fibres for medical textiles. Most notably it has demonstrated the feasibility of collagen functionalisation prior to spinning, followed by UV irradiation to create covalent crosslinks. The resulting crosslinked collagen hydrogel fibres also had good triple helix retention rates (82%), swelling, and mechanical

properties, suggesting that significant denaturation of the collagen material can be avoided using this manufacturing route.

Chapter 5

Manufacture and Characterisation of Collagen-Based Textile Structures

5.1 Introduction

The feasibility of converting vinylbenzylated collagen-based fibres into nonwovens and other textile structures is clearly of interest in determining scope for future applications in healthcare. Owing to the material's biocompatibility, low immunogenicity, and mechanical properties of collagen it is a valuable constituent of a range of medical devices, including those based on textile materials. Clinical uses of collagen-based medical devices, include tissue scaffolds, guided bone regeneration membranes, wound dressings and haemostats (Gottlieb, 2004; Schiefer et al., 2016; Vogt, 2015; Burak et al., 2011; He et al., 2014; Tonndorf et al., 2020). Manufacture of collagen-based nonwoven fabrics, including those composed of gelatin for medical devices has previously been reported by dry-laying followed by needlepunching, and by force-spinning and electrospinning (He et al., 2014; DeFrates et al., 2018; Ghasemi-Mobarakeh et al., 2008; Hlavata et al., 2017; Vogt, 2015).

The ability to convert f-collagen and f-gelatin fibres in to flexible, macroscopic structures such as nonwovens, braids and other textile structures is a pre-requisite to ensure effective clinical application of new devices. Accordingly, this chapter reports the feasibility of small-scale manufacture and characterisation of textile materials produced from the RTC-4VBC fibres reported in Chapter 4.

To provide context to this study, the application of collagen-based textile materials in the clinic is worthy of brief discussion. Clinically, wound dressings and skin substitutes are applied to wounds such as ulcers and burns to enhance the healing process by regulating liquid levels, preventing

infection, and stimulating new tissue growth. Wound dressings are applied to the wound site and replaced frequently to monitor healing and check for infection. By contrast, a skin substitute is effectively an acellular regenerative scaffold which works to recruit epithelial cells to the skin substitute substrate where new endogenous ECM is secreted, new tissue is generated and the initial scaffold is resorbed resulting in a reduced level of scar formation (Russell, 2004). Collagen-based devices contain motifs that attract cells and encourage cellular attachment and the material is therefore considered to be invaluable for such wound healing products.

Wound dressings and skins substitutes are required to manage wound exudate appropriately depending upon the stage of healing. Research has determined that the best healing environment is one with low levels of exudate, but with enough to prevent desiccation and to allow transport of cells and nutrients to and around the wound site. An excess of liquid is to be avoided to avoid maceration of the surrounding tissue and further breakdown (Cutting, 2003; Seaman, 2002). In practice, exudate levels are managed by wound dressings having appropriate levels of liquid absorbency, as well as the ability to redistribute the liquid within the dressing, and permit moisture vapour evaporation.

Infection control is another relevant factor. An effective approach involves blocking infiltration of antigens into the wound site with an external dressing layer containing either extremely small pores or barrier properties, whilst still allowing water vapour to evaporate from the wound if needed, but preventing penetration of micro-organisms (Rojas et al., 2002). Biocidal additives such as silver compounds can also aid in preventing infection as well as ensuring that there is full contact between the dressing and the wound bed, which reduces the regions in which bacteria can grow (Tigani et al., 2008).

The commercially established skin substitute, Integra ™ bilayer wound matrix (BWM) is made up on a semi-permeable silicone membrane which

facilitates fluid loss, increases the tear strength, and acts as a microbial barrier (IntegraLifeSciencesCorporation, 2010). The second layer is a Type I bovine collagen and shark chondroitin 6-sulfate glycosaminoglycan (GAG) matrix. This acts as a scaffold for cellular growth and revascularisation (Hodde et al., 2001; Powell, Heather M. and Boyce, 2006).

The collagenous Integra material is extremely porous with a 98% pore volume fraction and an average pore diameter of 30-120 μm, to allow for cellular invasion. The ideal pore size for fibroblast infiltration has been reported to be 100-200 μm (Vogt, 2015) and 20-125 μm (Nguyen et al., 2009).

This iniltration process normally takes around three weeks to occur. After about twenty one days, the silicone layer of the product is removed and replaced by a split thickness autograft taken from the patient's body (Bartis, 2011). Case studies on the use of the Integra^{TM} bilayer product have reported an improvement in healing outcomes (Papa et al., 2011; Loss et al., 2000; Gottlieb, 2004). However, this product cannot be applied to infected wounds, and it requires an autograft, which is unfavourable given it may lead to donor site morbidity.

Freudenberg have patented technology based on the centrifugal spinning of a biodegradable gelatin-based nonwoven with haemostatic compounds embedded in the product to induce clotting (Vogt, 2015). Spun using a 24 wt. % gelatin/ water solution at 120 ºC with integrated gentamicin (an antibiotic) and crosslinked with PEG diglycidylether, the nonwoven has fibre diameters of 0.5-500 μm and an average pore size of 50 μm. Studies of healing time in micro-pig full thickness wounds using gelatin nonwovens with a pore size of 35-70μm have concluded that multiple application speeds up wound closure although it was unclear whether this was due to formation of scar tissue or re-epithelialisation (Schiefer et al., 2016).

Regenerative medicine and tissue engineering scaffolds are an additional avenue for the application of collagen nonwovens. Fibrous scaffolds or meshes for the regeneration of bone, cartilage, ligaments, skin, neurons and vasculature have been thoroughly researched (He et al., 2014; Argento et al., 2012; Kalaithong et al., 2017; Enea et al., 2013; Kew et al., 2011; Venugopal et al., 2008; Powell, H. M. and Boyce, 2009; Timnak et al., 2011). These studies have led to significant understanding about the value of nonwovens as components in medical devices, but given that the bulk of the previous research has focused on electrospinning, which is only one method of nonwoven formation, it is likely that the full potential is yet to be established. Electrospinning has inherent limitations in that it produces a predominantly 2D scaffold architecture, with porosity and pore size dimensions that can inhibit cell infiltration, and with regard to collagen, because of the solvent systems needed, combined with high voltage, leads to denaturation of the protein (Kalaithong et al., 2017; Zeugolis, Dimitrios I. et al., 2008).

In a very small number of studies, the needle punching process has been applied in the preparation collagen-based nonwoven scaffolds (Sutherland, F.W.H. et al., 2005; Yim et al., 2007; He et al., 2014; Guan et al., 2015), wherein the purpose was development of high thickness collagen devices for articular cartilage and for bone regeneration (He et al., 2014; Guan et al., 2015).

An interesting mode of nonwoven composite formation involved using fibre bundles to reinforce a collagen-chondroitin-6-sulphate sponge (Shepherd, J.H. et al., 2013). In this process crosslinked regenerated collagen fibres were submerged in an aligned array into a collagen/ chondroitin slurry and freeze dried to form a sponge which was then further crosslinked using 1-ethyl-3-(3-dimethylaminopropyl) carbodiimide (EDC). The result was a highly porous composite material with the ability to withstand higher mechanical forces due to the fibrous scaffold within.

Other collagenous textile materials have been developed for medical devices such as knitted fabrics and braids (Zheng et al., 2017; Tonndorf et al., 2020) to modulate the bulk scale mechanical properties. In the case of knitted structures, extensibility and elasticity can be engineered due to the intermeshed loop structure. Tonndorf *et al* succeeded in producing a knitted collagen textiles. Multifilament yarns comprised of 6 GTA crosslinked filaments of approximately 80µm were wet-spun. These were then mechanically knitted together to produce a fabric targeted to tissue engineering applications (Tonndorf et al., 2020).

Twisting and braiding bundles of fibres is another approach, aimed at increasing extension at break and tensile strength, which can be useful in terms of mimicking the stress-strain response of high load bearing tissues such as ligaments and tendons (Freeman et al., 2007; Walters et al., 2012).

Herein, the potential for small-scale manufacture of the wet-spun RTC-4VBC fibres formed in Chapter 4 in to nonwovens and braids is investigated. To enable this, a novel solvent bonding approach was developed, and Gel-4VBC film/RTC-4VBC composite fibre materials were prepared and characterised. A feasibility study on the formation of braided structures comprising the RTC-4VBC fibres is also described.

5.2 Experimental

5.2.1 Materials

Gelatin was functionalised with 4VBC as detailed in Section 3.2.2, RTC-4VBC fibres were produced by coagulation in ethanol as per Section 4.2.4. *Clostridium* collagenase powder (9001-12-1), auxiliary chemicals, and L929 murine fibroblasts were purchased from Sigma Aldrich.

5.2.2 Solvent bonding

Five (5) mg of non-crosslinked RTC-4VBC fibres (EtOH-8) were dry laid in to the form of a web, sprayed with 1ml 10 mM HCl, and left for 5 min and 30 s to induce partial dissolution of fibres at the intersecting crossover points. Solidification was induced by immersion in 90 vol. % ethanol, 1 wt.% Irgacure I2959 and UV irradiated using the lamp detailed in Section 3.2.7 for 30 min, then air dried for 1 h.

5.2.3 Gel bonding

Gel-4VBC was dissolved in 17.4mM acetic acid at concentrations of 10, 15, and 20 wt. %. Five (5) mg of crosslinked RTC-4VBC fibres (EtOH-8) were dry laid in to the form of a web and submerged in 0.1, 0.2, or 0.3 ml of Gel-4VBC solution. Phase separation was then induced by adding 90 vol. % ethanol and crosslinking using 1 wt.% Irgacure 2925/ethanol solution for 30 min then air dried for 1 h.

5.2.4 Fibre braiding

Crosslinked collagen-4VBC filaments spun into ethanol (EtOH-8) were cut into sections of 160 mm. The fibres were bundled into three groups of six and braided together manually by consecutively moving one bundle of fibres from the outer side into the middle, alternating between each side (Freeman et al., 2007; Silver et al., 2003; Walters et al., 2012) ImageJ was then used to determine the braiding angle, measuring from 90º to the direction of the braid (n=10).

5.2.5 Scanning Electron Microscopy

Scanning Electron Microscopy was conducted in accordance with the methodology detailed in Section 3.2.10 Scanning Electron Microscopy

5.2.6 Water uptake

Water uptake was measured gravimetrically, based on the methodology given in section and according to Equation 3.4, Section 3.2.13 Fibre and nonwoven scaffold swelling

5.2.7 Degradation with Collagenase

Samples of RTC-4VBC gel bonded nonwovens were evaluated to determine enzymatic weight loss. A ratio of 5 mg fabric to 0.2 ml of Gel-4VBC solution were measured (n=6). The procedure is detailed in Section 4.2.11. For the positive and negative controls, lyophilised RTC sponge and PCL nonwoven were used, respectively. Weight loss by collagenase degradation was calculated using Equation 4.5 in Section 4.2.12.

5.2.8 Tensile testing

Wet strength of the braids were measured. Samples were immersed in PBS for 24 hrs at 20ºC and braid thickness were measured at minimum 10 points along the length of the sample. Braids (n=3) were fixed within a 1 cm frame and measured using a Testex TB400C tensile tester with a load cell of 2.5N at extension rate of 10mm/min (Testex, Switzerland).

5.2.9 Cytotoxicity testing

Cytotoxicity studies were undertaken using the procedure given in Section 3.2.14 Cytotoxicity testing. Gel bonded nonwovens produced using 5 mg of fibres bound with 0.2 ml of 15 wt. % Gel-4VBC solution were evaluated, with a PCL nonwoven control (n=5). 10-20mg of material was used. Confocal microscopy (Microsystems L2, Leica, Germany) was used to image scaffolds using LIVE/DEAD staining at wavelengths of 530 nm and 645 nm. Stacked images through the z-plane were compiled to form a 3D image.

3.2.10 Statistical analysis

OriginPro software was used for Normality tests, means comparisons using Tukey testing, and One-Way ANOVA providing normal distribution was observed. Data are presented as average ± standard deviation.

5.3 Results and Discussion

5.3.1 Bonded Fabric Structure

Non-crosslinked RTC-4VBC fibre webs were partially dissolved by spraying with a solvent, before neutralisation and crosslinking to form bonded junctions at the fibre intersections. This method was inspired by the solvent bonding approach previously applied for the stabilisation of synthetic and man-made fibre webs (Hudson Jr, 1971).

Optical micrographs of the resulting fabric structure (Figure 5.1: Optical micrograph of solvent bonded f-collagen 4VBC nonwovens. A-B: 5 min acid exposure; C-D: 30 s acid exposure

Figure 5.2: Optical micrograph of solvent bonded f-collagen 4VBC nonwovens. A-B: 5 min acid exposure; C-D: 30 s acid exposure

) reveal film formation particularly in the region of the fibre intersections. The extent to which this occurred was dependent on the solvent exposure time (30s - 5 min). It was therefore evident that bonding point morphologies in the resulting fabrics could be readily modulated by adjustment of the temporal solvent treatment conditions.

However, this method of bonding produced a fragile and rigid fabric due to the partial dissolution of the fibres and the formation of a more anisotropic polypeptide chain organisation within these regions than in the undissolved fibres. It has been previously reported that solvent bonding can lead to an increase in electrospun nylon web tensile modulus, toughness and strength,

at the expense of reduced elongation due to fusion points preventing fibre slippage (Xiang and Frey, 2016).

Although this technique was successful in forming a bonded nonwoven fabric and could potentially be useful as a wound dressing or medical device component, the approach was further developed with a view to producing a less brittle fabric and a ‘gel bonding’ approach was focussed upon. Essentially, this involved the application of f-gelatin to the f-collagen fibre web, prior to UV irradiation, to produce a bonded crosslinked fabric.

In the collagen gel bonding technique that was devised herein, Gel-4VBC solutions were used to encapsulate and bond RTC-4VBC fibre webs together after crosslinking. Thereby, the Gel-4VBC hydrogel effectively acted as an adhesive binder to adhere the RTC-4VBC fibre webs, similar to chemical bonding in nonwoven fabric manufacture (**Error! Reference source not found.**). 4VBC-mediated crosslinking between the Gel-4VBC matrix and the RTC-4VBC fibres is also possible. This would enable the formation of a nanoscale-integrated structure with increased elasticity compared to phase-segregated composite materials (Mahony et al., 2010).

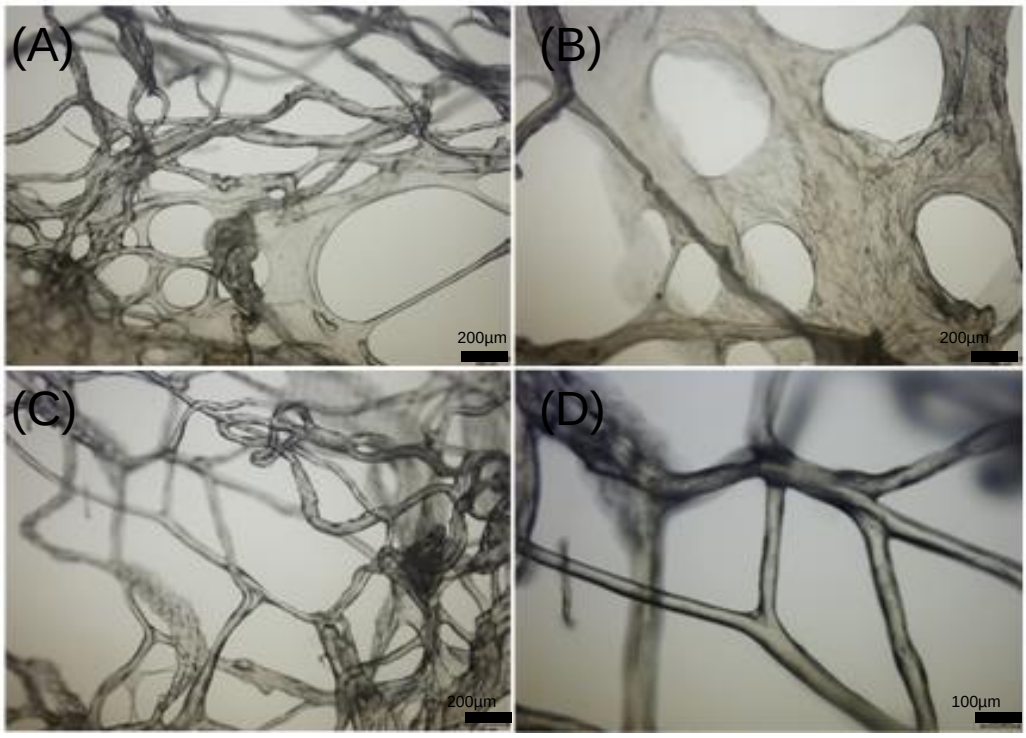

Figure 5.1: Optical micrograph of solvent bonded f-collagen 4VBC nonwovens. A-B: 5 min acid exposure; C-D: 30 s acid exposure

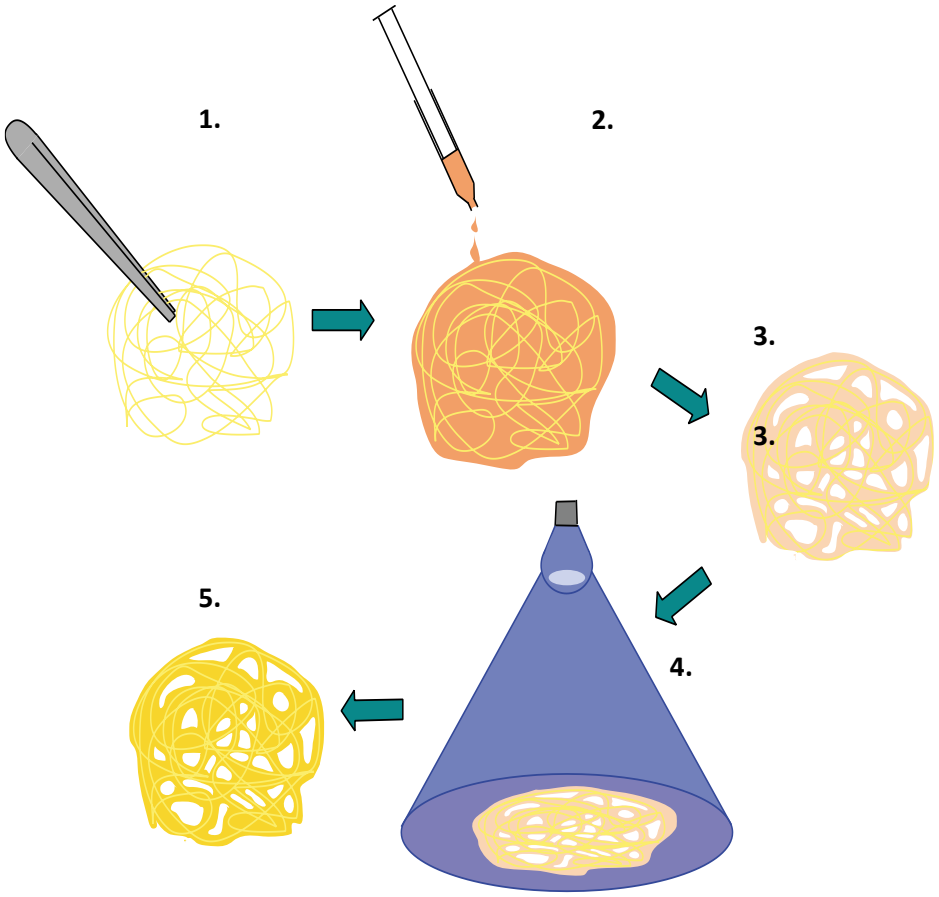

Figure 5.2: Schematic procedure for the manufacture of Gel-4VBC/ RTC-4VBC gel-bonded f-collagen nonwovens 1: Formation of a drylaid RTC-4VBC fibre web. 2: Impregnation of the web with Gel-4VBC solution. 3: EtOH added to solidify Gel-4VBC binder. 4: Incubation in I2925 + EtOH with UV light exposure to crosslink Gel-4VBC binder. 5: Gel-4VBC/ RTC-4VBC gel bonded nonwoven fabric

Micrographs of the resulting gel-bonded fabric structure and bond points are shown in Figure 5.3 and reveal the retention of the underlying fibre morphology as well as inter-fibre regions and coating over the fibres consisting of Gel-4VBC. The new collagen-based gel bonding approach enabled a collagen-based biocompatible fabric to be produced without the use of synthetic binders, potentially simplifying the clinical translation pathway, from a regulatory perspective, as well ensuring no potential for toxicity issues associated with the use of a secondary adhesive.

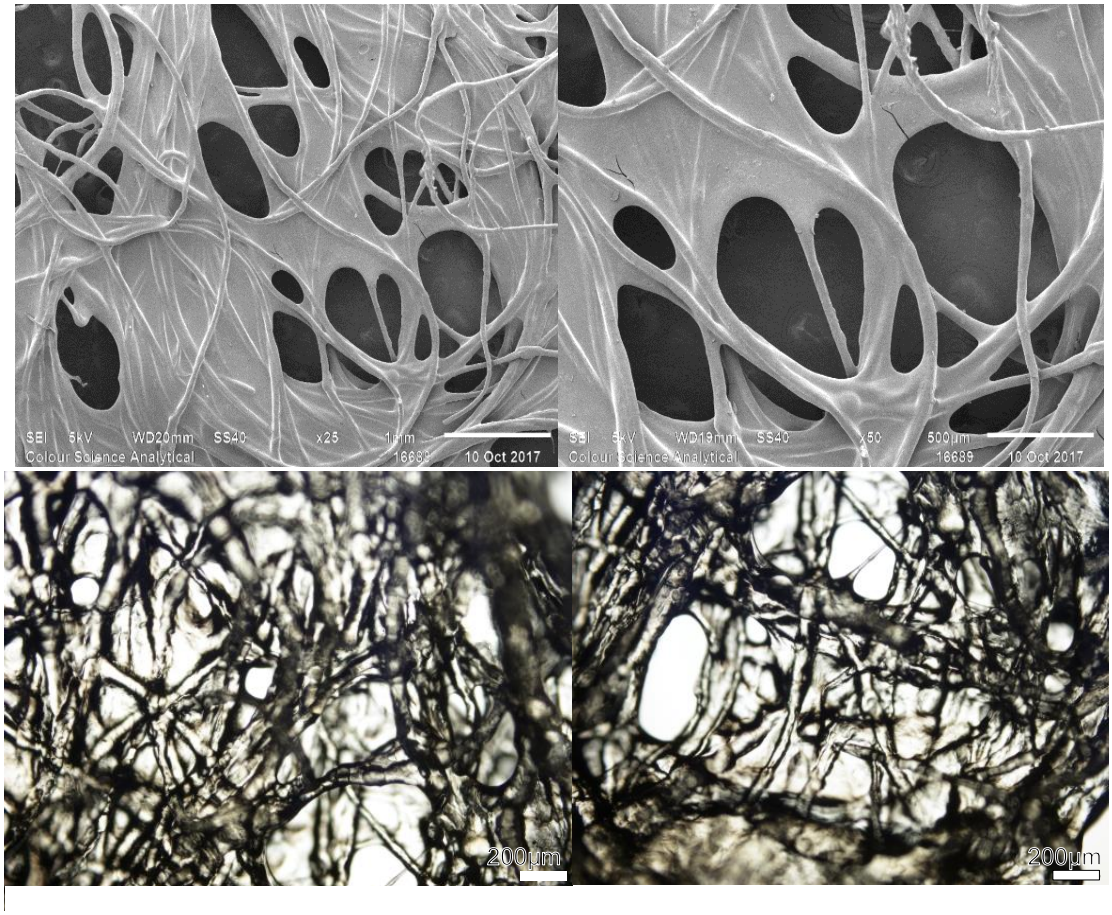

Figure 5.3: Gel-4VBC bonded RTC-4VBC prototype nonwovens (ratio of fibre to gel = 5 mg:0.3 ml). Top row: SEM micrographs of initial gel bonded RTC-4VBC collagen nonwoven x25 (left) and x50 (right). Bottom row: Optical micrograph of initial gel bonded RTC-4VBC collagen nonwoven x10

Using this approach, the presence of an amorphous hydrophilic crosslinked Gel-4VBC (f-gelatin) phase in the fabric can also be expected to assist in the management of liquid exudate when in situ, providing cells with the necessary nutrients vital for survival, and removing waste (Haslauer, 2014). Being collagen-based there is also the potential to act as a sacrificial polypeptide to manage undesirable upregulation of collagenases, which can delay healing in chronic wounds (Cullen et al., 2002; Jabłońska-Trypuć et al., 2016; Kim, S. et al., 2016; Tronci et al., 2016b).

Finally, unlike with needle punching and solvent bonding, the gel bonding process subjects the fibres to neither a high mechanical stress or partial

chemical dissolution, respectively, nor are there any associated issues of fibre breakage and deterioration in fibre mechanical properties.

To further explore the conditions required to accomplish gel bonded nonwoven fabric fabrics using Gel-4VBC, the concentration of the gel bonding solution was varied. The mass of the fabrics before and after gel-bonding was measured. All fibre webs weighed 5 mg prior to bonding. These were laid into a circular template of 2 cm diameter, or 3.14 cm^2 making a basis weight of approximately 15.9 g/m^2. The post bonding dried weights are shown in Table 5.1.

No statistical difference between fibre mass:Gel-4VBC ratio and basis weight was observed (p=0.2). However, SEM imaging did show some subtle morphological changes in the resulting fabrics Figure 5.4). In addition to coating of fibre surfaces, greater occlusion of pores between proximal fibres occurred as the coating volume was increased from 0.1ml of solution (Figure 5.4 A-B) to 0.3ml (Figure 5.4E-F).

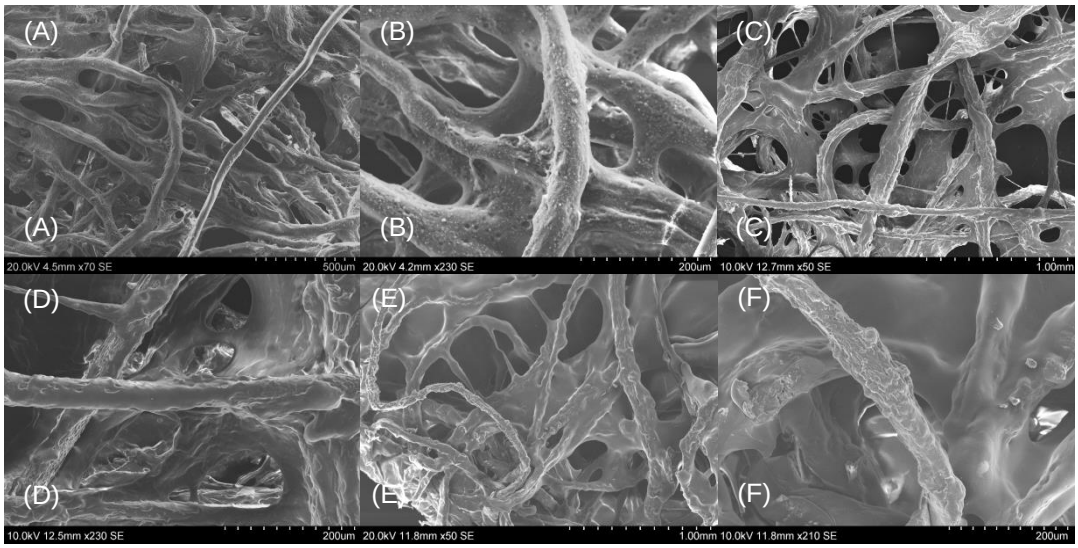

Figure 5.4: SEM micrographs of gel-bonded f-collagen nonwovens formed using different fibre mass: Gel-4VBC solution ratios (mg : ml); A&B = 5:0.1; C&D = 5:0.2; E&F = 5:0.3

The lack of a statistical difference in basis weight is likely due to excess Gel-4VBC being removed during the gel coagulation stage leaving only a residual quantity of Gel-4VBC coating the fibres and held at fibre crossover junctions. A higher volume of Gel-4VBC would therefore not contribute additional mass, as excess material would be removed.

A difference in mass was observed when increasing the concentration of Gel-4VBC from 10 wt % (16.4 ± 3 g m^{-2}) to 20 wt % (25.5 ± 4 g m^{-2}, p=0.03). As increasing concentration increases the viscosity of the solution, a thicker coating of Gel-4VBC would adhere to the fibres during the coagulation stage due to increased shear resistance preventing the solution from flowing off the fibre structure when precipitation occurs.

Fibre mass: Gel-4VBC vol ratio (mg:ml)	Gel-4VBC conc (% wt)	Basis weight g m^{-2} (n=5)	WU m% (n=5)
5: 0.1	15	22.7 ± 4	311 ± 137
5: 0.2	10	16.4 ± 3 *	75 ± 26 *,**
5: 0.2	15	21.3 ± 6	218 ± 50 *
5: 0.2	20	25.5 ± 4*	218 ± 63 **
5: 0.3	15	24.6 ± 2	238 ± 34

Table 5.1: Gel-bonded f-collagen nonwoven basis weight and water uptake m% with respect to varied fibre mass:Gel-4VBC bonding solution volume ratio, and Gel-4VBC bonding solution concentration. * indicates statistical differences (p<0.05)

5.3.2 Gel-bonded f-collagen nonwoven fabric liquid uptake

The ratio of fibre mass to Gel-4VBC solution volume in the gel bonded and crosslinked nonwovens did not significantly alter the water uptake % of the resulting fabrics (p=0.4) (Figure 5.13A). However a significant increase was seen when the Gel-4VBC concentration was increased (Figure 5.5). A WU of 75 ± 26 m % was observed for nonwovens bonded with 10 wt % Gel-4VBC compared to 218 ± 50 m % for 15 wt % solutions, and 218 ± 63 m % for 20 wt % solutions (p=0.001).

It can be speculated that an increase in the volume of Gel-4VBC relative to the fibre in the fabric could potentially increase the water uptake due to the increase in overall amorphous gelatin content. This was confirmed by the basis weight measurements of nonwoven fabrics formed using various Gel-

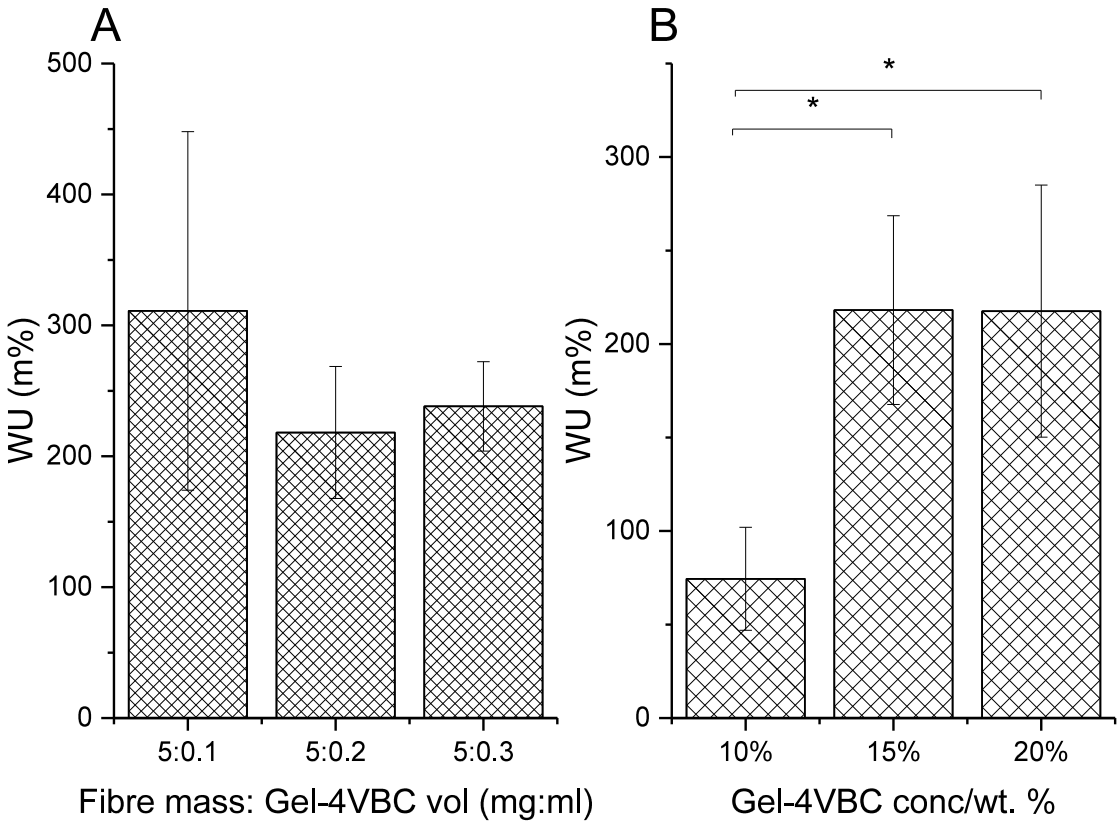

Figure 5.5: Water uptake of manufactured f-collagen nonwoven samples: A) *gel bonded nonwoven fabric mass (mg): 15% wt Gel-4VBC binding solution volume (ml)* ratio; B) wt. % of Gel-4VBC binding solution used in 5 mg : 0.2 ml ratio

4VBC solution concentrations. This f-gelatin component would more readily absorb liquid than the fibrous f-collagen component due to the increased space between amorphously organised polypeptide chains, which water molecules could more easily access and be held within.

5.3.3 Degradation by Collagenase

To determine the degradation behaviour of the fabrics in simulated biological conditions,RTC-4VBC gel bonded nonwoven samples were incubated in *Clostridium* collagenase for four days and the percentage mass loss was quantified (Figure 5.6). After the incubation period, the rat tail collagen sponge (control) was almost completely degraded (99.6 ± 0.2 m%), while the PCL control was subject to minimal mass loss of only 4 ± 1 m%. The gel-bonded nonwoven sample produced with 0.2 ml of 15% Gel-4VBC was degraded to an intermediate extent of 37 ± 2 m% ($p=0$ for all sample comparisons).

This was as expected given the collagen sponge contained comprised collagenase motifs over which the enzymes could degrade and possessed no crosslinks to stabilise the material. Furthermore, the sponge format means a high surface area to volume ratio, maximising penetration of the enzymatic liquid to the internal surfaces. The small weight loss in the PCL sample, which possessed no collagen motifs, can be attributed to hydrolysis of ester linkages, which can occur under physiological conditions (Baghersad et al., 2018; Antipova et al., 2018; Shojaei et al., 2019).

The RTC-4VBC nonwoven sample exhibited markedly lower levels of enzymatic degradation compared to the collagen sponge control, due to the higher level of crosslinking within the structure, and possibly because of the gel bonding material covering the fibre surfaces. It is hypothesised that the presence of the crosslinked gelatin coating acts to protect the fibrous structure

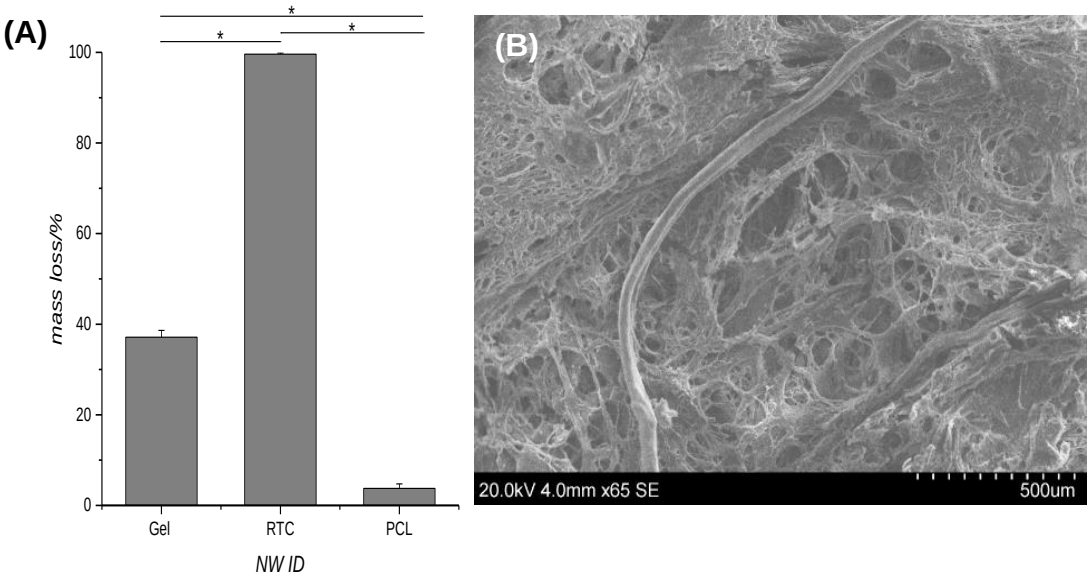

Figure 5.6: A) % mass loss post collagenase degradation with relation to gel-bonded (Gel) RTC-4VBC nonwoven, Rat tail collagen sponge (RTC), and Polycaprolactone (PCL) nonwoven; B) SEM micrograph of collagenase degraded gel bonded RTC-4VBC nonwoven

of the fabric, by providing a sacrificial material, which is preferentially degraded.

Note that the level of mass loss in the gel-bonded RTC-4VBC nonwoven was over double that of single RTC-4VBC fibres as measured in Section 4.3.8 (37% vs 18%), and SEM micrographs of the fibres confirmed that they remained mostly intact, while the gelatin was more readily degraded (Figure 5.6 **Error! Reference source not found.**B). The rapid degradation of the gelatin component can be attributed as its lower molecular weight and crystallinity, caused by helical uncoiling at 37 ºC, lead to higher solubility (Tigani et al., 2008; Zhao et al., 2016; Shubhra et al., 2011; Lynn et al., 2004; Zeugolis, Dimitrios I. et al., 2008).

The RTC-4VBC gel-bonded nonwoven structure therefore provides opportunities to control the rate of degradation of the bulk structure, by modulating the relative volume fraction of gelatin and RTC-4VBC fibres in the fabric. This control can be readily accomplished as the fabric is manufactured.

5.3.4 Cytotoxicity

For clinical applications cytotoxicity is a further important consideration governing suitability for use. Murine fibroblasts were seeded onto PCL (control) and the gel bonded RTC-4VBC collagen nonwoven sample (formed using 0.2ml of 15 wt. % Gel-4VBC binder with 5 mg of fibres) and incubated for 7 days. As expected, after day 7, a significant difference between cell metabolism was observed using an alamar Blue assay ($p=0.003$) due to the presence of cell attachment motifs in the collagen protein (Figure 5.12).

3D confocal micrography revealed multiple live (green) cells attached directly to the fibres in the gel bonded RTC-4VBC collagen nonwoven sample. As the collagen fibres also absorbed the red EH-1, it was difficult to distinguish dead cells, because the fibres themselves appear red. However, considering

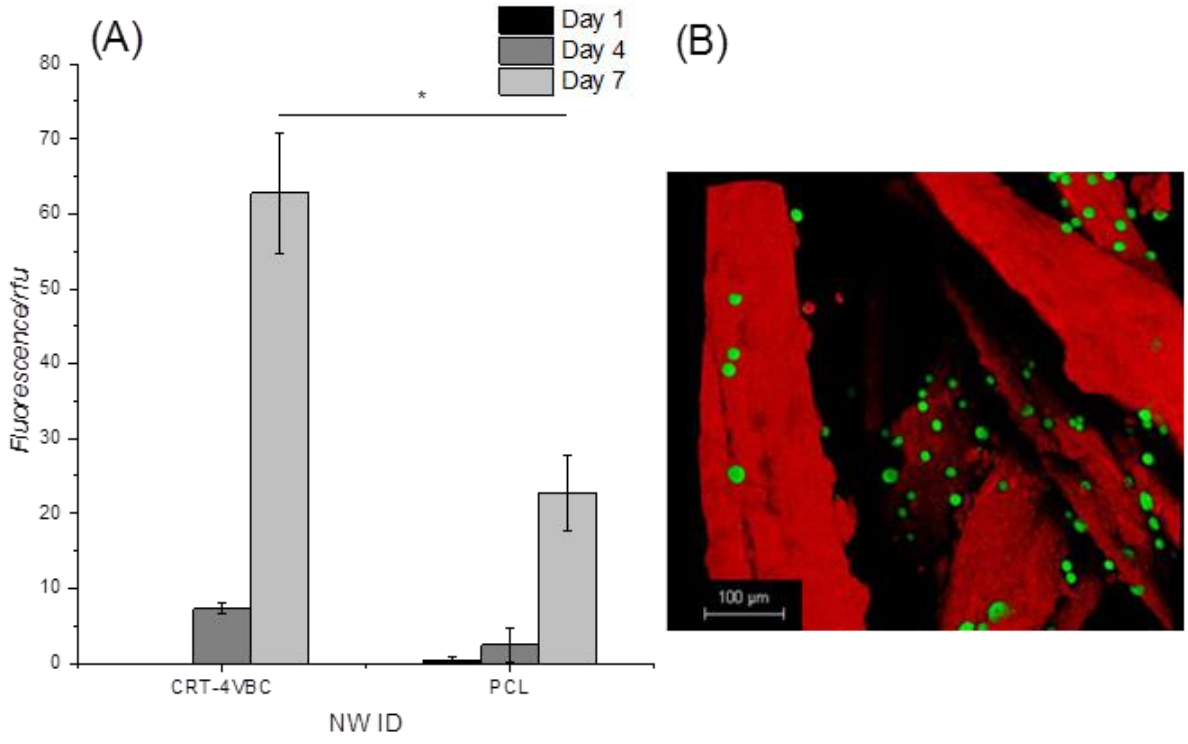

Figure 5.7: A) alamarBlue cell metabolism assay; B) Confocal micrograph of gel bonded RTC-4VBC nonwoven after 7 days incubation and LIVE/DEAD staining

the high level of cell activity that was observed relative to the inert PCL control, the suitability of the samples for use as biomaterials was confirmed.

Although there is no existing precedent for the use of gelatin-based binders to bond collagen nonwovens, there have been reports of other biomaterials used to support collagenous material. Examples include polyglactin 910, which induces the laydown of collagen, and fibrin glue in dural substitutes (Maurer and McDonald, 1985; Terasaka et al., 2006). Terasaka et al. sprayed biodegradable polyglycolic acid (PGA) with fibrin glue and found the resulting product had excellent biocompatibility, with infiltration of inflammatory cells, and laydown of collagen fibres by fibroblasts after 1 month in dural substitutes implanted in beagles. After 2 months, the substitute was mostly absorbed, vascularisation had occurred and no inflammatory cells were present.

In conclusion, it was determined that the gel bonded RTC-4VBC collagen nonwovens, were more biocompatible than the PCL (control) which is a material already commonly used in medical devices (Baghersad et al., 2018; Dias et al., 2013). This suggested that this substrate is also be suited to supporting cell growth and would be a useful tool in the manufacture of medical devices.

5.3.5 Feasibility of forming RTC-4VBC filament braids

Applications for collagen-based materials in the clinic extend beyond nonwoven fabrics to more mechanically competent assemblies, where load bearing behaviour is important. Braids can be useful as biomaterials for the replacement of fibrous, directionally aligned tissues with anisotropic mechanical properties, such as ligament and tendons because of the ability to build load bearing structural architectures. To determine the feasibility of delivering the new RTC-4VBC fibres in a braided format, the constituent fibres have to possess sufficient strength and flexibility to conform to small bending radii.

A RTC-4VBC 18 strand braid was manually manufactured using UV-irradiated and crosslinked 160 mm long staple fibres. Herein, the filaments were based on the EtOH-8 coagulated samples (as reported in Section 4.2.4) to demonstrate the ability of the material to be used in textile processes other than nonwoven formation. Figure 5.8 shows the morphology of the prototype braid, forming a compact structure with a braid angle of 63º ± 2. This refers to the angle of the yarns relative to the braiding direction (Cichosz and Hut, 2016).

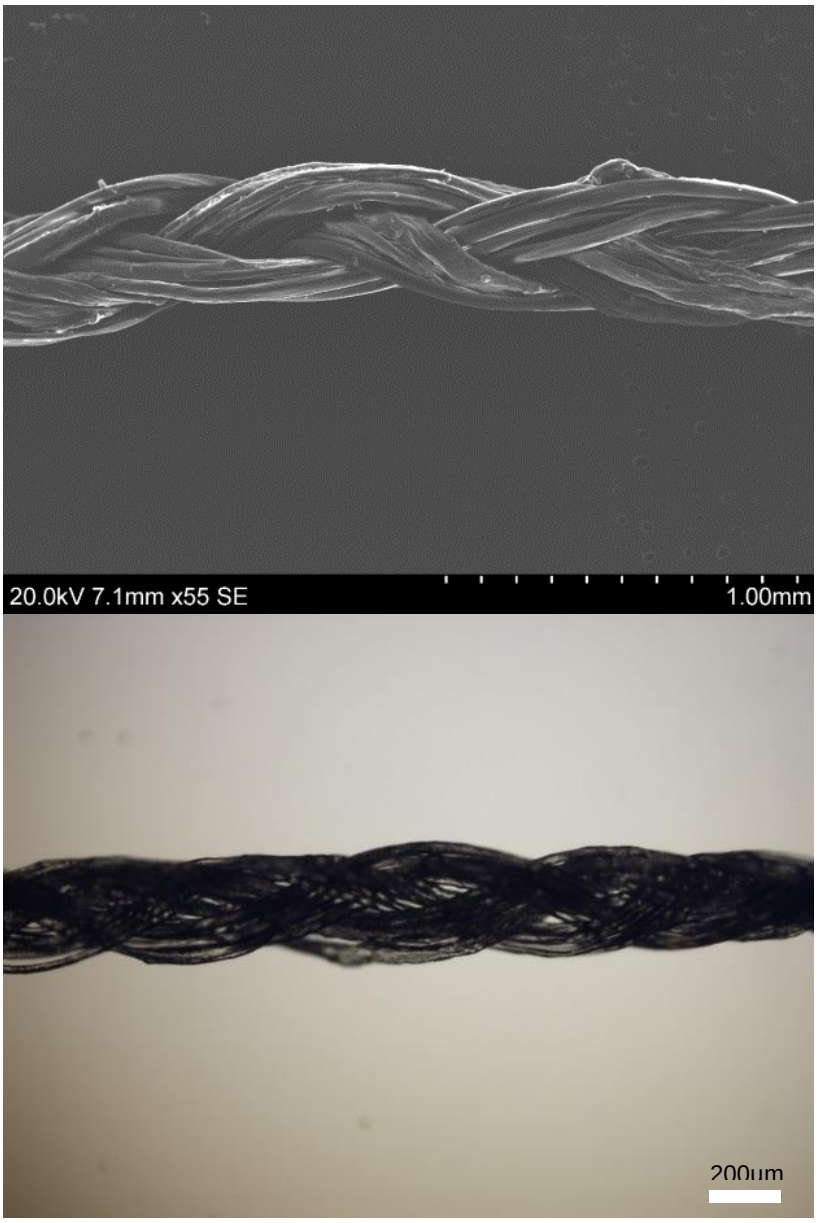

Figure 5.8: SEM x55 (top) and optical x10 (bottom) micrographs of an eighteen strand braid formed from three yarns comprised of six continuous filaments made of RTC-4VBC.

Adoption of a simple braided structure was sufficient in this preliminary study to demonstrate that braid formation is possible using the new RTC-4VBC filament materials. To enable future upscaling, inclusion of producer twist into the collagen filaments would likely increase the load bearing capacity and should be considered in future development of this material. (Freeman et al., 2007).

Hydrated tensile testing of the braids gave a low UTS of 1.4 ± 0.2 MPa, but were they possessed remarkable extensibility with a measured mean strain of 41.4 ± 10.3%. The longer gauge length of 40 mm used for the braids, compared to the 20mm used for the staple fibres, lead to a reduction in tensile strength being recorded due to the necking region (or region which begins to deform under tension) making up a larger proportion of longer materials (Naito et al., 2012).

5.4 Conclusions

Small-scale manufacture of RTC-4VBC nonwoven fabrics was accomplished, producing structures suitable for manual handling and future clinical evaluation. Two approaches were introduced for bonding RTC-4VBC fibre webs. The first was an acid-based solvent bonding system and the second, a novel gel-bonding technique wherein fibre webs were impregnated with a UV-crosslinking Gel-4VBC formulation. Both approaches enabled nonwoven fabrics to be produced from homogeneous crosslinked collagenous materials, but the gel bonded nonwovens yielded fabrics with superior handling properties compared to solvent bonding, and additionally, could be tuned to control the rate of degradation in the presence of collagenase.

Gel-bonding appeared to provide a sacrificial layer for collagenase during the degradation study due to the lower polypeptide content than the RTC-4VBC fibres. After 4 days of collagenase degradation a 37 ± 2 m% of the gel bonded RTC-4VBC nonwoven was degraded, compared to only 4 ± 1 m% of the PCL, and 100 ± 0 m% of the RTC sponge. The cell supporting capacity

of the gel-bonded f-collagen nonwoven was seen to favourably compare to the widely used biomaterial, polycaprolactone (PCL).

Swelling was not affected by the ratio of fibre to Gel-4VBC but increasing the concentration of the Gel-4VBC solution lead to a higher water uptake ratio, likely due to the increase in amorphous gelatin within the material. This was confirmed by measuring the material basis weight. Gel-bonded nonwovens bonded using 20 wt. % Gel-4VBC has a mean basis weight of 25.5 ± 4 g · m^{-2} compared to those bonded using 10 wt. % Gel-4VBC with a weight of 16.4 ± 3 g · m^{-2} ($p=0.03$).

To further illustrate the potential scaling of the fibre manufacture, to produce macroscopic structures, an eighteen strand braid was produced from RTC-4VBC. These studies demonstrate that RTC-4VBC and Gel-4VBC materials can be converted into nonwoven and textile structures with load bearing, degradation and cytotoxicity properties relavant to future surgical applications.

Chapter 6

Conclusions and Recommendations for Further work

6.1 General Conclusions

This research aimed to determine the feasibility of developing a new manufacturing route for wet spinning of collagen-based materials with a grafted 4-vinylbenzyl moiety for the purpose of post-spinning UV-photoactivation to form a covalently crosslinked network within fibres. The basic approach has been demonstrated for both functionalised gelatin and collagen starting materials. In so doing, the purpose was to avoid existing chemical crosslinking treatments post-spinning for collagen, which have the drawback of leading to potential cytotoxic effects due to the presence of residual reagent in the fibre.

Chapter 2 presented a critical review of previous approaches to manufacturing collagen materials by wet spinning and related techniques and highlighted the challenges of achieving wet stability in collagen fibre materials, whilst preserving the native triple helix structure. Based on a recently developed method of producing photoactive collagen-based materials, Chapter 3 investigated the feasibility of producing crosslinked fibres from gelatin functionalised with a photoactive moiety.

Gel-4VBC fibres were successfully wet spun using an automated rotary deposition system (ARDS). Wet-spinning was studied with different coagulants and compared to the conventionally used photoactive gelatin Gel-MA (Shi et al., 2015; Yue et al., 2015). It was found that using a PEG supplemented bath for phase separation resulted in stronger fibres with more homogenous morphologies, increased fibre swelling capacity, and higher strength and extensive properties than those spun into a salt solution. This

was hypothesised to be due to the presence of the ‘reptating’ PEG molecules and the modulation of diffusional exchange during precipitation which occurred due to the more viscous bath.

It was found that Gel-4VBC had significant advantages for spinning into fibres for biomaterials over Gel-MA. These included increased strength and handling ability with significantly stronger fibres (mean UTS = 73 MPa ±3) being spun. Most importantly the ease of spinning was much improved with the Gel-4VBC material. This was due to the reduced viscosity of dopes theorised to be caused by the lower level of functionalisation of vinylbenzylated materials. Gel-4VBC was able to be spun into an aqueous bath at room temperature as opposed to an ethanol bath at -20ºC, the conditions at which Gel-MA fibres could be made as previously reported in literature. Cellular compatibility as measured using a metabolic assay was also improved in Gel-4VBC fibres. This work indicates that 4VBC is superior to the more established MA for the crosslinking of gelatin with respect to spinning fibres.

Chapter 4 reported the feasibility of translating the wet spinning and crosslinking method for functionalised collagen materials. RTC was functionalised and spun into a PEG subsidised coagulant and ethanol. The process was shown to preserve up to 82% of collagen triple helices, the slight level of denaturation being attributed to the bulky 4VBC side chains disrupting the helical structure. The rate of diffusional exchange benefitted the EtOH fibre, with incomplete exchange occurring in PEG fibres leading to a heterogeneous, highly porous morphology which adversely affected the fibre mechanical strength. Ethanol coagulated fibres had a circular cross section with no visible pores, and smaller diameters. It was also found that EtOH was the more suitable coagulant for the spinning process as the solvent’s low density allowed the fibres to sink to the bottom of the coagulant container and be stretched allowing for additional fibre tuning.

Uniaxial tension exploiting the drag forces in a rotating coagulating bath was shown to raise the crystallinity of the fibres, demonstrated by changes in mechanical, and enzymatic resistance of the fibres although overstretching was apparent between the two collection rates to confirm this effect additional collection rates should be investigated in the future.

The slower relative collection rate caused by faster extrusion lead to higher die swelling which counteracted the increase in shear stress induced alignment within the die. This resulted in increased fibre diameter, fibre density, and strength. Aperture size also affected fibre characteristics with significantly finer fibres with regards to tensile strength. Fibres increased to a UTS of 286 ± 38 MPa and YM of 4 ± 0.5 GPa from 126 ± 6 MPa and 1.4 ± 1 GPa when spun with a needle of 0.6 mm diameter compared to 0.8 mm. Hydrated crosslinked fibres showed significantly higher tensile strength than uncrosslinked samples with a UTS of 3.3 ± 2.9 MPa vs 0.6 ± 0.3 MPa. Accounting for water content crosslinked fibres required significantly more force to be broken. Although comparable to some literature on hydrated collagen fibres, increasing the strength of the hydrated fibres could be achieved by increasing 4VBC functionalisation and photoactivation within the fibre during the processing.

Furthermore, an experimental one step wet spinning and crosslinking production route was also investigated and was found to be feasible. Reducing manufacturing time and the necessity to handle weak uncrosslinked fibres was also mitigated. Fibre swelling data for resulting fibres using the one step approach, confirmed crosslinking within these fibres. A significantly lower swelling level was seen in the two-step process compared to the three-step process. This is hypothesised to be caused by increased photoinitiator penetration into the coagulating fibre. Further work could be performed to investigate whether the change in non-solvent, and stage in the spinning process at which UV exposure occurs significantly affects the fibre’s heirarchical architecture.

The results reported herein provide a basis to consider scaling up studies using the principle of the ARDS system utilized in this study. This would in turn permit increasing the collection rates of these fibres to ensure the optimal level of fibre stretching. The mechanical testing of physiologically conditioned fibres is also important to include in further work.

The feasibility of converting the functionalised collagen-based materials into nonwovens and a braid indicated that RTC-4VBC fibres had adequate mechanical properties for braiding and for nonwoven formation. New modes of fibre bonding for nonwoven fabric production were experimented with. In the first approach, a solvent bonding technique, not previously utilized with f-collagen fibres was attempted. The resulting nonwovens were deemed too fragile to handle, although improvements were made to the material by reducing the acid exposure time. In a second approach, gel-bonding of f-collagen fibre webs with f-gelatin binder agents was shown to produce promising bonded fabric structures, in terms of handling ability when compared to solvent bonding. Gel bonding involved use of Gel-4VBC as a binding agent within a RTC-4VBC fibre mesh resulting in a crosslinked gelatin matrix holding together the collagen fibres ensuring that the entire material was composed of collagen derived material. It is hypothesised that some f-collagen and f-gelatin bonding may have occurred further reinforcing the material.

Concentration and volume of Gel-4VBC dope was experimented with in terms of basis weight and swelling properties. No significant changes were observed in basis weight or water uptake by increasing the volume of Gel-4VBC solution added to the fibre web. However, increasing the concentration of the Gel-4VBC from 10 to 20 wt. % increased the basis weight of the material significantly ($p=0.03$). It is hypothesised that this increase in mass was due to the Gel-4VBC solution’s increased viscosity. The increase in quantity of Gel-4VBC within the nonwoven also likely lead to the significant increase in water uptake observed in the materials formed with 15 and 20 wt. % Gel-4VBC when compared to the 10 wt % Gel-4VBC formed material.

Collagenase and cytotoxicity assays in conjunction with confocal and SEM imaging indicated that the f-gelatin component in the nonwoven fabric could act as a sacrificial polypeptide for MMPs within chronic wounds and that it was significantly more biocompatible than a nonwoven control. Over 4 days of collagenase degradation 37 ± 2 m% of the gel bonded RTC-4VBC nonwoven was degraded, significantly higher than the PCL control, and significantly lower than the RTC sponge. Overall this points to the nonwovens having properties relevant for use in medical devices.

Overall, the feasibility of wet spinning vinylbenzylated collagen-based fibres combined with crosslinking based on UV irradiation rather than liquid reagents was successfully demonstrated. Furthermore, a one step, combined spinning and crosslinking methodology has also been demonstrated, resulting in reduced levels of fibre swelling following subsequent hydration. Finally, it is apparent that these new photo-crosslinked collagen-based fibre materials have the capability of being made into macroscopic structures based on nonwoven or textile processes.

6.2 Recommendations for Further Work

Further work will enable the physical properties and biocompatibility of the vinylbenzylated materials to be tuned by further study of process-structure-property relationships. The effects of drawing and post-processing of fibres in particular, are worthy of further study. Further investigation aimed at tuning of Gel-4VBC fibre properties would enable further optimisation of the approach and the development of structure-property relationships.

This could include investigation into use of non-solvent, and stage in the spinning process at which UV exposure occurs significantly affects fibre characteristics by altering photoinitator penetration into the fibre.

Development of the filament drawing technique with a narrower needle aperture could also be included, which would serve to align polypeptide chains more efficiently. This could be done in conjunction with scaling up the spinning process. Bioprinting, the process of using a computer controlled extruder to lay down fibres into precise 3D architectures could also be integrated into this spinning process by either moving the coagulant bath or the syringe pump.

Clearly, looking towards clinical applications, there is significant scope to investigate scale-up opportunities for the manufacturing methods developed herein, combined with studies of the uniformity of physical properties. There is also considerable scope to study the physical and biological properties of resulting macroscopic nonwoven and textile structure, together with associated structure-property relationships. Finally, the behaviour of the functionalised collagen-based fibres in pre-clinical animal models should be thoroughly studied to assess immune response and degradation profile.

References

Abbasi, N. and Wu, X.S. 1996. Preparation of gelatin nanospheres for protein and peptide drug delivery. *Abstracts of Papers of the American Chemical Society.* **211**, pp.184-BIOT.

Adanur, S. 1995. *3.2 Wet-spinning.* CRC Press.

Agren, M.S., Taplin, C.J., Woessner, J.F., Eaglstein, W.H. and Mertz, P.M. 1992. COLLAGENASE IN WOUND-HEALING - EFFECT OF WOUND AGE AND TYPE. *Journal of Investigative Dermatology.* **99**(6), pp.709-714.

Ahn, J.-I., Kuffova, L., Merrett, K., Mitra, D., Forrester, J.V., Li, F. and Griffith, M. 2013. Crosslinked collagen hydrogels as corneal implants: Effects of sterically bulky vs. non-bulky carbodiimides as crosslinkers. *Acta Biomaterialia.* **9**(8), pp.7796-7805.

Aishanjiang, D., Green, E.C., Li, H. and Minus, M.L. 2016. Advances Toward Forming Synthetic Mimetic Tendon. *Mrs Advances.* **1**(18), pp.1283-1288.

Akbari, M., Tamayol, A., Laforte, V., Annabi, N., Najafabadi, A.H., Khademhosseini, A. and Juncker, D. 2014. Composite Living Fibers for Creating Tissue Constructs Using Textile Techniques. *Advanced Functional Materials.* **24**(26), pp.4060-4067.

Al-Shammari, B., Al-Fariss, T., Al-Sewailm, F. and Elleithy, R. 2011. The effect of polymer concentration and temperature on the rheological behavior of metallocene linear low density polyethylene (mLLDPE) solutions. *Journal of King Saud University - Engineering Sciences.* **23**(1), pp.9-14.

Alconcel, S.N.S., Baas, A.S. and Maynard, H.D. 2011. FDA-approved poly(ethylene glycol)–protein conjugate drugs. *Polymer Chemistry.* **2**(7), pp.1442-1448.

Alexander, F.A., Johnson, L., Williams, K. and Packer, K. 2019. A Parameter Study for 3D-Printing Organized Nanofibrous Collagen Scaffolds Using Direct-Write Electrospinning. *Materials.* **12**(24).

Aloglu, A.K. and Harrington, P.D. 2018. Differentiation of Bovine, Porcine, and Fish Gelatins by Attenuated Total Reflectance Fourier Transform Infrared Spectroscopy (ATR-FTIRS) Coupled with Pattern Recognition. *Journal of Aoac International.* **101**(1), pp.221-226.

Alrubaiy, L. and Al-Rubaiy, K.K. 2009. Skin substitutes: a brief review of types and clinical applications. *Oman medical journal.* **24**(1), pp.4-6.

Antipova, T.V., Zhelifonova, V.P., Zaitsev, K.V., Nedorezova, P.M., Aladyshev, A.M., Klyamkina, A.N., Kostyuk, S.V., Danilogorskaya, A.A. and Kozlovsky, A.G. 2018. Biodegradation of Poly-epsilon-caprolactones and Poly-l-lactides by Fungi. *Journal of Polymers and the Environment.* **26**(12), pp.4350-4359.

Arafat, M.T., Tronci, G., Yin, J., Wood, D.J. and Russell, S.J. 2015. Biomimetic wet-stable fibres via wet spinning and diacid-based crosslinking of collagen triple helices. *Polymer.* **77**, pp.102-112.

Arellano-Olivares, R.M., Yanez, K.J., Hernandez-Tellez, B., Pinon-Zarate, G., Herrera-Enriquez, M.A. and Castell-Rodriguez, A.E. 2016. Characterization of a Gelatin-Hyaluronic Acid Scaffold for Dressing Wound Healing. *Tissue Engineering Part A.* **22**, pp.S138-S139.

Argento, G., Simonet, M., Oomens, C.W.J. and Baaijens, F.P.T. 2012. Multi-scale mechanical characterization of scaffolds for heart valve tissue engineering. *Journal of Biomechanics.* **45**(16), pp.2893-2898.

Badrossamay, M.R., Balachandran, K., Capulli, A.K., Golecki, H.M., Agarwal, A., Goss, J.A., Kim, H., Shin, K. and Parker, K.K. 2014. Engineering hybrid polymer-protein super-aligned nanofibers via rotary jet spinning. *Biomaterials.* **35**(10), pp.3188-3197.

Baghersad, S., Bahrami, S.H., Mohammadi, M.R., Mojtahedi, M.R.M. and Milan, P.B. 2018. Development of biodegradable electrospun gelatin/aloe-vera/poly (epsilon-caprolactone) hybrid nanofibrous scaffold for application as skin substitutes. *Materials Science & Engineering C-Materials for Biological Applications.* **93**, pp.367-379.

Bai, Z.H., Reyes, J.M.M., Montazami, R. and Hashemi, N. 2014. On-chip development of hydrogel microfibers from round to square/ribbon shape. *Journal of Materials Chemistry A.* **2**(14), pp.4878-4884.

Baker, S., Begum, R., Zalupski, P., Durham, M. and Fitch, A. 2004. Polyethylene glycol penetration into clay films: real time experiments. *Colloids and Surfaces a-Physicochemical and Engineering Aspects.* **238**(1-3), pp.141-149.

Balasubramanian, P., Prabhakaran, M.P., Sireesha, M. and Ramakrishna, S. 2013. Collagen in Human Tissues: Structure, Function, and Biomedical Implications from a Tissue Engineering Perspective. *Polymer Composites - Polyolefin Fractionation - Polymeric Peptidomimetics - Collagens.* **251**, pp.173-206.

Bartis, D., J. Pongrácz. 2011. *Three dimensional tissue cultures and tissue engineering: http://www.tankonyvtar.hu/hu/tartalom/tamop425/0011_1A_3D_en_book/ch01s14.html.* [Online]. [Accessed 13/3/2015].

Basu, P., Kumar, U.N. and Manjubala, I. 2017. Wound healing materials - a perspective for skin tissue engineering. *Current Science.* **112**(12), pp.2392-2404.

Bigi, A., Cojazzi, G., Panzavolta, S., Rubini, K. and Roveri, N. 2001. Mechanical and thermal properties of gelatin films at different degrees of glutaraldehyde crosslinking. *Biomaterials.* **22**(8), pp.763-768.

Bohn, G., Liden, B., Schultz, G., Yang, Q.P. and Gibson, D.J. 2016. Ovine-Based Collagen Matrix Dressing: Next-Generation Collagen Dressing for Wound Care. *Advances in Wound Care.* **5**(1), pp.1-10.

Bota, P.C.S., Collie, A.M.B., Puolakkainen, P., Vernon, R.B., Sage, E.H., Ratner, B.D. and Stayton, P.S. 2010. Biomaterial topography alters healing in vivo and monocyte/macrophage activation in vitro. *Journal of Biomedical Materials Research Part A.* **95A**(2), pp.649-657.

Briefer, M. and Cohen, J.H. 1927. A study of gelatin viscosity and related problems. *Industrial and Engineering Chemistry.* **19**(1), pp.252-257.

BSI. 1996. *BS EN ISO 5079 Determination of breaking force and elongation at break of individual fibres.* UK: BSI.

Bubnis, W.A. and Ofner, C.M. 1992. The determination of epsilon-amino groups in soluble and poorly soluble proteinaceous materials by a spectrophotometric method using trinitobenzesulfonic acid *Analytical Biochemistry.* **207**(1), pp.129-133.

Burak, S., Soichi, O. and Joung, H.L. 2011. Non-watertight dural reconstruction in meningioma surgery: results in 439 consecutive patients and a review of the literature. *Journal of Neurosurgery JNS.* **114**(3), pp.714-718.

Camangi-Corp. 2020. *https://www.umorfil.com/product.html.* [Online]. [Accessed 26/02/2020].

Cavallaro, J.F., Kemp, P.D. and Kraus, K.H. 1994. Collagen fabrics as biomaterial. *Biotechnology and Bioengineering.* **43**(8), pp.781-791.

Caves, J.M., Kumar, V.A., Wen, J., Cui, W., Martinez, A., Apkarian, R., Coats, J.E., Berland, K. and Chaikof, E.L. 2010. Fibrillogenesis in Continuously Spun Synthetic Collagen Fiber. *Journal of Biomedical Materials Research Part B-Applied Biomaterials.* **93B**(1), pp.24-38.

Cebi, N., Durak, M.Z., Toker, O.S., Sagdic, O. and Arici, M. 2016. An evaluation of Fourier transforms infrared spectroscopy method for the classification and discrimination of bovine, porcine and fish gelatins. *Food Chemistry.* **190**, pp.1109-1115.

Centanni, J.M., Straseski, J.A., Wicks, A., Hank, J.A., Rasmussen, C.A., Lokuta, M.A., Schurr, M.J., Foster, K.N., Faucher, L.D., Caruso, D.M., Comer, A.R. and Allen-Hoffmann, B.L. 2011. StrataGraft Skin Substitute Is Well-tolerated and Is Not Acutely Immunogenic in Patients With Traumatic

Wounds Results From a Prospective, Randomized, Controlled Dose Escalation Trial. *Annals of Surgery.* **253**(4), pp.672-683.

Chandra, G.S. 2017. Effective Drug Delivery Alginate-gelatin polymer blends. *Current Science.* **112**(9), pp.1799-1799.

Chaparro, F.J., Matusicky, M.E., Allen, M.J. and Lannutti, J.J. 2016. Biomimetic microstructural reorganization during suture retention strength evaluation of electrospun vascular scaffolds. *Journal of Biomedical Materials Research Part B-Applied Biomaterials.* **104**(8), pp.1525-1534.

Chen, W., Villa-Diaz, L.G., Sun, Y., Weng, S., Kim, J.K., Lam, R.H.W., Han, L., Fan, R., Krebsbach, P.H. and Fu, J. 2012. Nanotopography Influences Adhesion, Spreading, and Self-Renewal of Human Embryonic Stem Cells. *Acs Nano.* **6**(5), pp.4094-4103.

Cheng, H.M., Rashid, S., Yu, Z.X., Yoshizumi, A., Hwang, E.L. and Brodsky, B. 2011. Location of Glycine Mutations within a Bacterial Collagen Protein Affects Degree of Disruption of Triple-helix Folding and Conformation. *Journal of Biological Chemistry.* **286**(3), pp.2041-2046.

Chaochai, T.; Imai, Y.; Furuike, T.; Tamura, H. Preparation and Properties of Gelatin Fibers Fabricated by Dry Spinning. Fibers 2016, **4** (2). https://doi.org/10.3390/fib4010002

Choi, Y.S., Hong, S.R., Lee, Y.M., Song, K.W., Park, M.H. and Nam, Y.S. 1999. Study on gelatin-containing artificial skin: I. Preparation and characteristics of novel gelatin-alginate sponge. *Biomaterials.* **20**(5), pp.409-417.

Cichosz, J. and Hut, V.D. 2016. *Experimental Characterization and Numerical Modeling of the Mechanical Response for Biaxial Braided Composites.* Dr. Hut.

Cong, H.-P., Ren, X.-C., Wang, P. and Yu, S.-H. 2012. Wet-spinning assembly of continuous, neat, and macroscopic graphene fibers. *Scientific Reports.* **2**, p613.

Cook, G. 2001. 3 - Protein Fibres. *Woodhead Publishing Series in Textiles.* **2**, pp.115 - 147.

Cullen, B., Watt, P.W., Lundqvist, C., Silcock, D., Schmidt, R.J., Bogan, D. and Light, N.D. 2002. The role of oxidised regenerated cellulose/collagen in chronic wound repair and its potential mechanism of action. *International Journal of Biochemistry & Cell Biology.* **34**(12), pp.1544-1556.

Cumming, M.H., Leonard, A.R., LeCorre-Bordes, D.S. and Hofman, K. 2018. Intra-fibrillar citric acid crosslinking of marine collagen electrospun nanofibres. *International Journal of Biological Macromolecules.* **114**, pp.874-881.

Cutting, K. 2003. Wound exudate: composition and functions. *British journal of community nursing.* **8**(3), pp.4-9.

DeFrates, K.G., Moore, R., Borgesi, J., Lin, G.W., Mulderig, T., Beachley, V. and Hu, X. 2018. Protein-Based Fiber Materials in Medicine: A Review. *Nanomaterials.* **8**(7).

Deible, C.R., Petrosko, P., Johnson, P.C., Beckman, E.J., Russell, A.J. and Wagner, W.R. 1999. Molecular barriers to biomaterial thrombosis by modification of surface proteins with polyethylene glycol. *Biomaterials.* **20**(2), pp.101-109.

Delyth, E.E., Fred, J.D., Geoffrey, R.M. and Robert, H.O. 2009. Structure development in electrospun fibres of gelatin. *Journal of Physics: Conference Series.* **183**(1), p012021.

Di Giuseppe, M., Law, N., Webb, B., Macrae, R.A., Liew, L.J., Sercombe, T.B., Dilley, R.J. and Doyle, B.J. 2018. Mechanical behaviour of alginate-gelatin hydrogels for 3D bioprinting. *Journal of the Mechanical Behavior of Biomedical Materials.* **79**, pp.150-157.

Dias, J.R., Antunes, F.E. and Bartolo, P.J. 2013. Influence of the Rheological Behaviour in Electrospun PCL Nanofibres Production for Tissue Engineering Applications. *Icheap-11: 11th International Conference on Chemical and Process Engineering, Pts 1-4.* **32**, pp.1015-1020.

Elmogahzy, Y., R. Farag. 2018. *Tensile properties of cotton fibers: importance, research, and limitations.* Woodhead Publishing.

Enea, D., Gwynne, J., Kew, S., Arumugam, M., Shepherd, J., Brooks, R., Ghose, S., Best, S., Cameron, R. and Rushton, N. 2013. Collagen fibre implant for tendon and ligament biological augmentation. In vivo study in an ovine model. *Knee Surgery Sports Traumatology Arthroscopy.* **21**(8), pp.1783-1793.

Enea, D., Henson, F., Kew, S., Wardale, J., Getgood, A., Brooks, R. and Rushton, N. 2011. Extruded collagen fibres for tissue engineering applications: effect of crosslinking method on mechanical and biological properties. *Journal of Materials Science-Materials in Medicine.* **22**(6), pp.1569-1578.

Engel, J. and Bachinger, H.P. 2005. Structure, stability and folding of the collagen triple helix. *Collagen: Primer in Structure, Processing and Assembly.* **247**, pp.7-33.

Everaerts, F., Torrianni, M., Hendriks, M. and Feijen, J. 2007. Quantification of carboxyl groups in carbodiimide cross-linked collagen sponges. *Journal of Biomedical Materials Research Part A.* **83A**(4), pp.1176-1183.

Farzamfar, S., Naseri-Nosar, M., Samadian, H., Mahakizadeh, S., Tajerian, R., Rahmati, M., Vaez, A. and Salehi, M. 2018. Taurine-loaded poly (epsilon-caprolactone)/gelatin electrospun mat as a potential wound dressing material: In vitro and in vivo evaluation. *Journal of Bioactive and Compatible Polymers.* **33**(3), pp.282-294.

Frantz, C., Stewart, K.M. and Weaver, V.M. 2010. The extracellular matrix at a glance. *Journal of Cell Science.* **123**(24), pp.4195-4200.

Freeman, J.W., Woods, M.D. and Laurencin, C.T. 2007. Tissue engineering of the anterior cruciate ligament using a braid-twist scaffold design. *Journal of Biomechanics.* **40**(9), pp.2029-2036.

Fukae, R., Maekawa, A. and Sangen, S. 2005. Gel-spinning and drawing of gelatin. *Polymer.* **46**(25), pp.11193-11194.

Fukae, R. and Midorikawa, T. 2008. Preparation of Gelatin Fiber by Gel Spinning and Its Mechanical Properties. *Journal of Applied Polymer Science.* **110**(6), pp.4011-4015.

Gabbott, P. 2008. *A Practical Introduction to Differential Scanning Calorimetry.* Oxford: Blackwell Publishing Ltd.

Gelse, K., Poschl, E. and Aigner, T. 2003. Collagens - structure, function, and biosynthesis. *Advanced Drug Delivery Reviews.* **55**(12), pp.1531-1546.

Ghasemi-Mobarakeh, L., Prabhakaran, M.P., Morshed, M., Nasr-Esfahani, M.H. and Ramakrishna, S. 2008. Electrospun poly(epsilon-caprolactone)/gelatin nanofibrous scaffolds for nerve tissue engineering. *Biomaterials.* **29**(34), pp.4532-4539.

Ginalska, G., Osinska, M., Uryniak, A., Urbanik-Sypniewska, T., Belcarz, A., Rzeski, W. and Wolski, A. 2005. Antibacterial activity of gentamicin-bonded gelatin-sealed polyethylene terephthalate vascular prostheses. *European Journal of Vascular and Endovascular Surgery.* **29**(4), pp.419-424.

Gopinath, A., Reddy, S.M.M., Madhan, B., Shanmguam, G. and Rao, J.R. 2014. Effect of aqueous ethanol on the triple helical structure of collagen. *European Biophysics Journal with Biophysics Letters.* **43**(12), pp.643-652.

Gorgieva, S., Kokol, K. 2011. Collagen- vs. Gelatine-Based Biomaterials and Their Biocompatibility: Review and Perspectives. In: Pignatello, R. ed. *Biomaterials.*

Gottlieb, M., Jennifer Furman. 2004. Successful Management and Surgical Closure of Chronic and Pathological Wounds using Integra. *Journal of Burns & Surgical Wound Care.* **3**(4).

Gough, J.E., Scotchford, C.A. and Downes, S. 2002. Cytotoxicity of glutaraldehyde crosslinked collagen/poly(vinyl alcohol) films is by the mechanism of apoptosis. *Journal of Biomedical Materials Research.* **61**(1), pp.121-130.

Guan, J.J., Yang, J., Dai, J.Q., Qin, Y.H., Wang, Y., Guo, Y.P., Ke, Q.F. and Zhang, C.Q. 2015. Bioinspired nanostructured hydroxyapatite/collagen three-dimensional porous scaffolds for bone tissue engineering. *Rsc Advances.* **5**(46), pp.36175-36184.

Gunzler, H., H.U. Gremlich. 2002. *IR Spectroscopy.* Weinheim: Wiley-Vch.

Haghi, A.K. 2012. *Electrospinning of nanofibers in textiles.*

Hashemi, J., Chandrashekar, N. and Slauterbeck, J. 2005. The mechanical properties of the human patellar tendon are correlated to its mass density and are independent of sex. *Clinical Biomechanics.* **20**(6), pp.645-652.

Hashimoto, Y., Hattori, S., Sasaki, S., Honda, T., Kimura, T., Funamoto, S., Kobayashi, H. and Kishida, A. 2016. Ultrastructural analysis of the decellularized cornea after interlamellar keratoplasty and microkeratome-assisted anterior lamellar keratoplasty in a rabbit model. *Scientific Reports.* **6**.

Haslauer, C.M., et al. 2014. Translating textiles to tissue engineering: Creation and evaluation of microporous, biocompatible, degradable scaffolds using industry relevant manufacturing approaches and human adipose derived stem cells. *Journal of Biomedical materials Research B: Applied Biomaterials.* **00B**(0), pp.1-9.

Haynl, C., Hofmann, E., Pawar, K., Förster, S. and Scheibel, T. 2016. Microfluidics-Produced Collagen Fibers Show Extraordinary Mechanical Properties. *Nano Letters.*

He, N.F., Ke, Q.F., Huang, C., Yang, J. and Guo, Y.P. 2014. Needle-Punched Nonwoven Matrix from Regenerated Collagen Fiber for Cartilage Tissue Engineering. *Journal of Applied Polymer Science.* **131**(13).

Helling, A.L., Tsekoura, E.K., Biggs, M., Bayon, Y., Pandit, A. and Zeugolis, D.I. 2017. In Vitro Enzymatic Degradation of Tissue Grafts and Collagen Biomaterials by Matrix Metalloproteinases: Improving the Collagenase Assay. *Acs Biomaterials Science & Engineering.* **3**(9), pp.1922-1932.

Hiramatsu, H., Hori, A., Yajima, Y., Yamada, M., Seki, M. and Ieee. 2016. Microfluidics-based Wet Spinning of Protein Microfibers as Solid Scaffolds for 3D Cell Cultivation. *2016 International Symposium on Micro-Nanomechatronics and Human Science (Mhs).*

Hlavata, J., Suchy, T., Supova, M., Pokorny, M., Kostakova, E.K., Czech Soc New, M., Technol, Region Ctr Adv, T. and Mat. 2017. A comparison of centrifugal force spinning and electrospinning of collagen under different conditions. *8th International Conference on Nanomaterials - Research & Application (Nanocon 2016).* pp.514-519.

Hoch, E., Schuh, C., Hirth, T., Tovar, G.E.M. and Borchers, K. 2012. Stiff gelatin hydrogels can be photo-chemically synthesized from low viscous gelatin solutions using molecularly functionalized gelatin with a high degree of methacrylation. *Journal of Materials Science: Materials in Medicine.* **23**(11), pp.2607-2617.

Hodde, J.P., Record, R.D., Liang, H.A. and Badylak, S.F. 2001. Vascular endothelial growth factor in porcine-derived extracellular matrix. *Endothelium-New York.* **8**(1), pp.11-24.

Hodges, J.A. and Raines, R.T. 2005. Stereoelectronic and steric effects in the collagen triple helix: Toward a code for strand association. *Journal of the American Chemical Society.* **127**(45), pp.15923-15932.

Holmes, R., Yang, X.B.B., Dunne, A., Florea, L., Wood, D. and Tronci, G. 2017. Thiol-Ene Photo-Click Collagen-PEG Hydrogels: Impact of Water-Soluble Photoinitiators on Cell Viability, Gelation Kinetics and Rheological Properties. *Polymers.* **9**(6).

Huang, Y.F., Meek, K.M., Ho, M.W. and Paterson, C.A. 2001. Anaylsis of birefringence during wound healing and remodeling following alkali burns in rabbit cornea. *Experimental Eye Research.* **73**(4), pp.521-532.

Huang, Z.L. and Jiang, G.J. 2006. Manufacture of gelatin/chitosan wound dressing and experimental study on its biological evaluation. *Tissue Engineering.* **12**(4), pp.1070-1071.

Hudson Jr, R.E., W. C. Monk Jr 1971. *Solvent bonding of synthetic fibers*.

Hulmes, D.J.S., Miller, A., Parry, D.A.D., Piez, K.A. and Woodhead.J. 1973. Analysis of primary structure of collagen for origins of molecular packing. *Journal of Molecular Biology.* **79**(1), pp.137-148.

IntegraLifeSciencesCorporation. 2010. *INTEGRA™ Bilayer Matrix Wound Dressing: Product makeup, http://www.ilstraining.com/bmwd/bmwd/bmwd_it_03.html.* [Online]. [Accessed 6/3/2015].

Jabłońska-Trypuć, A., Matejczyk, M. and Rosochacki, S. 2016. Matrix metalloproteinases (MMPs), the main extracellular matrix (ECM) enzymes in collagen degradation, as a target for anticancer drugs. *Journal of Enzyme Inhibition and Medicinal Chemistry.* **31**(sup1), pp.177-183.

Jarvinen, T.A.H., Jarvinen, T.L.N., Kannus, B.B., Jozsa, L. and Jarvinen, M. 2004. Collagen fibres of the spontaneously ruptured human tendons display decreased thickness and crimp angle. *Journal of Orthopaedic Research.* **22**(6), pp.1303-1309.

Jones, A.C., Arns, C.H., Hutmacher, D.W., Milthorpe, B.K., Sheppard, A.P. and Knackstedt, M.A. 2009. The correlation of pore morphology, interconnectivity and physical properties of 3D ceramic scaffolds with bone ingrowth. *Biomaterials.* **30**(7), pp.1440-1451.

Juhar, G., Saqan, S. & Zihlif, A. M. 2001. The plastic deformation of fibrous polymers via Weibull model. *Polymers & Polymer Composites*, **9,** 473-481.

Juncker, David & Rooij, N.. (2002). Capillary microfluidic systems for bio/chemistry.

Kadler, K.E., Hill, A. and Canty-Laird, E.G. 2008. Collagen fibrillogenesis: fibronectin, integrins, and minor collagens as organizers and nucleators. *Current Opinion in Cell Biology.* **20**(5), pp.495-501.

Kalaithong, W., Molloy, R., Theerathanagorn, T. and Janvikul, W. 2017. Novel Poly(L-lactide-co-caprolactone)/Gelatin Porous Scaffolds for Use in Articular Cartilage Tissue Engineering: Comparison of Electrospinning and Wet Spinning Processing Methods. *Polymer Engineering and Science.* **57**(8), pp.875-882.

Kaneka-Corporation. 2013. *http://www.kanecaron.com/cef/en/index.html*. [Online]. [Accessed 26/2/2020].

Kanokpanont, S., Damrongsakkul, S., Ratanavaraporn, J. and Aramwit, P. 2012. An innovative bi-layered wound dressing made of silk and gelatin for accelerated wound healing. *International Journal of Pharmaceutics.* **436**(1-2), pp.141-153.

Kato, Y.P. and Silver, F.H. 1990. FORMATION OF CONTINUOUS COLLAGEN-FIBERS - EVALUATION OF BIOCOMPATIBILITY AND MECHANICAL-PROPERTIES. *Biomaterials.* **11**(3), pp.169-175.

Kew, S.J., Gwynne, J.H., Enea, D., Abu-Rub, M., Pandit, A., Zeugolis, D., Brooks, R.A., Rushton, N., Best, S.M. and Cameron, R.E. 2011. Regeneration and repair of tendon and ligament tissue using collagen fibre biomaterials. *Acta Biomaterialia.* **7**(9), pp.3237-3247.

Kew, S.J., Gwynne, J.H., Enea, D., Brookes, R., Rushton, N., Best, S.M. and Cameron, R.E. 2012. Synthetic collagen fascicles for the regeneration of tendon tissue. *Acta Biomaterialia.* **8**(10), pp.3723-3731.

Khan, M.Y., Samanta, A., Ojha, K. and Mandal, A. 2009. Design of Alkaline/Surfactant/Polymer (ASP) Slug and its use in Enhanced Oil Recovery. *Petroleum Science and Technology.* **27**(17), pp.1926-1942.

Khorshidi, S., Solouk, A., Mirzadeh, H., Mazinani, S., Lagaron, J.M., Sharifi, S. and Ramakrishna, S. 2016. A review of key challenges of electrospun scaffolds for tissue-engineering applications. *Journal of Tissue Engineering and Regenerative Medicine.* **10**(9), pp.715-738.

Kiernan, B.J., Smoak, E.M., Server, K. and Banerjee, I.A. 2010. Fabrication of gelatin and gelatin-siloxane nanoparticles on peptide based nanotubes and their applications in drug delivery. *Abstracts of Papers of the American Chemical Society.* **239**.

Kim, J.Y., Kim, J.I., Park, C.H. and Kim, C.S. 2019. Design of a modified electrospinning for the in-situ fabrication of 3D cotton-like collagen fiber bundle mimetic scaffold. *Materials Letters.* **236**, pp.521-525.

Kim, S., Ahn, S.H., Lee, J.S., Song, J.E., Cho, S.H., Jung, S., Kim, S.K., Kim, S.H., Lee, K.P., Kwon, K.S. and Lee, T.H. 2016. Differential Matrix

Metalloprotease (MMP) Expression Profiles Found in Aged Gingiva. *Plos One.* **11**(7).

Kovalenko, G.M., Bokova, E.S., Filatov, I.Y. and Mirontseva, V.V. 2017. Electrospun fibrous materials made of collagen and chitin derivatives. *Fibre Chemistry.* **48**(6), pp.466-469.

Lamke, L.O., Nilsson, G.E. and Reithner, H.L. 1977. The evaporative water loss from burns and the water-vapour permeability of grafts and artificial membranes used in the treatment of burns. *Burns.* **3**(3), pp.159-165.

Larson, C.E. and Greenberg, D.M. 1933. A paradoxical solubility phenomenon with gelatin. *Journal of the American Chemical Society.* **55**, pp.2798-2799.

Lee, B.H., Lum, N., Seow, L.Y., Lim, P.Q. and Tan, L.P. 2016. Synthesis and Characterization of Types A and B Gelatin Methacryloyl for Bioink Applications. *Materials.* **9**(10).

Lekakou, C., Lamprou, D., Vidyarthi, U., Karopoulou, E. and Zhdan, P. 2008. Structural hierarchy of biomimetic materials for tissue engineered vascular and orthopedic grafts. *Journal of Biomedical Materials Research Part B-Applied Biomaterials.* **85B**(2), pp.461-468.

Liang, H., Russell, S.J., Wood, D.J. and Tronci, G. 2018. Monomer-Induced Customization of UV-Cured Atelocollagen Hydrogel Networks. *Frontiers in chemistry.* **6**, pp.626-626.

Liu, H., Ding, X., Zhou, G., Li, P., Wei, X. and Fan, Y. 2013. Electrospinning of Nanofibers for Tissue Engineering Applications. *Journal of Nanomaterials.*

Liu, Y.X. and Chan-Park, M.B. 2010. A biomimetic hydrogel based on methacrylated dextran-graft-lysine and gelatin for 3D smooth muscle cell culture. *Biomaterials.* **31**(6), pp.1158-1170.

Loss, M., Wedler, V., Kunzi, W., Meuli-Simmen, C. and Meyer, V.E. 2000. Artificial skin, split-thickness autograft and cultured autologous keratinocytes combined to treat a severe burn injury of 93% of TBSA. *Burns.* **26**(7), pp.644-652.

Lu, T., Hu, H., Li, Y.Q., Jiang, Q.S., Su, J.L., Lin, H., Xiao, Y., Zhu, X.D. and Zhang, X.D. 2020. Bioactive scaffolds based on collagen filaments with tunable physico-chemical and biological features. *Soft Matter.* **16**(18), pp.4540-4548.

Luescher, M., Ruegg, M. and Schindler, P. 1974. Effect of hydration upon thermal-stability of tropocollagen and its dependence on presence of neutral salts. *Biopolymers.* **13**(12), pp.2489-2503.

Lynn, A.K., Yannas, I.V. and Bonfield, W. 2004. Antigenicity and immunogenicity of collagen. *Journal of Biomedical Materials Research Part B-Applied Biomaterials.* **71B**(2), pp.343-354.

Mackley, M. 2010. Stretching polymer chains. *Rheologica Acta.* **49**(5), pp.443-458.

Mahony, O., Tsigkou, O., Ionescu, C., Minelli, C., Ling, L., Hanly, R., Smith, M.E., Stevens, M.M. and Jones, J.R. 2010. Silica-Gelatin Hybrids with Tailorable Degradation and Mechanical Properties for Tissue Regeneration. *Advanced Functional Materials.* **20**(22), pp.3835-3845.

Mai, F., Tu, W., Bilotti, E. and Peijs, T. 2015. The Influence of Solid-State Drawing on Mechanical Properties and Hydrolytic Degradation of Melt-Spun Poly(Lactic Acid) (PLA) Tapes. *Fibers.* **3**(4), p523.

Marshall, A.S. and Petrie, S.E.B. 1980. Thermal transitions in gelatin and aqueous gelatin solutions. *Journal of Photographic Science.* **28**(3), pp.128-134.

Maurer, P.K. and McDonald, J.V. 1985. Vicryl (polyglactin 910) mesh as a dural substitute. **63**(3), p448.

Meyer, M., Baltzer, H. and Schwikal, K. 2010. Collagen fibres by thermoplastic and wet spinning. *Materials Science & Engineering C-Materials for Biological Applications.* **30**(8), pp.1266-1271.

Midorikawa, T., Lawal, O.S., Sasaki, Y. and Fukae, R. 2012. Structure and physical properties of gelatin fibers prepared by gel-spinning in ethylene glycol. *Journal of Applied Polymer Science.* **125**, pp.E332-E338.

Miles, A.C. and Bailey, J., A. 1999. *Thermal Denaturation of Collagen Revisited.*

Miles, C.A. and Ghelashvili, M. 1999. Polymer-in-a-Box Mechanism for the Thermal Stabilization of Collagen Molecules in Fibers. *Biophysical Journal.* **76**(6), pp.3243-3252.

Mukherjee, I. and Rosolen, M. 2013. Thermal transitions of gelatin evaluated using DSC sample pans of various seal integrities. *Journal of Thermal Analysis and Calorimetry.* **114**(3), pp.1161-1166.

Muyonga, J.H., Cole, C.G.B. and Duodu, K.G. 2004. Fourier transform infrared (FTIR) spectroscopic study of acid soluble collagen and gelatin from skins and bones of young and adult Nile perch (Lates niloticus). *Food Chemistry.* **86**(3), pp.325-332.

Naito, K., Yang, JM., Tanaka, Y. et al. 2012.The effect of gauge length on tensile strength and Weibull modulus of polyacrylonitrile (PAN)- and pitch-based carbon fibers. J *Mater Sc*i **47,** pp. 632–642

Neffe, A.T., Tronci, G., Alteheld, A. and Lendlein, A. 2010. Controlled Change of Mechanical Properties during Hydrolytic Degradation of Polyester Urethane Networks. *Macromolecular Chemistry and Physics.* **211**(2), pp.182-194.

Nguyen, D.T., Orgill, D.P. and Murphy, G.F. 2009. 4 - The pathophysiologic basis for wound healing and cutaneous regeneration. In: Orgill, D. and Blanco, C. eds. *Biomaterials for Treating Skin Loss.* Woodhead Publishing, pp.25-57.

O'Brien, F.J. 2011. Biomaterials & scaffolds for tissue engineering. *Materials Today.* **14**(3), pp.88-95.

OED. 2018. *"viscosity, n."* *http://www.oed.com/view/Entry/223901?redirectedFrom=viscosity*. [Online]. [Accessed 11/10]. Available from: http://www.oed.com/view/Entry/223901?redirectedFrom=viscosity

Okamoto, Y. and Saeki, K. 2013. Phase transition of collagen and gelatin. *Kolloid-Zeitschrift und Zeitschrift für Polymere.* **194**(2), p124.

Ovlaque, Pierre & Foruzanmehr, M.Reza & Elkoun, Saïd & Robert, Mathieu. 2019. Milkweed floss fiber/PLA composites: effect of alkaline and epoxy-silanol surface modifications on their mechanical properties. *Composite Interfaces*. **27**. 1-19.

Panwar, P., Du, X., Sharma, V., Lamour, G., Castro, M., Li, H.B. and Bromme, D. 2013. Effects of Cysteine Proteases on the Structural and Mechanical Properties of Collagen Fibers. *Journal of Biological Chemistry.* **288**(8), pp.5940-5950.

Papa, G., Pangos, M., Renzi, N., Ramella, V., Panizzo, N. and Marij, A.Z. 2011. Five Years of Experience Using a Dermal Substitute: Indications, Histologic Studies, and First Results Using a New Single-Layer Tool. *Dermatologic Surgery.* **37**(11), pp.1631-1637.

Patterson, J. and Hubbell, J.A. 2010. Enhanced proteolytic degradation of molecularly engineered PEG hydrogels in response to MMP-1 and MMP-2. *Biomaterials.* **31**(30), pp.7836-7845.

Paul, D.R. 1968. Diffusion during the coagulation step of wet-spinning. *Journal of Applied Polymer Science.* **12**(3), pp.383-402.

Peng, G.-q., Wen, Y.-f., Yang, Y.-g., Liu, L. and Wang, W. 2009. Effect of dope extrusion rate on the formation and characterization of polyacrylonitrile nascent fibers during wet-spinning. *Polymer Bulletin.* **62**(5), pp.657-666.

Pins, G.D., Christiansen, D.L., Patel, R. and Silver, F.H. 1997a. Self-assembly of collagen fibers. Influence of fibrillar alignment and decorin on mechanical properties. *Biophysical Journal.* **73**(4), pp.2164-2172.

Pins, G.D., Huang, E.K., Christiansen, D.L. and Silver, F.H. 1997b. Effects of static axial strain on the tensile properties and failure mechanisms of self-assembled collagen fibers. *Journal of Applied Polymer Science.* **63**(11), pp.1429-1440.

Powell, H.M. and Boyce, S.T. 2006. EDC cross-linking improves skin substitute strength and stability. *Biomaterials.* **27**(34), pp.5821-5827.

Powell, H.M. and Boyce, S.T. 2009. Engineered Human Skin Fabricated Using Electrospun Collagen-PCL Blends: Morphogenesis and Mechanical Properties. *Tissue Engineering Part A.* **15**(8), pp.2177-2187.

Power, G., Moore, Z. and O'Connor, T. 2017. Measurement of pH, exudate composition and temperature in wound healing: a systematic review. *Journal of Wound Care.* **26**(7), pp.381-397.

Poza, P., Perez-Rigueiro, J., Elices, M. & Llorca, J. 2002. Fractographic analysis of silkworm and spider silk. *Engineering Fracture Mechanics*, **69**, 1035-1048.

Puppi, D., Piras, A.M., Chiellini, F., Chiellini, E., Martins, A., Leonor, I.B., Neves, N. and Reis, R. 2011. Optimized electro- and wet-spinning techniques for the production of polymeric fibrous scaffolds loaded with bisphosphonate and hydroxyapatite. *Journal of Tissue Engineering and Regenerative Medicine.* **5**(4), pp.253-263.

Raiskup, F. and Spoerl, E. 2013. Corneal Crosslinking with Riboflavin and Ultraviolet A. I. Principles. *Ocular Surface.* **11**(2), pp.65-74.

Reneker, D.H. and Yarin, A.L. 2008. Electrospinning jets and polymer nanofibers. *Polymer.* **49**(10), pp.2387-2425.

Rojas, I.-G., Padgett, D.A., Sheridan, J.F. and Marucha, P.T. 2002. Stress-Induced Susceptibility to Bacterial Infection During Cutaneous Wound Healing. *Brain, Behavior, and Immunity.* **16**(1), pp.74-84.

Roseti, L., Cavallo, C., Desando, G., Parisi, V., Petretta, M., Bartolotti, I. and Grigolo, B. 2018. Three-Dimensional Bioprinting of Cartilage by the Use of Stem Cells: A Strategy to Improve Regeneration. *Materials.* **11**(9).

Rozario, T. and DeSimone, D.W. 2010. The extracellular matrix in development and morphogenesis: A dynamic view. *Developmental Biology.* **341**(1), pp.126-140.

Russell, S.J., Mao, N. 2004. Nonwoven Wound Dressings. *Textile Progress.* **36**(4), pp.1-57.

Sakakibara, S., Inouye, K., Shudo, K., Kishida, Y., Kobayashi, Y. and Prockop, D.J. 1973. Synthesis of (pro-hyp-gly)n of defined molecular-weights - evidence for stabilization of collagen triple helix by hydroxypyroline. *Biochimica Et Biophysica Acta.* **303**(1), pp.198-202.

Salgaller, M.L. and Bajpai, P.K. 1985. Immunogenicity of glutaraldehyde-treated bovine pericardial tissue xenografts in rabbits. *Journal of Biomedical Materials Research.* **19**(1), pp.1-12.

Schiefer, J.L., Rath, R., Held, M., Petersen, W., Werner, J.O., Schaller, H.E. and Rahmanian-Schwarz, A. 2016. Frequent Application of the New

Gelatin-Collagen Nonwoven Accelerates Wound Healing. *Advances in Skin & Wound Care.* **29**(2), pp.73-78.

Seaman, S. 2002. Dressing selection in chronic wound management. *Journal of the American Podiatric Medical Association.* **92**(1), pp.24-33.

Shaw, K.M. and Lewis, G. 1997. Tensile properties of human Achilles tendon. In: *16th Southern Biomedical Engineering Conference, Apr 04-06, Biloxi, Ms*. pp.338-341.

Shepherd, D.V., Shepherd, J.H., Ghose, S., Kew, S.J., Cameron, R.E. and Best, S.M. 2015. The process of EDC-NHS cross-linking of reconstituted collagen fibres increases collagen fibrillar order and alignment. *APL Materials.* **3**(1).

Shepherd, J.H., Ghose, S., Kew, S.J., Moavenian, A., Best, S.M. and Cameron, R.E. 2013. Effect of fiber crosslinking on collagen-fiber reinforced collagen-chondroitin-6-sulfate materials for regenerating load-bearing soft tissues. *Journal of Biomedical Materials Research Part A.* **101**(1), pp.176-184.

Shi, X.T., Ostrovidov, S., Zhao, Y.H., Liang, X.B., Kasuya, M., Kurihara, K., Nakajima, K., Bae, H., Wu, H.K. and Khademhosseini, A. 2015. Microfluidic Spinning of Cell-Responsive Grooved Microfibers. *Advanced Functional Materials.* **25**(15), pp.2250-2259.

Shojaei, S., Nikuei, M., Goodarzi, V., Hakani, M., Khonakdar, H.A. and Saeb, M.R. 2019. Disclosing the role of surface and bulk erosion on the viscoelastic behavior of biodegradable poly(epsilon-caprolactone)/poly(lactic acid)/hydroxyapatite nanocomposites. *Journal of Applied Polymer Science.* **136**(10).

Shoulders, M.D. and Raines, R.T. 2009. Collagen Structure and Stability. *Annual Review of Biochemistry.* **78**, pp.929-958.

Shubhra, Q.T.H., Alam, A. and Beg, M.D.H. 2011. Mechanical and degradation characteristics of natural silk fiber reinforced gelatin composites. *Materials Letters.* **65**(2), pp.333-336.

Silver, F.H., Freeman, J.W. and Seehra, G.P. 2003. Collagen self-assembly and the development of tendon mechanical properties. *Journal of Biomechanics.* **36**(10), pp.1529-1553.

Siriwardane, M.L., DeRosa, K., Collins, G. and Pfister, B.J. 2014. Controlled formation of cross-linked collagen fibers for neural tissue engineering applications. *Biofabrication.* **6**(1).

Skrzyński, S., Sionkowska, A. and Marciniak, A. 2009. DSC Study of Collagen in Disc Disease. *Journal of biophysics (Hindawi Publishing Corporation : Online).* **2009**, pp.819635-819635.

Stepanyan, R., Subbotin, A., Cuperus, L., Boonen, P., Dorschu, M., Oosterlinck, F. and Bulters, M. 2014. Fiber diameter control in electrospinning. *Applied Physics Letters.* **105**(17).

Stoessel, P.R., Krebs, U., Hufenus, R., Halbeisen, M., Zeltner, M., Grass, R.N. and Stark, W.J. 2015a. Porous, Water-Resistant Multifilament Yarn Spun from Gelatin. *Biomacromolecules.* **16**(7), pp.1997-2005.

Stoessel, P.R., Raso, R.A., Kaufmann, T., Grass, R.N. and Stark, W.J. 2015b. Fibers Mechanically Similar to Sheep Wool Obtained by Wet Spinning of Gelatin and Optional Plasticizers. *Macromolecular Materials and Engineering.* **300**(2), pp.234-241.

Sung, H.W., Chang, W.H., Ma, C.Y. and Lee, M.H. 2003. Crosslinking of biological tissues using genipin and/or carbodiimide. *Journal of Biomedical Materials Research Part A.* **64A**(3), pp.427-438.

Sung, H.W., Huang, R.N., Huang, L.L.H. and Tsai, C.C. 1999. In vitro evaluation of cytotoxicity of a naturally occurring cross-linking reagent for biological tissue fixation. *Journal of Biomaterials Science-Polymer Edition.* **10**(1), pp.63-78.

Sutherland, F.W.H., Perry, T.E., Yu, Y., Sherwood, M.C., Rabkin, E., Masuda, Y., Garcia, G.A., McLellan, D.L., Engelmayr, G.C., Sacks, M.S., Schoen, F.J. and Mayer, J.E. 2005. From stem cells to viable autologous semilunar heart valve. *Circulation.* **111**(21), pp.2783-2791.

Sutherland, J.C. 1996. *Circular Dichroism and the Conformational Analysis of Biomolecules.* Plenun Press.

Tamayol, A., Najafabadi, A.H., Aliakbarian, B., Arab-Tehrany, E., Akbari, M., Annabi, N., Juncker, D. and Khademhosseini, A. 2015. Hydrogel Templates for Rapid Manufacturing of Bioactive Fibers and 3D Constructs. *Advanced Healthcare Materials.* **4**(14), pp.2146-2153.

Tampieri, A., Celotti, G., Landi, E., Montevecchi, M., Roveri, N., Bigi, A., Panzavolta, S. and Sidoti, M.C. 2003. Porous phosphate-gelatine composite as bone graft with drug delivery function. *Journal of Materials Science-Materials in Medicine.* **14**(7), pp.623-627.

Teo, B.K.K., Wong, S.T., Lim, C.K., Kung, T.Y.S., Yap, C.H., Ramagopal, Y., Romer, L.H. and Yim, E.K.F. 2013. Nanotopography Modulates Mechanotransduction of Stem Cells and Induces Differentiation through Focal Adhesion Kinase. *Acs Nano.* **7**(6), pp.4785-4798.

Terasaka, S., Iwasaki, Y., Shinya, N. and Uchida, T. 2006. Fibrin glue and polyglycolic acid nonwoven fabric as a biocompatible dural substitute. *Neurosurgery.* **58**(2), pp.134-138.

Teule, F. 2008. Spinning of fibers from protein solutions. *Biologically Inspired Textiles.* (77), pp.44-73.

Tigani, D., Zolezzi, C., Trentani, F., Ragaini, A., Iafisco, M., Manara, S., Palazzo, B. and Roveri, N. 2008. Controlled release of vancomycin from cross-linked gelatine. *Journal of Materials Science-Materials in Medicine.* **19**(3), pp.1325-1334.

Tigner, T.J., Rajput, S., Gaharwar, A.K. and Alge, D.L. 2020. Comparison of Photo Cross Linkable Gelatin Derivatives and Initiators for Three-Dimensional Extrusion Bioprinting. *Biomacromolecules.* **21**(2), pp.454-463.

Timnak, A., Gharebaghi, F.Y., Shariati, R.P., Bahrami, S.H., Javadian, S., Emami, S.H. and Shokrgozar, M.A. 2011. Fabrication of nano-structured electrospun collagen scaffold intended for nerve tissue engineering. *Journal of Materials Science-Materials in Medicine.* **22**(6), pp.1555-1567.

Tonndorf, R., Aibibu, D. and Cherif, C. 2020. Collagen multifilament spinning. *Materials Science & Engineering C-Materials for Biological Applications.* **106**.

Tonndorf, R., Gossla, E., Aibibu, D., Lindner, M., Gelinsky, M. and Cherif, C. 2019. Wet spinning and riboflavin crosslin king of collagen type I/III filaments. *Biomedical Materials.* **14**(1).

Tracy, L.E., Minasian, R.A. and Caterson, E.J. 2016. Extracellular Matrix and Dermal Fibroblast Function in the Healing Wound. *Advances in Wound Care.* **5**(3), pp.119-136.

Tronci, G., Doyle, A., Russell, S.J. and Wood, D.J. 2013a. Triple-helical collagen hydrogels via covalent aromatic functionalisation with 1,3-phenylenediacetic acid. *Journal of Materials Chemistry B.* **1**(40), pp.5478-5488.

Tronci, G., Grant, C.A., Thomson, N.H., Russell, S.J. and Wood, D.J. 2015a. Multi-scale mechanical characterization of highly swollen photo-activated collagen hydrogels. *Journal of the Royal Society Interface.* **12**(102).

Tronci, G., Grant, C.A., Thomson, N.H., Russell, S.J. and Wood, D.J. 2016a. Influence of 4-vinylbenzylation on the rheological and swelling properties of photo-activated collagen hydrogels. *Mrs Advances.* **1**(8), pp.533-538.

Tronci, G., Kanuparti, R.S., Arafat, M.T., Yin, J., Wood, D.J. and Russell, S.J. 2015b. Wet-spinnability and crosslinked fibre properties of two collagen polypeptides with varied molecular weight. *International Journal of Biological Macromolecules.* **81**, pp.112-120.

Tronci, G., Neffe, A.T., Pierce, B.F. and Lendlein, A. 2010. An entropy-elastic gelatin-based hydrogel system. *Journal of Materials Chemistry.* **20**(40), pp.8875-8884.

Tronci, G., Russell, S.J. and Wood, D.J. 2013b. Photo-active collagen systems with controlled triple helix architecture. *Journal of Materials Chemistry B.* **1**(30), pp.3705-3715.

Tronci, G., Yin, J., Holmes, R.A., Liang, H., Russell, S.J. and Wood, D.J. 2016b. Protease-sensitive atelocollagen hydrogels promote healing in a diabetic wound model. *Journal of Materials Chemistry B.* **4**(45), pp.7249-7258.

Tronci G., e.a. 2014. Tunable drug-loading capability of chitosan hydrogels with varied network architectures. *Acta Biomaterialia.* **10**(2), pp.821-830.

Turker, E., Yildiz, U.H. and Yildiz, A.A. 2019. Biomimetic hybrid scaffold consisting of co-electrospun collagen and PLLCL for 3D cell culture. *International Journal of Biological Macromolecules.* **139**, pp.1054-1062.

Vandooren, J., Van den Steen, P.E. and Opdenakker, G. 2013. Biochemistry and molecular biology of gelatinase B or matrix metalloproteinase-9 (MMP-9): The next decade. *Critical Reviews in Biochemistry and Molecular Biology.* **48**(3), pp.222-272.

Vasudev, S.C. and Chandy, T. 1997. Effect of alternative crosslinking techniques on the enzymatic degradation of bovine pericardia and their calcification. *Journal of Biomedical Materials Research.* **35**(3), pp.357-369.

Venugopal, J., Low, S., Choon, A.T., Kumar, T.S.S. and Ramakrishna, S. 2008. Mineralization of osteoblasts with electrospun collagen/hydroxyapatite nanofibers. *Journal of Materials Science-Materials in Medicine.* **19**(5), pp.2039-2046.

Vogt, S., Copanaki, E., Grafahrend, D., Reibel, D., Neumüller, D.,. 2015. *Biodegradable nonwoven material for medical purposes*.

Wakuda, Y., Nishimoto, S., Suye, S. and Fujita, S. 2018. Native collagen hydrogel nanofibres with anisotropic structure using core-shell electrospinning. *Scientific Reports.* **8**.

Walters, V.I., Kwansa, A.L. and Freeman, J.W. 2012. Design and Analysis of Braid-Twist Collagen Scaffolds. *Connective Tissue Research.* **53**(3), pp.255-266.

Wang, K. 2012. Chapter 4: Die Swell of Complex Polymeric Systems. In: de Vicente, J. *Viscoelasticity - From Theory to Biological Applications*. InTech, p 77-96.

Wang, X.H., Ao, Q., Tian, X.H., Fan, J., Tong, H., Hou, W.J. and Bai, S.L. 2017. Gelatin-Based Hydrogels for Organ 3D Bioprinting. *Polymers.* **9**(9).

Wang, Y., Kankala, R.K., Zhu, K., Wang, S.B., Zhang, Y.S. and Chen, A.Z. 2019. Coaxial Extrusion of Tubular Tissue Constructs Using a Gelatin/GeIMA Blend Bioink. *Acs Biomaterials Science & Engineering.* **5**(10), pp.5514-5524.

Wenande, E. and Garvey, L.H. 2016. Immediate-type hypersensitivity to polyethylene glycols: a review. *Clinical and Experimental Allergy.* **46**(7), pp.907-922.

Xiang, C.H. and Frey, M.W. 2016. Increasing Mechanical Properties of 2-D-Structured Electrospun Nylon 6 Non-Woven Fiber Mats. *Materials.* **9**(4).

Yaari, A., Schilt, Y., Tamburu, C., Raviv, U. and Shoseyov, O. 2016. Wet Spinning and Drawing of Human Recombinant Collagen. *Acs Biomaterials-Science & Engineering.* **2**(3), pp.349-360.

Yang, C.Y., Chiu, C.T., Chang, Y.P. and Wang, Y.J. 2009. Fabrication of Porous Gelatin Microfibers Using an Aqueous Wet Spinning Process. *Artificial Cells Blood Substitutes and Biotechnology.* **37**(4), pp.173-176.

Yim, E.K.F., Liao, I.C. and Leong, K.W. 2007. Tissue compatibility of interfacial polyelectrolyte complexation fibrous scaffold: Evaluation of blood compatibility and biocompatibility. *Tissue Engineering.* **13**(2), pp.423-433.

Yue, K., Trujillo-de Santiago, G., Alvarez, M.M., Tamayol, A., Annabi, N. and Khademhosseini, A. 2015. Synthesis, properties, and biomedical applications of gelatin methacryloyl (GelMA) hydrogels. *Biomaterials.* **73**(Supplement C), pp.254-271.

Zaman, H.U., Islam, J.M.M., Khan, M.A. and Khan, R.A. 2011. Physico-mechanical properties of wound dressing material and its biomedical application. *Journal of the Mechanical Behavior of Biomedical Materials.* **4**(7), pp.1369-1375.

Zeugolis, D.I., Khew, S.T., Yew, E.S.Y., Ekaputra, A.K., Tong, Y.W., Yung, L.-Y.L., Hutmacher, D.W., Sheppard, C. and Raghunath, M. 2008. Electro-spinning of pure collagen nano-fibres – Just an expensive way to make gelatin? *Biomaterials.* **29**(15), pp.2293-2305.

Zeugolis, D.I., Paul, G.R. and Attenburrow, G. 2009a. Cross-linking of extruded collagen fibers-A biomimetic three-dimensional scaffold for tissue engineering applications. *Journal of Biomedical Materials Research Part A.* **89A**(4), pp.895-908.

Zeugolis, D.I., Paul, R.G. and Attenburrow, G. 2008a. Engineering extruded collagen fibers for biomedical applications. *Journal of Applied Polymer Science.* **108**(5), pp.2886-2894.

Zeugolis, D.I., Paul, R.G. and Attenburrow, G. 2008b. Extruded collagen-polyethylene glycol fibers for tissue engineering applications. *Journal of Biomedical Materials Research Part B-Applied Biomaterials.* **85B**(2), pp.343-352.

Zeugolis, D.I., Paul, R.G. and Attenburrow, G. 2008c. Post-self-assembly experimentation on extruded collagen fibres for tissue engineering applications. *Acta Biomaterialia.* **4**(6), pp.1646-1656.

Zeugolis, D.I., Paul, R.G. and Attenburrow, G. 2009b. Extruded Collagen Fibres for Tissue-Engineering Applications: Influence of Collagen Concentration and NaCl Amount. *Journal of Biomaterials Science-Polymer Edition.* **20**(2), pp.219-234.

Zeugolis, D.I., Paul, R.G. and Attenburrow, G. 2010. The influence of a natural cross-linking agent (Myrica rubra) on the properties of extruded collagen fibres for tissue engineering applications. *Materials Science & Engineering C-Materials for Biological Applications.* **30**(1), pp.190-195.

Zhao, X., Lang, Q., Yildirimer, L., Lin, Z.Y., Cui, W.G., Annabi, N., Ng, K.W., Dokmeci, M.R., Ghaemmaghami, A.M. and Khademhosseini, A. 2016. Photocrosslinkable Gelatin Hydrogel for Epidermal Tissue Engineering. *Advanced Healthcare Materials.* **5**(1), pp.108-118.

Zheng, Z.F., Ran, J.S., Chen, W.S., Hu, Y.J., Zhu, T., Chen, X., Yin, Z., Heng, B.C., Feng, G., Le, H.H., Tang, C.Q., Huang, J.Y., Chen, Y.W., Zhou, Y.T., Dominique, P., Shen, W.L. and Ouyang, H.W. 2017. Alignment of collagen fiber in knitted silk scaffold for functional massive rotator cuff repair. *Acta Biomaterialia.* **51**, pp.317-329.